DISSERTATION

The Hierarchical Reference Theory

An Application to Simple Fluids

ausgeführt zum Zwecke der Erlangung des akademischen Grades
eines Doktors der technischen Wissenschaften
unter der Leitung von

Ao.Univ.Prof. Dipl.-Ing. Dr.techn. Gerhard Kahl
E136
Institut für Theoretische Physik

eingereicht an der Technischen Universität Wien,
Fakultät für Technische Naturwissenschaften und Informatik,

von

Albert Reiner
Matrikelnummer 8901869
Schottenfeldgasse 10/11,
A–1070 Wien.

Wien, am 19. Februar 2002.

Albert Reiner

Kurzfassung

Während andere Integralgleichungsmethoden zur Beschreibung thermodynamischer Systeme im kritischen Bereich üblicherweise versagen und teils überhaupt kein, teils nur klassisches kritisches Verhalten zeigen, gelingt es der *Hierarchical Reference Theory* (HRT) diese Einschränkungen durch Anwendung renormierungsgruppentheoretischer Konzepte zu überwinden und in vielen Fällen sowohl die unmittelbare Umgebung des kritischen Punktes als auch die bei unterkritischen Temperaturen auftretenden Zweiphasengebiete erfolgreich zu beschreiben, ohne dabei jedoch strukturelle Information auf kleinen Längenskalen zu verlieren. Unter Beschränkung auf den Fall einfacher Einkomponentenfluide untersuchen wir die übliche Formulierung der HRT mit einer Schließungsbeziehung auf dem Zweiteilchenniveau im Geiste der *Lowest-Order γ-Ordered Approximation* bzw. der dazu äquivalenten *Optimized Random-Phase Approximation* sowie die relative Bedeutung verschiedener nötiger Näherungen auf analytischem, semi-analytischem sowie numerischem Weg; insbesondere erhellen wir den die Konvexität der freien Energie sicherstellenden Mechanismus und zeigen, dass er auch für die Steifheit des Gleichungssystems bei Temperaturen nahe der bzw. unterhalb der kritischen verantwortlich ist. Ebenso diskutieren wir die sogenannte Entkoppelungsannahme, die die Vernachlässigbarkeit gewisser Terme proportional zu dritten partiellen Ableitungen der geeignet modifizierten freien Energie zum Inhalt hat, und beweisen die Instabilität der Theorie in der gegenwärtigen Formulierung für vorwiegend repulsive Potentiale. Durch Anwendung der HRT auf Hartkugel-Yukawa- und *Square-Well*-Systeme bestätigen wir die erwartete Potentialreichweitenabhängigkeit der Qualität der Rechenergebnisse, beschäftigen uns mit Fragen der Konvergenz und Angemessenheit der bloß näherungsweise möglichen Berücksichtigung der Unmöglichkeit gegenseitiger Durchdringung der das Referenzsystem konstituierenden harten Kugeln, untersuchen die Bedeutung der Randbedingungen für die Lage der Binodale und die numerische Stabilität der diskretisierten Gleichungen und betrachten die unphysikalischen Verschiebungen der kritischen Temperatur, wie sie durch Unstetigkeiten im Störungsanteil des Potentials ausgelöst werden. Die numerischen Untersuchungen erfolgen unter Zuhilfenahme unserer vollständig modularen Neuimplementierung der Theorie, die programmtechnisch durch die Verwendung einer Metasprache und automatischer Codeerzeugungsmethoden, materiell jedoch durch den zur Sicherung der numerischen Signifikanz jedes Berechnungsschrittes getriebenen Aufwand gekennzeichnet ist.

Abstract

Combining renormalization group theoretical ideas with the integral equation approach to fluid structure and thermodynamics, the *Hierarchical Reference Theory* (HRT) is known to be successful even in the vicinity of the critical point and for sub-critical temperatures for a wide variety of systems. Restricting ourselves to the case of simple one-component fluids, we present analytical, semi-analytical and numerical results on the usual formulation of HRT and the customary closure reminiscent of the *Lowest-Order γ-Ordered Approximation* and the equivalent *Optimized Random-Phase Approximation*, investigating the necessary approximations' significance for the numerical procedure. In particular, we clarify the mechanism leading to a suppression of van der Waals loops and furthermore show that it gives rise to the equations' stiffness for close-to-critical and sub-critical temperatures; we also discuss the so-called decoupling assumption related to the elimination of terms proportional to third-order partial derivatives of a suitably modified free energy, and we prove the theory's instability for predominantly repulsive potentials. Applying HRT to both hard-core Yukawa and square-well fluids we confirm the trend of decreasing accuracy for narrower potentials, assess convergence and appropriateness of an approximate implementation of the core condition, consider the boundary conditions' relevance for the binodal's location and the numerical procedure, and we highlight the *rôle* of discontinuities in the potential's perturbational part in triggering unphysical shifts of the critical temperature predicted. The numerical investigations are carried out by means of our re-implementation of the theory in a fully modular software package relying heavily on the use of a meta-language and code construction techniques and going to great lengths to ensure the numerical soundness of the calculation.

Foreword

Looking back at the last years' work condensed into this slim volume I cannot fail but note that even the modest achievements documented here would not have been possible if it were not for the help of individuals and support from institutions.

First and foremost I would like to whole-heartedly thank my thesis' supervisor Prof. Gerhard Kahl who not only introduced me to HRT, a fascinating theory that turned out to hold more surprises than originally anticipated, but also patiently endured a long period lacking in constructive results; not the least do I thank him for accepting the peculiarities of my personality that must not have been easy to bear at times.

In the course of the work to be summarized here I also spent several months at the Chemistry Department of the State University of New York at Stony Brook; I am most grateful to Prof. George Stell for the hospitality extended towards me during this time and for the illuminating conversations we had; it was also during this time that Davide Pini, now in Milan, was most helpful both in mastering the difficulties of everyday life and in sharing his wealth of experience with HRT's numerical side as well as the `Fortran` code of what will be referred to as the "original implementation" in chapters 4 and on. — In the wake of a short encounter during the 4^{th} Liquid Matter Conference in Granada, Spain, in the fall of 1999 D.Ph. Giorgio Pastore invited me to Trieste for a week of inspiring discussions of HRT's current state and possible future. — I also gratefully acknowledge financial support from Österreichische Nationalbank under project 6241 and from Österreichischer Forschungsförderungsfonds under project P13062-TPH.

On a more personal note, the time during which the work reported here was carried out has not always been an easy one, and it is with a profound sense of thankfulness towards those I value — *sciunt qui sciant* — that I conclude these opening remarks.

Vienna, February 19, 2002. AR.

Table of Contents

I. Introduction

In a large part of the density-temperature plane integral equation theories are a reliable tool for studying thermodynamic and structural properties of, among others, simple one-component fluids [1]; unfortunately, in the vicinity of a liquid-vapor critical point integral equations are haunted by a host of difficulties leading to a variety of shortcomings such as incorrect and non-matching branches of the binodal, classical values at best for the critical exponents, or other deviations from the correct behavior at the critical singularity [2]. Asymptotically close to the critical point, on the other hand, renormalization group (RG) theory is the instrument of choice for describing the fluid; in general, however, RG approaches do not allow one to derive non-universal quantities from microscopic information only, *i. e.* from knowledge of the forces acting between the fluid's particles alone.

One of the theories devised to bridge the conceptual gap between these complementary approaches is the *Hierarchical Reference Theory* (HRT) first put forward by Parola and Reatto [2–13]: In this theory the introduction of a cut-off wavenumber Q inspired by momentum space RG theory and, for every value of Q, of a renormalized potential $v^{(Q)}(r)$ means that only non-critical systems have to be considered at any stage of the calculation; consequently, integral equations may successfully be applied to every system with $Q > 0$, and critical behavior characterized by non-classical critical exponents is recovered only in the limit $Q \to 0$.

An especially noteworthy trait of HRT is that it allows for a determination of structural and thermodynamic properties of various systems from first principles; in contrast, a similar scheme known under the name of global renormalization [14–17], originally developed by White and co-workers as an extension of Wilson's phase-space cell method [18] to the liquid state, while deemed computationally much less demanding than HRT, typically relies on at least one parameter that must be determined by a fitting procedure in order to correctly locate the critical point. Another distinguishing feature of HRT is its generality; indeed, after some early demonstration of the theory's applicability to various one-component systems the main focus of research shifted to the richer phase behavior of binary systems [19–21], and the theory has also been used in the context of quantum systems [22–24] or for the determination of an effective coarse-grained Hamiltonian to be used in a ϕ^4 RG theory [25]. Nevertheless, in the light of HRT's high promise and low penetration into the liquid physics community further study and critical

assessment of this theory seem worthwhile, even and foremost in the case of simple one-component fluids: indeed, it is in this comparatively simple setting that we may gain important insights into the numerical side of the theory, and barring special mechanisms relevant to some specific model system only any problems uncovered here must be expected to haunt more advanced applications of HRT, too.

In the work to be presented on the pages to follow[1] we set out to re-implement HRT independently of earlier programs and to undertake a systematic exploration of the computational nature of the problem posed by this particular theory; both the scope of our software and the results it typically yields will be demonstrated by applying HRT to two suitable types of model potentials, *viz.* the hard-core Yukawa (HCY) system and the square-well (SW) fluid; with effectively only one parameter each to vary, these systems provide convenient and popular test cases of liquid state theories, and they have been studied extensively. The present contribution, it should be noted, is the first application of HRT to SWs while this is one of the preferred models for the authors of the global renormalization scheme mentioned above [14–16].

Due to the large body of literature available on the HCY fluid and SWs the more recent of which will shortly be presented later on, and in view of some limitations of HRT in its current formulation we cannot expect to gain new insight into these model systems with a level of precision comparable to that of the more sophisticated simulation schemes. Instead, our focus of interest primarily lies on some aspects of HRT's numerical side and the *rôle* the potential's range plays; as far as the latter is concerned, the continuous nature of the HCY potential is in stark contrast to the finite domain of the SW interaction, and while the former, a system previously studied by HRT [28], is expected to be computationally rather unproblematic, the parametrization of the direct correlation functions in the usual closure to the theory on the two-particle level is clearly inappropriate for SWs in part of the phase diagram at least; indeed, even for less pronouncedly short-ranged potentials the computationally attractive but rather simlistic closure used almost exclusively has repeatedly been invoked as explanation of unsatisfactory aspects of HRT results [9, 11, 28, 29]. On the other hand, the main justification for using this particular closure relation comes from the need to avoid explicit Fourier transformations of quantities affected by the renormalized interparticle potential, with obvious repercussions for the implementation of the core condition. The additional approximations that this formulation of HRT necessitates raise further questions that are hardly mentioned in the literature and generally deemed unproblematic; in particular, the convergence properties of the correlation functions' expansions and the *rôle* of certain terms routinely neglected by invoking the so-called decoupling assumption are certainly not clear *a priori* and deserve closer study, the latter especially on account of the short-rangedness of the SW potential. Unfortunately, adoption of the decoupling assumption is dictated by the computational need for an additional approximation regarding some integrals of poor convergence

[1] Note that many of our results have also been summarized in the reports [26, 27]; in accordance with appendix F we will generally not reference these in the following.

whereas thermodynamic consistency mandates violation of this very assumption; not surprisingly, the resulting mathematical inconsistencies, not even mentioned in the literature to the best of our knowledge, adversely influence the numerical results as well as the theory's range of applicability. The closure and the chosen renormalization procedure — both coinciding with the usual choices for the kind of systems we are interested in — are also to blame for other restrictions on HRT's possible use: in particular, the presence of discontinuities in the potential is found to lead to unphysical shifts of the critical temperatures predicted, and we prove the equations' unconditional instability for predominantly repulsive inter-particle forces. By way of contrast, the pathological behavior of the theory's exact solution for high-compressibility thermodynamic states, here characterized for the first time, is linked to the very mechanism that also effectuates the suppression of van der Waals loops, one of the major feats of HRT, and is thus likely to be a generic trait of HRT; some of its numerical manifestations will again be discussed in the context of HCY and SW systems.

All of these issues will be considered in more detail by analytical, semi-analytical and purely numerical ways in the chapters to follow, and while the computational challenges it presents are, indeed, considerable, we still find HRT a viable theory of the liquid state well; however, because of the difficulties inherent in the theory any single calculation must be considered as of uncertain standing, and it is only by combining several related calculations and checking the respective solutions' appropriateness, internal consistency, and mutual compatibility that we are able to extract reliable and meaningful information from HRT calculations in the theory's current formulation.

In the remainder of this work we will first outline the underlying theory in chapter 2, taking care to properly motivate and preliminarily assess the approximations we introduce and discussing some general traits of the computational model of HRT so defined. After a short presentation of the physical systems that we consider as well as two additional types of potentials that we will make use of (chapter 3) we then give a superficial sketch of our recent re-implementation of HRT in the usual formulation for simple one-component fluids (chapter 4). Application of our software to the HCY and SW fluids then complements our earlier analytical considerations: chapter 5 characterizes the numerical problems that we find and provides a summary of their manifestations in the HCY and SW systems considered. The concluding remarks of chapter 6 once more summarize the most important of the points raised; they are followed only by several appendices where we collect some material the presence of which seems desirable on account of completeness but that would only hinder the flow of the exposition in the main text.

II. The Hierarchical Reference Theory for simple one-component fluids

Before we embark onto our excursion into some aspects of the application of HRT to simple one-component fluids we first have to familiarize ourselves with said theory and to motivate the approximate equations to be used in the numerical implementation of chapter 4, and with the more important of the properties of HRT some of which are hardly mentioned in the literature[1].

Despite being somewhat dated and not even mentioning the points to be raised in sections 2.3.2 and 2.4 as well as chapter 5, the review article [2] with its multitude of references of course remains the definite resource on HRT; in this chapter we limit ourselves to only a rough sketch of the theory as far as is relevant for the simple one-component fluids we will consider in chapter 5. In particular, in our work we found it convenient to restrict ourselves to the case of a spherically symmetric pure two-body interaction, and we took advantage of the additional simplifications possible by identifying the reference system with a pure hard sphere system, $v^{\mathrm{ref}} = v^{\mathrm{hs}}$, as can always be achieved *via* the well-known Weeks-Chandler-Andersen scheme [30–32]. Neither of these restrictions is, however, inherent to HRT itself, and the framework of our software (chapter 4) is in principle well able to accomodate a more general formulation of the theory if need be, *cf.* section 4.7. — In a similar vein, the extensive mathematical apparatus developed for, and applied in, deriving the basic hierarchy will not be considered, and despite the generality of HRT's approach to critical phenomena we will not consider any of the numerous other physical systems that HRT has been applied to, ranging from discrete [8] and continuous one component systems [5, 6, 11], the latter even including ones characterized by three-body interactions [9, 29], internal degrees of freedom [33], or non-hard-core reference systems [21], to various mixtures [19–21] and lately even including quantum systems [22–24].

[1] Except, of course, in the articles [26, 27] shortly presenting some of the work documented here.

2.1. Introduction of the Q-system and derivation of the exact hierarchy

The basic ingredient of HRT, already present in its precursor [12], is the gradual transition from a reference potential[2] $v^{\mathrm{ref}}(r,\varrho)$ at density ϱ, in our work chosen to coincide with the hard-sphere potential of diameter $\sigma(\varrho)$,

$$v^{\mathrm{ref}}(r,\varrho) = v^{\mathrm{hs}[\sigma(\varrho)]}(r) = \begin{cases} +\infty: & r < \sigma(\varrho) \\ 0: & r > \sigma(\varrho)\,, \end{cases} \tag{1}$$

to the full potential

$$v(r,\varrho) = v^{\mathrm{ref}}(r,\varrho) + w(r,\varrho) \tag{2}$$

describing the interaction between pairs of particles of a fluid, where any one of the intermediate potentials serves as a reference system with respect to which the properties of a successor potential are calculated. The two main differences between HRT and the theory presented in [12], however, are the differential nature of this transition (so that $\aleph_1$ intermediate systems are to be considered as opposed to a mere $\aleph_0$ in [12]) and the parametrization of the auxiliary potentials in terms of v^{ref} and w effecting the suppression of long-wavelength fluctuations typical of momentum-space RG calculations [34]. Correspondingly, a cut-off wavenumber Q varying from infinity to zero is introduced, and for every value of Q the potential $v^{(Q)} = v^{\mathrm{ref}} + w^{(Q)}$ is defined such that Fourier components $k < Q$ of the perturbational part $w^{(Q)}$ of the Q-potential $v^{(Q)}$ are strongly suppressed whereas those for $k > Q$ coincide with those of the original potential w. Consequently, the reference system and the fully interacting system are recovered in the limits $Q \to \infty$ and $Q \to 0$, respectively:

$$\begin{aligned} v^{(\infty)} &= v^{\mathrm{ref}}, \\ v^{(0)} &= v\,. \end{aligned} \tag{3}$$

The *rôle* of the Q-potential just introduced becomes clear when we consider a functional expansion in $\tilde{w}^{(Q)}$ of thermodynamic and structural properties of the system with pair interaction $v^{(Q)}$: as $\tilde{w}^{(Q)}(k)$, $k < Q$, is small, any integrals in the expansion corresponding to graphs with at least one loop are effectively truncated for $k < Q$; as HRT is constructed in such a way that only graphs with one or more loops are considered, use of the Q-potential is sufficient to implement the RG theoretical cut-off.

In principle, the precise manner in which the potential is cut off should not matter, and one can easily conceive of many different ways of doing so (*q. v.* subsection 2.4.2). On the other hand, for such a procedure to be usable it must not introduce instabilities when truncating the HRT hierarchy, which is usually done at the two-particle level. Apart from approaches valid only for special types of

[2] For the notation used cf. appendix F; in particular, superscripts signal the system a quantity is evaluated for and a tilde indicates Fourier transformation.

potentials (*cf.* section C.1), we are aware of only two cut-off procedures suitable at least for attractive potentials (*q. v.* sub-section 2.4.1); in our work we opted for the prescription presented in the review article [2] which seems to have been used almost exclusively so far [4–6, 11, 28] rather than the smooth cut-off formulation of [13], the latter being numerically cumbersome and predicting non-universal critical exponents (*q. v.* sub-section 2.4.2). Thus we define the Q-potential $v^{(Q)} = v^{\mathrm{ref}} + w^{(Q)}$ by

$$\tilde{w}^{(Q)}(k) = \begin{cases} \tilde{w}(k) : k > Q \\ 0 : k < Q \,, \end{cases} \tag{4}$$

and it is convenient to also introduce the symbol

$$\phi(r) = -\beta\, w(r) \tag{5}$$

where $\beta = 1/k_B\, T$, T is the temperature of the system considered and k_B is Boltzmann's constant.

A discussion of some questions regarding the properties of the Q-potential so defined can be found in section D.1; in particular, a simple calculation shows that $w^{(Q)}(r)$ differs from $w(r)$ by the addition of a convolution integral, *viz.*

$$w^{(Q)}(r) - w(r) = -\frac{1}{\pi r} \int_0^\infty \left(\frac{\sin Q\,(r'-r)}{r'-r} - \frac{\sin Q\,(r'+r)}{r'+r} \right) r'\, w(r')\, \mathrm{d}r' \tag{6}$$

so that the Q-potential is a rather artificial function in r-space hardly resembling the full potential except in the limits of eq. (3); furthermore, the range over which $v^{(Q)}(r)$ has to be considered is much larger than that of the original potential $v(r)$, a property immediately carrying over to related quantities, the direct correlation functions in particular. As an immediate consequence, numerical Fourier transformations involving the Q-potential or any of the correlation functions for the Q-system are computationally expensive and must be treated with extreme care; in fact, they should be avoided if possible at all, with obvious repercussions for the implementation of the core condition (*v. i.*).

Equipped with this sequence of Q-systems, the theoretical backbone of HRT is formed by a perturbative expansion treating the system at any value of Q as a starting point, or reference system, for obtaining the properties of the fluid with infinitesimally smaller cut-off $Q - \mathrm{d}Q$; as is well known from other theories, a reorganization and partial resummation of the resulting series is necessary in order to surpass the mean-field level. The procedure for arriving at the final hierarchy, summarized and discussed in some detail in [2, 4] so that we may confine ourselves to a mere sketch of the more important of the conceptual steps, is based upon standard expansion techniques [35] in the grand-canonical formalism; starting with the grand-canonical partition function of the $(Q - \Delta Q)$-system[3] and the splitting

$$v^{(Q-\Delta Q)} = v^{(Q)} + v^{(Q-\Delta Q)\leftarrow(Q)} \tag{7}$$

[3] Note that the HRT expansion (9) is a formally exact result that does not make use of the notion of a suppression of length scales that underlies the Q-system's definition (4) but, in principle, applies to arbitrary physical potentials under rather general assumptions. As we are interested only in the hierarchy's application within the framework of HRT, we identify the reference potential with $v^{(Q)}(r)$ and the target potential with $v^{(Q-\Delta Q)}$ right from the beginning.

of the potential with cut-off $Q - \Delta Q$, in order to arrive at expansions of the properties of the $(Q - \Delta Q)$-system in terms of those of the Q-system at the same density ϱ rather than at fixed fugacity z the transition from Q to $Q - \Delta Q$ must be accompanied by a shift in z formally corresponding to the effect of an as yet unknown external potential acting on the Q system that is implicitly determined by the condition of equality of the densities; and indeed, in [4] the authors of HRT provide an expansion of this external potential in a series the terms of which are naturally interpreted in terms of diagrams [35]. But from the density operator's definition as functional derivative of the partition function with respect to $\ln z$, and taking into account that $-\beta$ times the Helmholtz free energy A is just the Legendre transform of the partition function with respect to the density, $\ln z^{(Q-\Delta Q)}(\vec{r})$ is equal to $\delta(\beta A^{(Q-\Delta Q)})/\delta\varrho(\vec{r})$; as $\ln z^{(Q-\Delta Q)}$ differs from $\ln z^{(Q)}$ only by the external potential and a term proportional to $v^{(Q-\Delta Q)\leftarrow(Q)}(0)$ the expansion for the external potential acting on the Q-system (which is proportional to the difference of the logarithms of the fugacities) directly translates into an expansion for $A^{(Q-\Delta Q)} - A^{(Q)}$. In HRT it is customary and convenient to define the n-particle direct correlation functions as functional derivatives of the free energy with respect to the density, *viz.*

$$c_n^{(Q)}(\vec{r}_1, \ldots, \vec{r}_n) = \frac{\delta^n(-\beta A^{(Q)})}{\delta\varrho(\vec{r}_1)\cdots\varrho(\vec{r}_n)}$$

for arbitrary Q; repeated functional differentiation of the expansion for $A^{(Q-\Delta Q)}$ readily yields analogous expansions for the $c_n^{(Q)}$, $n \geq 1$. In this context it is important to note that the above definition of the direct correlation functions differs from the usual one by inclusion of terms corresponding to the ideal gas limit (given explicitly in eq. (5) of [4]); in particular, $\tilde{c}_2^{(Q)}(k)$ includes the term $-1/\varrho$ so that the Ornstein-Zernike (OZ, [36]) equation takes the form

$$\tilde{c}_2^{(Q)}(k) = -(1/\varrho) - \varrho\,\tilde{h}^{(Q)}(k)\,\tilde{c}_2^{(Q)}(k)\,, \tag{8}$$

where $g^{(Q)}(r) = h^{(Q)}(r) + 1$ is the pair distribution function of the Q-system.

The expansions for the free energy $A^{(Q-\Delta Q)}$ and the $c_n^{(Q-\Delta Q)}$, $n \geq 1$, so obtained are, however, still not suitable as a basis for HRT; indeed, in order to allow for non-classical critical behavior a re-summation has to be performed so that non-analyticities in the free energy as a function of β and ϱ may arise from expansions to finite order in ΔQ. To this end, the series for $A^{(Q-\Delta Q)}$ is ordered by the number of loops in the corresponding diagrams, and assuming translational invariance chains of perturbational interactions $\phi^{(Q-\Delta Q)\leftarrow(Q)} = -\beta\, v^{(Q-\Delta Q)\leftarrow(Q)}$ and suitable two-particle correlation functions of the Q-system (technically, the negative functional inverse of $c_2^{(Q)}$, related to $g^{(Q)}(r)$ or, in Fourier space, to the structure factor) can

be summed up: for the free energies this yields the relation

$$\begin{aligned}\frac{\beta A^{(Q-\Delta Q)}}{V} = \frac{\beta A^{(Q)}}{V} &- \frac{1}{2}\,\varrho^2\,\tilde{\phi}^{(Q-\Delta Q)\leftarrow(Q)}(0) \\ &+ \frac{1}{2}\int\limits_{\mathbb{R}^3}\frac{\mathrm{d}^3k}{(2\pi)^3}\,\ln\left(1+\frac{\tilde{\phi}^{(Q-\Delta Q)\leftarrow(Q)}(k)}{\tilde{c}_2^{(Q)}(k)}\right) \\ &+ \frac{1}{2}\,\varrho\,\phi^{(Q-\Delta Q)\leftarrow(Q)}(0) + \cdots\,,\end{aligned} \tag{9}$$

where the resummation's vestiges are clearly to be seen from the logarithm appearing in the integral on the right hand side and the ellipsis corresponds to the sum of all the relevant diagrams with a minimum of two loops; analogous results of course apply to the n-particle direct correlation functions.

The goal in developing the formal expansion of eq. (9) is to arrive at differential equations by taking the limit of $\Delta Q \to 0$ and retaining terms in the expansion only up to first order in ΔQ, which turn out to be exactly those displayed in eq. (9). For this program to succeed, however, both sides of eq. (9) as well as of its analogues for the direct correlation functions must be continuous in the cut-off wavenumber even in the limit $Q \to 0$; but from the definitions (7) of $\phi^{(Q-\Delta Q)\leftarrow(Q)}$ and (4) of the renormalized potential we immediately see that the zero-loop term proportional to $\tilde{\phi}^{(Q-\Delta Q)\leftarrow(Q)}(0) = \tilde{\phi}^{(Q-\Delta Q)} - \tilde{\phi}^{(Q)}(0)$ vanishes for $Q - \Delta Q > 0$ but coincides with $\tilde{\phi}(0)$ for $Q - \Delta Q = 0$. In order to eliminate this discontinuity we therefore define a modified free energy $\mathcal{A}^{(Q)}$ by formally subtracting this zero-loop contribution on both sides of eq. (9), and it is convenient to also treat the trivial part proportional to $\phi^{(Q-\Delta Q)\leftarrow(Q)}(0)$ of the one-loop term in the same way; all in all, $\mathcal{A}^{(Q)}$ is thus given by

$$\frac{\beta\mathcal{A}^{(Q)}(\varrho)}{V} = \frac{\beta A^{(Q)}(\varrho)}{V} - \frac{\varrho^2}{2}\left(\tilde{\phi}(0,\varrho) - \tilde{\phi}^{(Q)}(0,\varrho)\right) + \frac{\varrho}{2}\left(\phi(0,\varrho) - \phi^{(Q)}(0,\varrho)\right) \tag{10}$$

where we have added the density ϱ as an argument for the benefit of later use within the context of an approximate closure relying on thermodynamic consistency. An analogous discontinuity in $c_2^{(Q)}$ is similarly absorbed into the definition of a modified two-particle direct correlation function

$$\mathcal{C}^{(Q)}(r,\varrho) = c_2^{(Q)}(r,\varrho) + \phi(r,\varrho) - \phi^{(Q)}(r,\varrho)\,, \tag{11}$$

whereas the higher order correlation functions $c_n^{(Q)}$, $n \geq 1$, are free from zero-loop terms and do not have to be changed. With these definitions, the modified free energy $\mathcal{A}^{(Q)}$, the modified two-particle direct correlation function $\mathcal{C}^{(Q)}$ and the higher-order correlation functions $c_n^{(Q)}$, $n \geq 1$, are all continuous functions of Q even in the limit $Q \to 0$ and can thus be used for the construction of differential equations; on the other hand, from eqs. (10) and (11) it is obvious that their limits coincide with the physically meaningful unmodified quantities for the fully interacting system.

Assuming spherical symmetry, it is now simple to obtain the HRT hierarchy[4]: combining eq. (4) with the definition (7) of $\phi^{(Q-\Delta Q)\leftarrow(Q)}$ as the difference of $\phi^{(Q-\Delta Q)}$ and $\phi^{(Q)}$ (*v. s.*), we see that the integration on the right hand side of eq. (9) is to be extended over the shell with $Q-\Delta Q < k < Q$ only; but for $k < Q$ we have $\tilde{c}_2^{(Q)}(k) = \tilde{\mathcal{C}}^{(Q)}(k) - \tilde{\phi}(k)$ from eq. (11), and according to eq. (7) $\tilde{\phi}^{(Q-\Delta Q)\leftarrow(Q)}(k) = \tilde{\phi}(k)$ for $Q-\Delta Q < k < Q$. Writing d^3k as $4\pi\, k^2\, \mathrm{d}k$ by means of rotational invariance of v, invoking continuity of the integrand and taking the limit $\Delta Q \to 0$ we thus obtain

$$\begin{aligned}\frac{\mathrm{d}}{\mathrm{d}Q}\left(\frac{\beta\mathcal{A}^{(Q)}(\varrho)}{V}\right) &= -\frac{1}{2}\,\frac{4\pi}{(2\pi)^3}\,Q^2\,\ln\left(1+\frac{\tilde{\phi}(Q,\varrho)}{\tilde{\mathcal{C}}^{(Q)}(Q,\varrho)-\tilde{\phi}(Q,\varrho)}\right)\\ &= -\frac{Q^2}{4\pi^2}\,\ln\frac{\tilde{\mathcal{C}}^{(Q)}(Q,\varrho)}{\tilde{\mathcal{C}}^{(Q)}(Q,\varrho)-\tilde{\phi}(Q,\varrho)}\\ &= \frac{Q^2}{4\pi^2}\,\ln\left(1-\frac{\tilde{\phi}(Q,\varrho)}{\tilde{\mathcal{C}}^{(Q)}(Q,\varrho)}\right)\,.\end{aligned} \tag{12}$$

Analogous results can, of course, be obtained for the direct correlation functions but will not be given here as they will be considered no more in the remainder of this work; the interested reader may find the first few of these, in diagrammatic notation, in eqs. (26) to (28) of [4] or, in conventional notation but for $\mathcal{C}^{(Q)}$ alone, in eq. (4.27) of [2]. It is, however, important to note that the expression for $\mathrm{d}\tilde{c}_n^{(Q)}(k,\varrho)/\mathrm{d}Q$ involves the direct correlation functions from $\mathcal{C}^{(Q)}$ up to $c_{n+2}^{(Q)}$ so that the hierarchy of differential equations never terminates; on the other hand, even though an exact solution of this hierarchy is not available for non-trivial potentials, as the expansion underlying eq. (9) is formally exact, at every cut-off Q the isothermal compressibility $\kappa_T^{(Q)}$ of the Q-system as obtained from the volume integral of the two-particle direct correlation function or by differentiation of the free energy must coincide, which can be written in the simple form

$$\tilde{\mathcal{C}}^{(Q)}(0,\varrho) = -\frac{\mathrm{d}^2}{\mathrm{d}\varrho^2}\left(\frac{\beta\mathcal{A}^{(Q)}(\varrho)}{V}\right) \tag{13}$$

despite the additional terms introduced in eqs. (10) and (11). Also we wish to stress that all the calculations done so far were performed at fixed density ϱ, and that the hierarchy comprises ordinary differential equations (ODEs) in Q only; it is only for the benefit of later application that we included ϱ as an argument to various functions appearing in eqs. (9) to (12).

From among the interesting aspects of the theory the conceptual basis of which has just been presented we here only want to mention two: first of all, HRT not only draws considerable inspiration from RG theory, it can also be shown to be equivalent to an RG theoretical development by Nicoll and co-workers [2]; and

[4] Note that it is only now that identification of the reference system in the expansion with any of the Q-systems and of the target system with a system at slightly smaller cut-off is necessary.

exponent	classical	HRT	Ising
α	0	-0.07	0.1096(5)
β	0.5	0.345	0.32653(10)
γ	1	1.378	1.2373(2)
δ	3	5	4.7893(8)
η	0	0	0.03639(15)
ν	0.5	0.689	0.63012(16)

Table 1: The critical exponents for fluids in the three-dimensional Ising universality class as obtained from mean field theory ("classical" exponents), from HRT with an OZ *ansatz* for the structure factor [2], and from recent 25^{th}-order high-temperature series expansions [37].

secondly, the equations can be analyzed in the scaling regime which allows one to demonstrate universality, and with an Ornstein-Zernike *ansatz* for the structure factor (so that $\eta = 0$) the non-classical critical exponents listed in table 1 are found.

2.2. Approximate closure

Due to the non-terminating character of the hierarchy the derivation of which we just sketched, the need arises to introduce some approximate closure relation. In doing so, it is desirable to retain both the differential build-up of the relevant quantities mandated by the RG picture and thermodynamic consistency as embodied in the compressibility sum-rule (13); the derivatives with respect to ϱ present in the latter then mandate the transition from equations at fixed ϱ to a partial differential equation (PDE) in the (Q, ϱ)-plane with boundary conditions supplied at two densities, $\varrho_{\min}$ and $\varrho_{\max}$. In addition, we need to retain the core condition

$$g^{(Q)}(r) = 0\,, \qquad r < \sigma\,; \tag{14}$$

indeed it is one of HRT's main advantages to conserve information on length scales as diverse as the hard-sphere diameter $\sigma(\varrho)$ of the reference system at density ϱ and the cut-off wavelength $1/Q$ allowing criticality to arise from long-wavelength fluctuations in the limit $Q \to 0$ for low enough temperature.

As noted above and discussed in more detail in section D.1, the long-ranged nature of $w^{(Q)}$ and the correlation functions due to the cutting-off of eq. (4) is a strong argument in favor of any closure allowing an approximate implementation of the core-condition without the need for costly Fourier transforms. This is a likely reason for the up to now seemingly exclusive use of a closure in the spirit of the *Lowest-Order γ-ordered Approximation* (LOGA, [38, 39]) or the equivalent *Optimized Random-Phase Approximation* (ORPA, [40]) despite this closure's known deficiencies [9, 11, 28, 29] (*cf.* section 2.4). Just as in those approximations we introduce a set of Q-independent basis functions u_n and corresponding expansion

coefficients $\gamma_n^{(Q)}$, but unlike LOGA/ORPA we add one degree of freedom in order to be able to accomodate not only the core condition but also thermodynamic consistency (13) or some other condition (*cf.* sub-section 2.2.1):

$$\begin{aligned}
\mathcal{C}^{(Q)}(r,\varrho) &= \phi(r,\varrho) + \gamma_0^{(Q)}(\varrho)\, u_0(r,\varrho) + \mathcal{K}^{(Q)}(r,\varrho)\,, \\
\mathcal{K}^{(Q)}(r,\varrho) &= \mathcal{G}^{(Q)}(r,\varrho) + c_2^{\mathrm{ref}}(r,\varrho)\,, \\
\mathcal{G}^{(Q)}(r,\varrho) &= \sum_{n=1}^{\infty} \gamma_n^{(Q)}(\varrho)\, u_n(r,\varrho)\,.
\end{aligned} \tag{15}$$

Here, $u_0(r,\varrho)$ is usually taken to be proportional to $w(r,\varrho)$ (but *cf.* section A.3) and normalized to

$$\tilde{u}_0(0,\varrho) = 1\,, \tag{16}$$

and only the $u_n(r,\varrho)$ for $n \geq 1$ are taken to provide a basis for a suitable function space over $[0,\sigma(\varrho)]$ (*cf.* section D.2); LOGA/ORPA is recovered by dropping the γ_0-term necessary for thermodynamic consistency (*cf.* section 2.4).

With these provisions, the problem of implementing both thermodynamic consistency (13) and the core condition (14) reduces to that of an appropriate choice of the expansion coefficients $\gamma_n^{(Q)}(\varrho)$, $n \geq 0$, for every point (Q,ϱ) in the PDE's domain. As first demonstrated in [6] and shown in more detail in section D.2, when starting with a reference system that already meets both of these requirements the problem of determining the correct $\gamma_n^{(Q)}(\varrho)$ for all Q reduces to that of the solution of a countable set of ODEs coupled to each other as well as to the HRT-PDE at every density; with the short-hand notation

$$\alpha^{(Q)}(\varrho) = \frac{\partial^3}{\partial Q \partial \varrho^2} \left(\frac{\beta \mathcal{A}^{(Q)}(\varrho)}{V} \right) \tag{17}$$

(a quantity that will play an important *rôle* in sub-section 2.2.1 below) and the definition (D.9) for the auxiliary symbol $\hat{\mathcal{I}}^{(Q)}$ denoting a class of integrals extended over all of Fourier space, these ODEs are conveniently written as

$$\begin{aligned}
&\sum_{n=1}^{\infty} \hat{\mathcal{I}}^{(Q)} \left[\tilde{u}_j(k,\varrho)\, \left(\tilde{u}_n(k,\varrho) - \tilde{u}_0(k,\varrho)\, \tilde{u}_n(0,\varrho) \right), \varrho \right] \frac{\partial \gamma_n^{(Q)}(\varrho)}{\partial Q} \\
&\qquad = \alpha^{(Q)}(\varrho)\, \hat{\mathcal{I}}^{(Q)} \left[\tilde{u}_j(k,\varrho)\, \tilde{u}_0(k,\varrho), \varrho \right] \\
&\qquad\quad + \frac{Q^2}{2\pi^2} \frac{\tilde{\phi}(Q,\varrho)\, \tilde{u}_j(Q,\varrho)}{\tilde{\mathcal{C}}^{(Q)}(Q,\varrho)\, \left(\tilde{\mathcal{C}}^{(Q)}(Q,\varrho) - \tilde{\phi}(Q,\varrho) \right)}\,, \quad j \geq 1\,.
\end{aligned} \tag{18}$$

To fully specify the mathematical problem, the PDE must be amended by both initial and boundary conditions; the former take the simple form of vanishing expansion coefficients, *i. e.*

$$\gamma_n^{\mathrm{ref}}(\varrho) = 0\,, \qquad n \geq 0\,, \tag{19}$$

reflecting the reference system's compliance with both thermodynamic consistency and the core condition, whereas the question of the boundary conditions to be imposed upon the solution at high and low density will be discussed only in section 4.5.

As eq. (18) stands, it is no more amenable to direct numerical treatment than the underlying OZ relation (8) and the compressibility sum-rule (13); not only must this infinite-dimensional matrix equation be truncated to a finite number $1 + N_{\mathrm{cc}}$ of basis functions but even then the $\hat{\mathcal{I}}$-integrals (which, furthermore, turn out to converge only very slowly) need to be evaluated at every Q and ϱ — a tedious process no less demanding than the Fourier transformations this approach is meant to replace. It is only through the adoption of the simple, albeit not very well justified (*q. v.* section 5.2) approximation (D.11) for $\partial\hat{\mathcal{I}}^{(Q)}[f(k,\varrho),\varrho]/\partial Q$ detailed in section D.3 that this closure becomes manageable: following the steps leading up to eq. (D.11), the task of evaluating one of the integrals of eq. (18), or of eq. (D.8), reduces to only an initial integration for the reference system followed by the solution of an ordinary differential equation (ODE) coupled to the HRT-PDE as well as analogous ODEs for all the other integrals of the $\hat{\mathcal{I}}$-type.

2.2.1. Additional constraints

For future reference, let us shortly contemplate the effect of imposing some additional constraint on the solution at some density ϱ; in the following it is understood that the constraint considered is distinct from other conditions in the sense of not introducing redundancy into the equations. Under mild assumptions always fulfilled for the cases we will consider, as long as we retain the core condition such an additional constraint is already sufficient to determine the expansion coefficient $\gamma_0^{(Q)}$; consequently, thermodynamic consistency can no longer be imposed without introducing mathematical inconsistencies. By the same token, eq. (18) derived by incorporating the compressibility sum rule (13) into the core condition (*cf.* section D.1) is no longer valid but must be changed to

$$\begin{aligned}\sum_{n=1}^{\infty}\hat{\mathcal{I}}^{(Q)}\left[\tilde{u}_j(k,\varrho)\,\tilde{u}_n(k,\varrho),\varrho\right]\,\frac{\partial\gamma_n^{(Q)}(\varrho)}{\partial Q}\\ = -\hat{\mathcal{I}}^{(Q)}\left[\tilde{u}_j(k,\varrho)\,\tilde{u}_0(k,\varrho),\varrho\right]\,\frac{\partial\gamma_0^{(Q)}(\varrho)}{\partial Q}\\ + \frac{Q^2}{2\pi^2}\,\frac{\tilde{\phi}(Q,\varrho)\,\tilde{u}_j(Q,\varrho)}{\tilde{\mathcal{C}}^{(Q)}(Q,\varrho)\,\left(\tilde{\mathcal{C}}^{(Q)}(Q,\varrho)-\tilde{\phi}(Q,\varrho)\right)}\,,\quad j\geq 1,\end{aligned}\tag{20}$$

to reflect the transition from eq. (13) to said constraint determining the function $\gamma_0^{(Q)}(\varrho)$ appearing on the above equation's right hand side; furthermore, elimination of thermodynamic consistency obviously means decoupling the PDE to a set of ODEs at fixed density. Of course, eq. (18) is again recovered when inserting the expression (D.10) for $\partial\gamma_0^{(Q)}/\partial Q$ in eq. (20).

2.2.2. Decoupling assumption

Unfortunately it turns out that a scheme retaining $\alpha^{(Q)}(\varrho)$ in eq. (18) for $\varrho_{\min} < \varrho < \varrho_{\max}$ presents significant numerical problems for all but extremely high temperatures, precluding reaching $Q = Q_0$ at least for the potentials that we have looked at (*q. v.* sub-section 5.4.1). This is where the so-called "decoupling assumption" comes into play: based upon the different ranges of $u_0(r) \propto \phi(r)$ and $u_n(r)$, $n \geq 1$, the authors of [6] argue that terms related to third partial derivatives of the free energy might be ignored, thus effectively decoupling the long-range behavior driven by thermodynamic consistency from the constraint of eq. (14) acting on very short range[5]. Consequently they set

$$\alpha^{(Q)}(\varrho) = 0\,, \tag{21}$$

which obviously eliminates the $\hat{\mathcal{I}}$-integral on the right hand side of eq. (18); it turns out that this change, to the best of our knowledge adopted in all later publications on HRT for simple one-component fluids that aspire to implement the core condition at all, is often sufficient to allow generating a solution all the way to $Q = Q_0$, the smallest cut-off considered numerically. While a more detailed discussion of the decoupling assumption including numerical results will be presented in chapter 5, here we only point out that in the light of sub-section 2.2.1 eq. (21) is obviously incompatible not only with the LOGA/ORPA condition

$$\gamma_0^{(Q)}(\varrho) = 0 \tag{22}$$

retained in some numerical calculations for $\varrho = \varrho_{\max}$ (*q. v.* section 5.4) but also with thermodynamic consistency (13) altogether; furthermore, when consistently applying the approximation of eq. (21), the solution of eq. (15) is uniquely determined by the core condition (14) alone and the PDE thus reduced to a set of ODEs no longer capable of yielding clear phase boundaries (*cf.* section 5.3).

2.3. Reformulation in not-quite quasi-linear form and behavior of the solution for large isothermal compressibility

The formulation of section 2.2, treating core condition and thermodynamic consistency along the lines of sections D.2 and D.3, provides us with a set of equations implementing HRT with the LOGA/ORPA-like closure on the two-particle level that is, in principle, well suited for numerical processing; but while these expressions

[5] But note that the longest-ranged part in $c_2^{(Q)}(r, \varrho)$ is the zero-loop term for $Q \sim 1/\sigma$, *v. i.* section 2.4.

lend themselves to discretization in a straightforward way (*cf.* section B.1), it is computationally much more convenient to cast the PDE in a form superficially resembling a quasi-linear one [11] so that an implicit finite difference (FD) scheme requires only the inversion of a tridiagonal matrix. The re-writing we adopted — detailed in appendix A, very similar to the one of [11] — results in the introduction of an auxiliary function $f(Q,\varrho)$ *via* eq. (A.1) so that the PDE implied by eqs. (12) and (13) can be written in the form

$$\frac{\partial}{\partial Q} f(Q,\varrho) = d_{00}[f,Q,\varrho] + d_{01}[f,Q,\varrho]\,\frac{\partial}{\partial \varrho} f(Q,\varrho) + d_{02}[f,Q,\varrho]\,\frac{\partial^2}{\partial \varrho^2} f(Q,\varrho)\,, \quad (23)$$

with coefficients d_{0i} explicitly given in eq. (A.5); note that d_{01} vanishes for density-independent potential.

Apart from the technical advantages this re-writing affords and the clarification regarding the admissible basis functions it brings about (*cf.* section A.3), inspection of the expressions (A.5) for the PDE's coefficients d_{0i} with the definitions (A.3) readily yields the information that, for sufficiently small Q and large $\varepsilon(Q,\varrho) \propto \exp(f(Q,\varrho)\,\tilde{u}_0^2(Q,\varrho))$ as defined in eq. (A.3), the coefficients d_{0i} grow much more rapidly in modulus than $f(Q,\varrho)$ and its derivatives with respect to ϱ, *viz.*

$$\begin{aligned} d_{0i} &= \mathcal{O}(\varepsilon^1) \text{ for } i \in \{0,1,2\}\,, \\ \frac{\partial^i f}{\partial \varrho^i} &= \mathcal{O}(\varepsilon^0) \text{ for } i \in \{0,1,2\}\,, \\ \frac{\partial f}{\partial Q} &= \mathcal{O}(\varepsilon^1)\,; \end{aligned} \quad (24)$$

the last relation follows directly from eq. (23). This behavior, not easily seen from the relations (12), (13), and (15) underlying eq. (23), both provides us with some insight regarding the mechanism leading to the suppression of van der Waals loops in an implementation like that presented in chapter 4 and allows us to demonstrate the PDE's stiffness in the region where the isothermal compressibility's divergence builds up. Note, however, that neither of these is directly linked to the re-formulation of the PDE but merely more conveniently discussed in this framework as relations analogous to eq. (24) are not readily available in a formulation relying on the modified free energy $\mathcal{A}^{(Q)}(\varrho)$ rather than $f(Q,\varrho)$: indeed, the emergence of rigorously flat isotherms in the coexistence region and the corresponding direct accessibility of the binodal have long been regarded as among HRT's main advantages over other integral-equation based theories, and stiffness is probably at the heart of the problems preventing [6] from solving the HRT equations for sub-critical temperatures and its effects were also seen in an earlier version of our program that did not rely on the rewriting of appendix A (*cf.* section B.1).

2.3.1. Suppression of van der Waals loops

Interest in the case of large $\varepsilon(Q,\varrho)$ mainly derives from relation (A.4): as the isothermal compressibility κ_T of the fully interacting system must diverge in

the phase diagram's coexistence region[6], so must appendix A's $\varepsilon(0,\varrho)$ and, from eq. (A.3), $f(0,\varrho)$; continuity of the limit $Q \to 0$ (*cf.* eqs. (11) and (10)) then brings about that $\varepsilon(Q,\varrho)$ and $f(Q,\varrho)$ must be large already for non-vanishing but sufficiently small cut-off Q, while the RG mechanism with its suppression of long-wavelength fluctuations as implemented *via* eq. (4) precludes any divergences for $Q \neq 0$. In this and the following sub-section we will restrict ourselves to close-to-critical and subcritical temperatures only and concentrate on that part of the (Q,ϱ)-plane where ε is large and eq. (24) applies.

Let us consider $f(Q,\varrho)$ at some fixed, non-vanishing and not too large[7] value of the cut-off Q: in the following we take the potential's ϱ-dependence to be sufficiently small to allow us to ignore the d_{01}-term in eq. (23); furthermore, for sake of argument we assume that $f(Q,\varrho)$ is a smooth function of ϱ that remains small for most of the density interval $[0,\varrho_{\max}]$ but becomes large for intermediate ϱ. Note that the assumption of smoothness is not justified for the PDE's true solution (*cf.* sub-section 2.3.2); on the other hand, when relying on a FD scheme akin to that of chapter 4, for any practical density grid the numerical procedure can only produce an approximate solution that does not properly reflect the true solution's irregular behavior in the ϱ-domain and again appears sufficiently smooth (*cf.* section 5.5, table 5.4 in particular). Strictly speaking some of the arguments put forward in this sub-section thus apply only to a FD approximation to the PDE rather than to the PDE itself. Under these assumptions, inspection of the coefficients (A.5) shows that both d_{00} and d_{02} are negative whereever $f(Q,\varrho)$ and, hence, the Q-system's isothermal compressibility are large. Then, as $|\partial^2 f/\partial\varrho^2|$ is assumed small, wherever $f(Q,\varrho)$ is sufficiently large already, $\mathrm{d}f = (\partial f/\partial Q)\,\mathrm{d}Q = -(\partial f/\partial Q)\,|\mathrm{d}Q| > 0$ and f further increases to ever larger values as Q decreases towards $Q \to 0$. On the other hand, for the kind of $f(Q,\varrho)$ assumed, $\partial^2 f/\partial\varrho^2 < 0$ for most of the density interval where f is large, with a change of signs only where f falls off to small values again; consequently, the d_{02}-term in eq. (23) reduces $|\partial f/\partial Q|$ where f is largest and enhances it closer to the edge of the region of large f, thereby effectively safeguarding that $|\partial^2 f/\partial\varrho^2|$ remains rather small, as assumed; at the same time, the boundary between the regions of large and small f becomes ever more sharply defined.

Taken together the above considerations not only show that, indeed, the result of following the discretized HRT equations all the way to $Q \to 0$ is certainly free of a van der Waals loop; furthermore, it is not difficult to see that binodal and spinodal coincide under the smoothness assumptions stated, *i. e.* that $1/\kappa_T^{(0)} \propto 1/\bar{\varepsilon}(0,\varrho)$ is continuous at ϱ_v and ϱ_l.

---

[6] Recall that, in three dimensions, binodal and spinodal as predicted by HRT coincide, *i. e.* $1/\kappa_T^{(0)}$ remains continuous at the phase boundary. The boundaries of the density interval of diverging $\kappa_T^{(0)}$ are naturally identified with the densities ϱ_v and ϱ_l of the coexisting vapor and liquid, respectively.

[7] Typically, Q must be smaller than the location of the first minimum of $\tilde{\phi}(k,\varrho)$; there is, however, some numerical evidence for a much larger range of validity in the systems discussed in chapter 5.

2.3.2. Stiffness for large isothermal compressibility

As already mentioned, however, the PDE's true solution is certainly not smooth on the scales considered numerically for close-to-critical and sub-critical temperatures. In the following we will demonstrate the PDE's pathological behavior in the region of large $f(Q,\varrho)$; in doing so we restrict ourselves to even smaller Q than in sub-section 2.3.1, *viz.* to so low a Q that $\tilde{u}_0(Q,\varrho)$ may be replaced by unity by virtue of this basis function's normalization (16); extension of the argument to a larger Q-range is cumbersome but straightforward and cannot be expected to yield qualitatively different results.

As before, we base our considerations upon the orders cited for the various terms in the PDE (23); furthermore, for the time being we only consider an ODE at some fixed density ϱ, which is possible without loss of generality as the exact solution of the PDE exists and could, in principle, be imposed as discussed in sub-section 2.2.1. According to eq. (24), $\mathrm{d}f/\mathrm{d}Q$ is of order $\mathcal{O}(\varepsilon^1)$ and can thus be written as

$$\begin{aligned} \frac{\mathrm{d}f(Q)}{\mathrm{d}Q} &= e^{f(Q)} d_0(Q)\,, \\ d_0(Q) &= \mathcal{O}(1)\,, \end{aligned} \tag{25}$$

where the order given for d_0 is valid only with the assumption of sufficiently small Q mentioned earlier; note that a negative sign of d_0 corresponds to the rise of $f(Q)$ expected as Q approaches naught from above. But as the exponential in the above relation's right hand side cannot vanish, it may also be read as a definition for $d_0(Q)$ in terms of the exact solution f of the HRT-PDE; on the other hand, with the $d_0(Q)$ so obtained eq. (25) is also an exact ODE for $f(Q,\varrho)$, and imposing a correct starting value for f at some cut-off Q' the solution at any other cut-off Q is trivially obtained as

$$f(Q) = -\ln\left(e^{-f(Q')} - \int_{Q'}^{Q} d_0(q)\,\mathrm{d}q\right).$$

As stated already at the beginning of sub-section 2.3.1, $f(Q)$ must be large but finite for non-vanishing Q but diverge in the limit $Q \to 0$; inspecting the argument of the logarithm in the above solution, these requirements are readily translated as

$$\begin{aligned} \int_{Q'}^{Q} d_0(q)\,\mathrm{d}q &< e^{-f(Q')}\,, \\ \lim_{Q\to 0} \int_{Q'}^{Q} d_0(q)\,\mathrm{d}q &= e^{-f(Q')}\,. \end{aligned}$$

Thus the mean of $d_0(Q)$ over the interval $]0,Q[$ is $-1/(Q\,\varepsilon(Q))$, while $|d_0(Q)|$ itself still is of order unity; these statements are compatible only if d_0 is a rapidly oscillating function of Q, with both amplitude and period no larger than approximately $1/(Q\,\varepsilon(Q))$. Reverting to the HRT-PDE and the auxiliary function $f(Q,\varrho)$

we conclude that $f(Q,\varrho)$ as a function of Q also oscillates rapidly on a scale of the order of $1/(Q\,\varepsilon(Q,\varrho))$ but with both the average slope and an upper bound for the oscillations' amplitudes growing like $1/Q$; this erratic behavior immediately carries over to the solution's ϱ-dependence due to the estimate of eq. (24) for $\partial f(Q,\varrho)/\partial\varrho$.

The PDE's stiffness so demonstrated is, of course, a major obstacle in the numerical implementation of HRT, especially in view of the diverging upper bound on the oscillations' amplitudes; the above considerations, however, are rather general and rely only on some general properties of HRT in the current formulation as applied to one-component fluids, *viz.* divergence of the isothermal compressibility in the coexistence region, continuity of the limit $Q \to 0$, and suppression of divergences for $Q > 0$; only the remaining ingredient essential to our reasoning, *viz.* the behavior of the ratio of the Q- and the ϱ-derivatives as the divergence in the compressibility builds up, while obvious in the formulation of eq. (23), could only be obtained by reasoning about third- and second-order derivatives of $\mathcal{A}^{(Q)}(\varrho)$ rather than first- and second-order ones if we were to repeat the arguments without resorting to the re-writing of appendix A — after all, f is basically the modified free energy's derivative with respect to Q. Still, this last aspect is intimately linked to the continuous build-up of the isothermal compressibility for small Q so that none of the properties we invoked appear specific to the closure adopted or any of the other approximations introduced so far, and stiffness must be expected to arise in other formulations and more advanced applications of HRT, too.

2.4. Further considerations regarding the choice of closure

Before setting about the implementation of the theory just sketched, let us pause for a moment to reflect some more upon the properties of the closure adopted without taking recourse to our numerical results: first of all, it is instructive to write the LOGA/ORPA-*ansatz* (15) for the true two-particle direct correlation function rather than for $\mathcal{C}^{(Q)}$; from eq. (11) we immediately find

$$c_2^{(Q)}(r,\varrho) = c_2^{\mathrm{ref}}(r,\varrho) + \phi^{(Q)}(r,\varrho) + \gamma_0^{(Q)}(\varrho)\,u_0(r,\varrho) + \sum_{n=1}^{\infty}\gamma_n^{(Q)}(\varrho)\,u_n(r,\varrho)\,;$$

for the moment adopting the LOGA/ORPA condition (22) and ensuring the core condition by an appropriate choice of the other expansion coefficients this is immediately recognized as the well-known LOGA/ORPA closure for the Q-system with potential $v^{\mathrm{ref}} + w^{(Q)}$:

$$\begin{cases} c_2^{(Q)}(r,\varrho) = c_2^{\mathrm{ref}}(r,\varrho) - \beta\,w^{(Q)}(r,\varrho)\,, & r > \sigma(\varrho) \\ g^{(Q)}(r,\varrho) = 0\,, & r < \sigma(\varrho)\,. \end{cases}$$

But as soon as we relax the condition of vanishing $\gamma_0^{(Q)}(\varrho)$, with the usual choice[8] of $u_0(r,\varrho) \propto w(r,\varrho)$ the direct correlation function acquires a contribution from the full potential $w(r,\varrho)$ rather than from $w^{(Q)}(r,\varrho)$ alone. This is certainly inappropriate for a description of the Q-system, especially as the derivation of the exact HRT hierarchy in section 2.1 clearly treats the Q-system, despite its artificial potential, as a real physical system and not just as a formal device in the construction; indeed, the expansion (9) that all of HRT is based upon remains valid for any choice of reference and target system provided the potentials' difference is non-singular. — As a corollary we note that, from section D.1, the longest ranged component of $c_2^{(Q)}(r,\varrho)$ by far is not the term $\gamma_0^{(Q)}(\varrho)\,u_0(r,\varrho)$ used for implementing thermodynamic consistency but rather the convolution integral resulting from the renormalization (4) of the potential, an observation that casts some doubt on the decoupling assumption's justification first presented in [6] and re-iterated ever since (*q. v.* section 5.2).

Let us now assume that a given potential $v(r)$ vanishes identically beyond some finite interparticle distance (as is the case for the square well and multi-step systems to be introduced in chapter 3), or else that it decreases sufficiently rapidly for large r to ensure convergence of the relevant integrals[9] (like, *e. g.*, the exponential in eq. (3.2)): then, from the closure (15) we immediately conclude that all moments of $\mathcal{C}^{(Q)}(r,\varrho)$ and of $c_2^{(Q)}(r,\varrho)$ exist throughout the Q-system's phase diagram, which is clearly at variance with the correct behavior near the critical singularity [41]. While existence of all moments of $\mathcal{C}^{(Q)}(r,\varrho)$ is obvious from the short-rangedness and regularity of the terms in eq. (15), for the analogous conclusion regarding the physically meaningful $c_2^{(Q)}$ at non-vanishing Q we need to also invoke eq. (11) in conjunction with the relation of any function's moments to the derivatives of its Fourier transform with respect to the wavenumber k at $k = 0$; application to the zero-loop terms in the definition of $\mathcal{C}^{(Q)}$ then yields the desired result.

2.4.1. Instability for repulsive potentials

Another aspect of the closure (15) that can easily be seen is the instability of the PDE for repulsive potentials, a restriction only hinted at in [2], *v. i.*; as the core condition cannot be expected to be relevant in this context, for simplicity's sake we adopt the approximation of vanishing LOGA/ORPA function, *i. e.* we set $\mathcal{G}^{(Q)}(r,\varrho) = 0$ or, equivalently, $N_{\mathrm{cc}} = 0$. The HRT equations then provide a PDE

[8] As noted in appendix A, $u_0(r,\varrho)$ does not have to be strictly proportional to $w(r,\varrho)$ as long as it meets the requirements laid out in section A.3; but even then similar considerations apply unless we adopt Q-dependent basis functions, a possibility more general than the *ansatz* of appendix A.

[9] As we will shortly see, for the following considerations it is sufficient that all moments of $v(r,\varrho)$ exist, which, it should be noted, is not the case for, *e. g.*, a Lennard-Jones potential.

for $\gamma_0^{(Q)}(\varrho)$: By differentiating the compressibility sum rule (13) in the form

$$\gamma_0^{(Q)}(\varrho) = -\frac{\partial^2}{\partial\varrho^2}\frac{\beta\mathcal{A}^{(Q)}(\varrho)}{V} - \tilde{c}_2^{\mathrm{ref}}(0,\varrho) - \tilde{\phi}(0,\varrho)\,, \tag{26}$$

with respect to Q as well as eq. (12) twice with respect to ϱ and equating the resulting expressions for $-\alpha^{(Q)}(\varrho)$ we readily obtain this PDE, *viz.*

$$\frac{\partial\gamma_0^{(Q)}(\varrho)}{\partial Q} = -\frac{Q^2}{4\pi^2}\frac{\partial^2}{\partial\varrho^2}\ln\left(1 - \frac{\tilde{\phi}(Q,\varrho)}{\tilde{c}_2^{\mathrm{ref}}(Q,\varrho) + \tilde{\phi}(Q,\varrho) + \gamma_0^{(Q)}(\varrho)\,\tilde{u}_0(Q,\varrho)}\right).$$

Let us now assume that, at some stage of the computation, $\gamma_0^{(Q)}(\varrho)$ differs from the above PDE's true solution by only a small amount $\delta\gamma_0^{(Q)}(\varrho)$; performing the corresponding substitution

$$\gamma_0^{(Q)}(\varrho) \Longrightarrow \gamma_0^{(Q)}(\varrho) + \delta\gamma_0^{(Q)}(\varrho)\,,$$

expanding up to first order in $\delta\gamma_0$ and simplifying we find the PDE governing $\delta\gamma_0$, *viz.*

$$\frac{\partial\delta\gamma_0^{(Q)}(\varrho)}{\partial Q} = \frac{Q^2\,\tilde{\phi}(Q,\varrho)\,\tilde{u}_0(Q,\varrho)}{4\pi^2}\frac{\partial^2}{\partial\varrho^2}\left(\frac{\delta\gamma_0^{(Q)}(\varrho)}{\tilde{\mathcal{C}}^{(Q)}(Q,\varrho)\left(\tilde{\mathcal{C}}^{(Q)}(Q,\varrho) - \tilde{\phi}(Q,\varrho)\right)}\right).$$

For the HRT-PDE to be stable $\mathrm{d}\delta\gamma_0^{(Q)}(\varrho)$, the total change of $\delta\gamma_0^{(Q)}(\varrho)$ as the cut-off is lowered from Q to $Q+\mathrm{d}Q = Q-|\mathrm{d}Q|$ at constant density, must counteract the perturbation $\delta\gamma_0^{(Q)}(\varrho)$, *i. e.* $\mathrm{d}\delta\gamma_0^{(Q)}(\varrho)/\delta\gamma_0^{(Q)}(\varrho)$ must be negative; as $\mathrm{d}\delta\gamma_0^{(Q)}(\varrho) = (\partial\delta\gamma_0^{(Q)}(\varrho)/\partial Q)\,\mathrm{d}Q$, this is equivalent to positive $\partial\delta\gamma_0^{(Q)}(\varrho)/\delta\gamma_0^{(Q)}(\varrho)\,\partial Q$. Assuming that $\delta\gamma_0^{(Q)}$ is a sufficiently well-behaved[10] function of ϱ, for low enough density the second ϱ-derivative is dominated by the ideal-gas term $-1/\varrho$ in $\tilde{\mathcal{C}}^{(Q)}$: for $\varrho \to 0$ we may therefore neglect $\tilde{\phi}(Q,\varrho)$ in the denominator and move $\delta\gamma_0^{(Q)}$ out of the derivative; the remaining differentiation of the ideal-gas direct correlation function is trivial, and dropping manifestly positive factors we immediately find that $\tilde{\phi}(Q,\varrho)\,\tilde{u}_0(Q,\varrho) > 0$ is a necessary but not sufficient condition for stability, which is just another way of stating that the signs of $\tilde{\phi}(Q,\varrho)$ and of $\tilde{u}_0(Q,\varrho)$ should coincide, *cf.* [2] (p. 264). Note, however, that eq. (26) relies on the normalization (16) of u_0; combining this with the condition for stability just found, we conclude that the HRT-PDE with a closure of the type of eq. (15) is unconditionally unstable for repulsive potentials, *i. e.* for systems where the volume integral of the perturbational part of the potential, $\tilde{w}(0,\varrho)$, is positive, contrary to what is claimed in [21].

Concluding this short discussion of the problem's stability we should stress that our reasoning pertains to the PDE itself rather than to the related FD equation (FDE) obtained by discretization as discussed in chapter 4; consequently our conclusions are independent of the properties of the density grid used in the numerical work, and the only ϱ-scale relevant here is the separation ϱ from the ideal gas singularity at $\varrho = 0$. Also, $\tilde{w}(0) < 0$ is only a necessary but by no means sufficient condition for the PDE's stability.

[10] In particular, it should be continuous and non-singular for $\varrho \to 0$.

2.4.2. Motivation for using the LOGA/ORPA-like closure

As we have seen, the closure (15) suffers from various defects: in addition to the clearly unphysical traits (dependence of the Q-system on the full potential, existence of all moments of $c_2^{(Q)}$ for all Q-systems and all thermodynamic states, *v. s.*), its inability to treat repulsive potentials — a restriction not expected on the basis of the derivation of the HRT equations — seems particularly unattractive; still, it is this closure that has been used almost exclusively so far even though it has repeatedly been blamed for sub-optimal results obtained in HRT calculations [9, 11, 28]. There are, however, good reasons why application of eq. (15) is worthwhile even though any other closure popular in liquid state theory such as, *e. g.*, the hypernetted chain (HNC) approximation could concievably be used[11] in very much the same way in which LOGA/ORPA provides the conceptual basis for eq. (15). The most important reason seems to be that its use is computationally feasible while other approximations incur substantial difficulties: with eq. (15) the PDE is stable at least for many attractive potentials, the FDE allows generating some solution all the way to very small Q in remarkably many cases despite the PDE's stiffness for low temperatures (*q. v.* section B.1), and a convenient approximate treatment of the core condition without the need for costly and complicated Fourier transformations is available (*cf.* sections D.2 and D.3); indeed, the latter can hardly be expected in a more realistic *ansatz* for $\mathcal{C}^{(Q)}$.

In addition, the form of the zero-loop terms in eq. (11) makes it natural to choose a closure expressing the two-particle direct correlation function $c_2^{(Q)}(r)$ of the Q-system as the sum of the correct limiting term for $r \to \infty$, *i. e.* $\phi^{(Q)}(r)$, and a simple expression of shorter range; the transition to $\mathcal{C}^{(Q)}(r)$ then only involves exchanging the long-ranged summand $\phi^{(Q)}(r)$ by $\phi(r)$. In this context, however, it should be noted that eqs. (10) and (11) are direct consequences of the definition (4) of the Q-potential: if instead we define a cut-off procedure that does not introduce a discontinuity in $\tilde{w}^{(Q)}(0,\varrho)$ at $Q = 0$, the HRT-PDE might just as well be formulated in terms of the original quantities $A^{(Q)}$ and $c_2^{(Q)}$ even though the modified functions may still provide some technical advantages [13]. However, for cut-off procedures like that of the smooth cut-off formulation [13] of HRT or, *e. g.*, ones that replace the discontinuity of eq. (4) by a continuous function over a limited k-range (so that, other than in [13], $\partial\mathcal{A}^{(Q)}(\varrho)/\partial Q$ does not involve an integral over all of Fourier space), in the light of the findings reported in [13] we must expect the critical exponents to turn out non-universal and to depend on the details of the definition of the renormalized potential. On the other hand, we

[11] Formally, it is only necessary to include an additional degree of freedom in the *ansatz* for $c_2^{(Q)}(r,\varrho)$ corresponding to the $\gamma_0^{(Q)}(\varrho)$-term in eq. (15), provided $\tilde{\mathcal{C}}^{(Q)}(0,\varrho)$ invertibly depends on the corresponding parameter; as mixed closure theories typically involve some switching parameter [1], some of these might even be applied without further modifications. For practical applications, however, both stability and regularity properties would still have to be discussed.

should recover potential-independent critical exponents when defining, *e. g.*,

$$\tilde{w}^{(Q)}(k) = \begin{cases} \tilde{w}(k) : k > Q \\ \tilde{w}(Q) : k < Q \,, \end{cases}$$

even though they might differ from those listed in table 1; however, as this definition obviously cannot be used to implement the suppression of long-wavelength fluctuations typical of RG theory it will come as no surprise that reasoning analogous to that of sub-section 2.4.1 readily shows the PDE following from a LOGA/ ORPA-like closure on the two-particle level to be unstable except maybe for highly contrived potentials.

All in all, despite the closure's undisputable short-comings (*v. s.*) its adoption is almost dictated by the need to avoid explicit Fourier transformations and the requirement of stability of the PDE; consequently, the remainder of the work reported here will be based upon the formulation of HRT presented in sections 2.1 to 2.3, with eqs. (4) and (15) at its very core. Still, even within this framework there is ample freedom regarding the details of the equations to be solved numerically; this will be discussed in the superficial sketch of our software in chapter 4 and put to good use in chapter 5.

III. The physical systems considered and their pair potentials

Let us now shortly introduce the physical systems that we will apply the theory just outlined to and present some of the literature data that will be used in assessing the method's numerical qualities: in particular, we here define the SW and the HCY fluids, while other potentials of limited interest for the remainder of this work are only shortly touched upon. Note that the full set of parameters defining a given type of interaction is displayed here but suppressed in most of the remainder of this work (*cf.* sub-section F.1.1); also, the reference system unvaryingly identified with a pure hard-sphere fluid (*q. v.* section 4.7) has already been defined in section 2.1's eq. (2.1). Some seemingly awkward signs in the parametrizations were adopted for reasons of compatibility with the literature.

3.1. Square wells

Throughout our numerical work on HRT, the primary test case for the implementations to be presented in chapter 4 as well as appendices B and C was the density-independent SW fluid of range λ given by

$$\begin{aligned} v^{\mathrm{sw}[-\epsilon,\lambda,\sigma]}(r) &= v^{\mathrm{hs}[\sigma]}(r) + w^{\mathrm{sw}[-\epsilon,\lambda,\sigma]}(r)\,, \\ w^{\mathrm{sw}[-\epsilon,\lambda,\sigma]}(r) &= \begin{cases} -\epsilon: & r < \lambda\,\sigma \\ 0: & r > \lambda\,\sigma\,, \end{cases} \end{aligned} \tag{1}$$

the perturbational part of which has

$$\tilde{w}^{\mathrm{sw}[-\epsilon,\lambda,\sigma]}(k) = -4\pi\,\epsilon\,\frac{\sin\lambda\,\sigma\,k - \lambda\,\sigma\,k\,\cos\lambda\,\sigma\,k}{k^3}$$

as its Fourier transform.

As noted in chapter 1, after fixing the ϱ-independent hard-core diameter σ and the well depth ϵ as units of length and energy, respectively, we are left with the

potential range λ as the only free parameter; in this work we will study values of λ from slightly above unity up to 3.6. With just one parameter, *viz.* λ, to vary, SWs obviously make for a convenient test case of HRT and, indeed, of liquid state theories in general, and they can also be considered as among the simplest model systems exhibiting phase separation; consequently, a great many simulational and theoretical efforts have been directed at this system and studies of its phase behavior abound [14, 15, 42–52]. But square wells are also of interest in their own right, serving as — albeit somewhat crude — models of a wide variety of physical systems including, *e. g.*, ^{3}He, Ne, Ar, H_2, CO_2, CH_4, C_2H_6, *n*-pentane and *n*-butane [14, 16, 17] while current interest in this system derives mainly from the finding that square wells capture the essential features of the interactions found in colloidal systems [53–57]; also, the recent, very accurate simulation study [52] of the system with $\lambda = 1.5$ confirmed and quantified the presence of the Yang-Yang (YY) anomaly expected and experimentally found for asymmetric fluids [58, 59].

3.1.1. Non-HRT results on the critical point of square wells of variable range

For comparison purposes we compile in tables 1 and 2 the critical temperatures T_c and densities ϱ_c of various square well systems as obtained from simulations (table 1) or by purely theoretical means (table 2); the data given have been published within the last decade.

Of the simulation based results included in table 1, only those of [47] for $\lambda \in \{1.25, 1.375, 1.5, 1.75, 2\}$ were obtained by molecular dynamics (MD); most of the other simulation studies rely on one or the other variant of the Monte Carlo (MC) method: Among these, the Gibbs ensemble MC (GEMC) calculations of [42] set out to determine critical exponents, β in particular; that work's finding of $\beta \sim 1/2$ for $\lambda = 2$ as opposed to the expected $\beta \sim 1/3$ (*cf.* table 2.1) found for λ up to 1.75 prompted re-examination of the square well fluid with $\lambda = 2$ by GEMC augmented by finite-size scaling (FSS) techniques [43], refuting the mean field value for the effective exponent. — Especially in the critical regime, grand canonical MC (GCMC) simulations incorporating histogram re-weighting and FSS offer some advantage over GEMC due to the latter's restriction to fixed temperature; such an approach has been applied to square wells with $\lambda = 1.5$ and 3 in [44]; a more elaborate GCMC scheme not biased towards but confirming the Ising universality class and taking into account the YY anomaly has recently been applied to $\lambda = 1.5$ [52], *v. s.* Yet another method goes under the name of thermodynamic- or temperature-and-density-scaling MC (TDSMC); it was applied to the case of $\lambda = 1.5$ and analyzed in terms of an effective Hamiltonian in [45, 46]. — Also included in table 1 are the results of [48], employing an MC scheme modified to take advantage of a speed-up possible by combining simulation data with an analytical *ansatz* for the chemical potential; the efficiency of this approach originally devised to study phase separation allows a large number of systems to be considered. (The error

λ	$k_B\,T_c(\lambda)/\epsilon$	$\varrho_c\,\sigma^3$	method
1.05	0.3751(1)	0.496(26)	mod. MC [48]
1.1	0.4912(4)	0.458(9)	mod. MC [48]
1.15	0.5942(35)	0.434(1)	mod. MC [48]
1.2	0.692(1)	0.415(3)	mod. MC [48]
1.25	0.764(4)	9.370(23)	GEMC [42]
	0.78	—	MD [47]
	0.7880(6)	0.392(1)	mod. MC [48]
1.3	0.8857(7)	0.370(1)	mod. MC [48]
1.375	0.974(10)	0.355(45)	GEMC [42]
	1.01	—	MD [47]
1.4	1.076(8)	0.329(1)	mod. MC [48]
1.5	1.2179(3)	0.3067(4)	GCMC [52]
	1.2180(2)	0.310(1)	GCMC [44]
	1.219(8)	0.299(23)	GEMC [42]
	1.222	—	TDSMC [45, 46]
	1.226	—	TDSMC [45, 46]
	1.246(5)	0.329(6)	TDSMC [45, 46]
	1.27	—	MD [47]
	1.302(8)	0.322(5)	mod. MC [48]
1.65	1.645(5)	0.282(3)	mod. MC [48]
1.75	1.79	—	MD [47]
	1.811(13)	0.284(9)	GEMC [42]
1.8	2.062(8)	0.249(3)	mod. MC [48]
2	2.61	—	MD [47]
	2.648(14)	0.249(8)	GEMC+FSS [43]
	2.666(85)	0.238(81)	GEMC+FSS [43]
	2.678(27)	0.244(8)	GEMC+FSS [43]
	2.6821(8)	—	GEMC+FSS [43]
	2.684(51)	0.235(82)	GEMC+FSS [43]
	2.721(89)	0.228(85)	GEMC+FSS [43]
	2.730(14)	0.235(8)	GEMC+FSS [43]
	2.764(23)	0.225(18)	GEMC [42]
	2.778(7)	0.241(1)	mod. MC [48]
2.2	3.80(1)	0.258(1)	mod. MC [48]
2.4	5.08(2)	0.267(1)	mod. MC [48]
3	9.87(1)	0.257(1)	GCMC [44]

Table 1: The critical temperature T_c and critical density ϱ_c of square well systems for various values of λ as predicted by simulations and simulation-based theoretical analyses, and the corresponding references. The acronyms used for labeling the method employed in obtaining these results are given in sub-section 3.1.1 of the text, *q. v.* appendix F.

bounds given for these "modified MC" results in table 1 have been obtained from the numbers displayed in [48] for different parameter settings.)

λ	$k_B\,T_c(\lambda)/\epsilon$	$\varrho_c\,\sigma^3$	method
1.125	0.587	0.71	APT2 [50]
1.25	0.751	0.253	HSVDW [49]
	0.850	0.48	APT2 [50]
1.375	0.978	0.253	HSVDW [49]
	1.08	0.36	APT2 [50]
1.5	1.249	0.253	HSVDW [49]
	1.33	0.29	APT2 [50]
1.625	1.61	0.26	APT2 [50]
1.75	1.859	0.253	HSVDW [49]
	1.93	0.24	APT2 [50]
1.85	2.23	0.23	APT2 [50]
2	2.506	0.253	HSVDW [49]
	2.79	0.23	APT2 [50]

Table 2: The critical temperature T_c and critical density ϱ_c of square well systems for various values of λ as predicted by purely theoretical means, and the corresponding references. The acronyms used for labeling the method employed in obtaining these results are given in subsection 3.1.1 of the text, *q. v.* appendix F.

The theoretical predictions for the critical temperature listed in table 2 comprise a second-order analytic perturbation theory (APT2, [50]) applicable to $1 < \lambda \leq 2$ and claimed accurate for $\lambda \geq 1.4$ as well as the hard-sphere van der Waals (HSVDW, [49]) equation of state (EOS). In addition, though not listed in table 2, we have utilized the non-square-well-specific Okumura-Yonezawa (OY) estimate for β_c of [60], *viz.*

$$\frac{k_B\,T_c}{\epsilon} = 0.203\,\frac{2\pi}{3}\,\lambda^3 - 0.273\,,$$

primarily as a starting point when looking for the critical temperature in our HRT calculations.

3.2. Hard-core Yukawa fluid

Another potential we considered is the density-independent HCY potential parametrized as

$$\begin{aligned} v^{\mathrm{hcy}[-\epsilon_0,-\epsilon,z,\sigma]}(r) &= v^{\mathrm{hs}[\sigma]}(r) + w^{\mathrm{hcy}[-\epsilon_0,-\epsilon,z,\sigma]}(r)\,, \\ w^{\mathrm{hcy}[-\epsilon_0,-\epsilon,z,\sigma]}(r) &= \begin{cases} -\epsilon_0: & r < \sigma \\ -\epsilon\,\dfrac{\sigma}{r}\,e^{-z\,(r-\sigma)}: & r > \sigma\,, \end{cases} \end{aligned} \tag{2}$$

where the parameter $-\epsilon_0$, the value of $w(r)$ inside the core, defaults to the contact value $-\epsilon = w^{\mathrm{hcy}}(\sigma+)$, a choice actually dictated by numerical stability requirements in practical calculations (*cf.* section 4.3). Such a dependence of HRT's results

$k_B\,T_c(\lambda)/\epsilon$	$\varrho_c\,\sigma^3$	method
1.193	0.326	MHNC [28]
1.199	0.312	GMSA [28]
1.21	0.28	MHNC [68]
1.212(2)	0.312(2)	MC [67]
1.214	0.312	HRT [28]
1.219	0.314	SCOZA [28]

Table 3: The critical temperature T_c and critical density ϱ_c of the HCY system with $z = 1.8/\sigma$ as predicted by simulation and purely theoretical means, and the corresponding references. The acronyms used for labeling the method employed in obtaining these results are given in section 3.2 of the text.

on the perturbational part of the potential inside the core may be unexpected at first, but bear in mind that even in the exact HRT hierarchy without any approximations and with arbitrary cut-off procedure the renormalized potential $w^{(Q)}(r)$ outside the core will depend on $w(r)$ inside the core, and with the cut-off method of eq. (2.4) any discontinuities of $w(r)$ will feature prominently[1] in the Fourier transforms; only in the limit $Q \to 0$ are the exact results guaranteed to only depend on $v(r)$ rather than on $w(r)$, but so low a Q is unattainable at least numerically if[2] $\epsilon_0 \neq \epsilon$.

In comparison to SWs, the HCY fluid will play only a minor *rôle* in the presentation in the later chapters of this work; the reason for this is the richer set of numerical difficulties displayed by SWs as opposed to the HCY system, where the same considerations (with the exception of those of section 5.6) apply as in SWs but are less of a reason for concern due to the usually much less pronounced defects of the solution obtained. As far as assessing HRT as a general theory of the liquid state is concerned, the HCY fluid is of interest mainly because it allows direct comparison [28] with the *Self-Consistent Ornstein-Zernike Approximation* (SCOZA, [61–63]) by Stell and Høye as application of that theory benefits greatly from an analytical solution to the mean spherical approximation in the case of an HCY system; other than that, a direct comparison of HRT and SCOZA has only been performed for the three-dimensional lattice gas model isomorphic to the Ising model [64, 65].

For comparison purposes, in table 3 we again compile some results on the critical point's location for the system with inverse screening length $z = 1.8/\sigma$; the data are taken from [28] and comprise that contribution's results as obtained from SCOZA, the generalized mean spherical approximation (GMSA), the modified hypernetted

[1] Take into account that, from section D.1 and the obvious continuity of the convolution integral of eq. (2.6) for finite Q, the renormalized potential $w^{(Q)}(r)$ is bound to sport exactly the same discontinuities as $w(r)$ itself except in the limit of $Q \to \infty$; put differently, the cut-off procedure (2.4) only affects the potential's continuous component. The same, by the way, is also true for the smooth cut-off formulation of [13].

[2] Of course, similar considerations apply to other potentials just as well. In the light of this discussion it might be worthwhile to consider the numerical properties of HRT when confronted with a different form of the HCY potential that even remains differentiable at $r = \sigma$.

chain (MHNC) approximation and HRT[3], as well as MC simulations with FSS [67] and a variant of MHNC relying on Verlet-Weis results for the bridge functions [68].

3.3. Other potentials

Two more types of potentials will briefly be mentioned below; the first of these, *viz.* the general multi-step potential $v^{\mathrm{st}'}(r)$, can be obtained as a superposition of a finite number of square well potentials with common hard-sphere diameter σ, *i. e.*

$$\begin{aligned} v^{\mathrm{st}'[(-\delta_1,\lambda_1),(-\delta_2,\lambda_2),\ldots;\sigma]}(r) &= v^{\mathrm{hs}[\sigma]}(r) + w^{\mathrm{st}'[(-\delta_1,\lambda_1),(-\delta_2,\lambda_2),\ldots;\sigma]}(r)\,, \\ w^{\mathrm{st}'[(-\delta_1,\lambda_1),(-\delta_2,\lambda_2),\ldots;\sigma]}(r) &= \sum_{i\in I} w^{\mathrm{sw}[-\delta_i,\lambda_i,\sigma]}(r)\,, \end{aligned} \tag{3}$$

with a suitable set I of indices; this obviously defines a piecewise constant function vanishing for $r > \max_{i\in I}\lambda_i$, with jumps of height $\delta_i = v^{\mathrm{st}'}(\lambda_i+) - v^{\mathrm{st}'}(\lambda_i-)$ at each of the λ_i. A more natural parametrization uses the sequence of constant values ϵ_i of the potential, *i. e.* $\epsilon_i = v^{\mathrm{st}}(\lambda_i-)$,

$$\begin{aligned} v^{\mathrm{st}[(\epsilon_1,\lambda_1),(\epsilon_2,\lambda_2),\ldots;\sigma]} &= v^{\mathrm{hs}[\sigma]}(r) + w^{\mathrm{st}[(\epsilon_1,\lambda_1),(\epsilon_2,\lambda_2),\ldots;\sigma]}\,, \\ w^{\mathrm{st}[(\epsilon_1,\lambda_1),(\epsilon_2,\lambda_2),\ldots;\sigma]} &= \begin{cases} \epsilon_1: & r < \lambda_1 \\ \epsilon_i: & \lambda_{i-1} < r < \lambda_i, \text{ where } \{i-1,i\}\subseteq I \\ 0: & r > \max\limits_{i\in I}\lambda_i\,; \end{cases} \end{aligned} \tag{4}$$

of course, the ϵ_i are related to the δ_i in a straightforward way.

Yet another potential that will be useful in sub-section 5.2.1 is what we call the "core" potential v^{core} obtained by restricting one of the more realistic types of interaction like those defined in this chapter to within the hard-sphere diameter σ: for arbitrary function $\psi(r)$, we define the corresponding core potential as

$$\begin{aligned} v^{\mathrm{core}[\psi(r),\sigma]}(r) &= v^{\mathrm{hs}[\sigma]}(r) + w^{\mathrm{core}[\psi(r),\sigma]}(r)\,, \\ w^{\mathrm{core}[\psi(r),\sigma]}(r) &= \psi(r)\,\Theta(\sigma - r)\,. \end{aligned} \tag{5}$$

As can easily be seen, $v^{\mathrm{core}} = v^{\mathrm{hs}}$; but applying the cut-off Q as in eq. (2.4) we obtain

$$\begin{aligned} \lim_{Q\to\infty} v^{\mathrm{core}(Q)} &= v^{\mathrm{hs}} \\ \lim_{Q\to 0} v^{\mathrm{core}(Q)} &= v^{\mathrm{hs}} \\ v^{\mathrm{core}(Q)} &\neq v^{\mathrm{hs}}, \qquad 0 < Q < \infty\,, \end{aligned} \tag{6}$$

which allows for simple reasoning the conclusions of which are of some relevance for very short ranged potentials (*cf.* sub-section 5.2.1).

[3] Using what is referred to as the "original implementation" in chapter 4; these calculations were carried out with a setting of $N_{\mathrm{cc}} = 5$ [66], but *q. v.* section 5.2.

IV. Implementation of HRT for simple one-component fluids

From the discussion of chapter 2 it should be clear that HRT holds high promise for the study of, among others, simple one-component fluids especially in the two-phase region where it renders Maxwell constructions obsolete, or in the critical region where the theory produces a true singularity characterized by non-classical critical exponents without loosing information on short length-scales as is often the case in RG theoretical methods. Still, adoption of this theory by the liquid physics community has been lagging, and while this reluctance to adopt so powerful a tool may partially be attributed to the theory's inherent difficulties and high computational cost, lack of an easy to use yet flexible, well-documented implementation of HRT may also have played a *rôle*. To fill this gap we have written software[1] suited as a general framework for the exploration and application of HRT to simple one-component fluids with hard sphere reference systems with various combinations of physical systems, approximations, and solution algorithms; together with appendix C the present chapter will provide a short overview of our implementation, its facilities and limitations.

4.1. General characteristics and comparison with earlier programs

Of course, the software to be presented here is not the first implementation of HRT for simple one-component fluids: indeed, there has been a series of earlier programs [6, 9, 13] by the authors of the theory and their collaborators, but it was the one used in [11, 28], henceforth referred to as the "original" implementation, that was a vital step in demonstrating the viability of HRT for continuous systems below the critical temperature; though never published or formally released, it has been circulating among interested physicists for quite some time, serving as a valuable resource for us, too, as it solves in its own way some of the problems inherent to

[1] Available on the world wide web from `http://purl.oclc.org/NET/ar-hrt-1/`.

the theory in the formulation chosen; also, we point out that the current version of our software which we will be concerned with in the remainder of this chapter evolved through various stages shortly presented in appendix B, each of which provided us with a host of new insights into the theoretical, numerical and practical aspects of applying HRT to the systems considered (*cf.* chapter 3). Still, there are good reasons for producing yet another implementation of the theory, and indeed does the one at hand differ from its precursors in many respects: adoption of a meta-language in our version, programming style, and documentation-to-code ratio may be most obvious, number and nature of hard-coded limitations (*e. g.* the number of basis functions in the closure), important details of the numerical procedure (*e. g.* the manner of discretization, a general preference for analytic expressions over interpolation on grids, and some basic control of error terms and convergence checks with clearly defined criteria to be met or explicitly overridden) and a possible speed gain through generation of customized code (*cf.* section C.1) might be less apparent. Most importantly, though, the original implementation's structure makes experimentation with different combinations of approximations, PDE solving algorithms, parameter settings and physical potentials rather cumbersome; in contrast, the fully modular approach adoption of a meta-language (*cf.* section C.1) allowed us to take seems far better suited to a more general survey of HRT's numerical side.

In addition to the necessary flexibility of our software, great care has been taken to ensure the numerical soundness of every step in the calculation and hence of the results produced; as a secondary goal we also strive for efficiency of the implementation but without sacrificing correctness, which entails an almost uniform distribution of the generation of numerical errors necessarily arising from finite-precision arithmetic and a FD approximation to the underlying PDE over all of the problem's domain. To this end we introduce one central parameter, $\epsilon_{\#}$, characteristic of the maximum relative error introduced at any step; together with a number of criteria relying on $\epsilon_{\#}$ this parameter governs virtually all of the numerics. Where the mathematical structure of the HRT-PDE or limited computer resources necessitate a deviation from the criteria usually employed to maintain the numerical quality indicated by $\epsilon_{\#}$ this is made explicit (*v. i.* sub-section 4.6.2), as are all the other approximations entering the calculation.

On a more technical note, in view of the well-known advantages of this programming language for numerical work that we did not want to forgo, we decided to strive for an implementation in fully standards-conforming [69] `Fortran-90`; the only non-standard feature we make use of is the availability of the special values `NaN` and $\pm$`Inf` for numerically undefined values and signed overflows, respectively, as defined in the IEEE floating-point standard [70]. These requirements should not pose a serious restriction for our software's prospective users: after all, `Fortran-90` compilers have been available for a wide range of platforms for several years, and the desired floating-point behavior can usually be requested — albeit at a small performance penalty — *via* compiler switches; also, the next revision of the `Fortran` language informally known as `Fortran-2000` (due in 2004) is set to include a formal specification on floating-point exception handling [71], which will

probably spur compliance with [70] on an even wider range of platforms. — But despite the chosen language's indisputable merits, experience with prior versions of our code (*cf.* appendix B) taught us that the kind of flexibility we need cannot be accommodated within the rather rigid framework `Fortran-90`'s modules with their one-way flow of information provide. Instead we opted for the simple meta-language `arfg`[2] for self-configuring construction of code customized to the chosen combination of approximations and the physical system at hand, at the same time enhancing readability and maintainability of the source and encouraging modularization; for a more detailed discussion of this approach, the numerous technical advantages it affords, and of the meta-language itself we refer the reader to section C.1.

4.2. The program's computational framework

As a direct consequence of the adoption of a meta-language our software is more appropriately described as a collection of mutually compatible building blocks rather than as a monolithic program so that the details of the numerical procedure are best left to these; however, for the combination of different selections of implementations of these parts to jointly define a valid numerical realization of the theory outlined in chapter 2 all of the code must adhere to a common view of the computation.

Most obviously, we have to make the transition from the PDE's domain, *viz.* the infinite strip $[0, \infty) \times [\varrho_{\min}, \varrho_{\max}]$, to a discrete mesh defined by a finite number of discrete points in a finite part $[Q_0, Q_\infty] \times [\varrho_{\min}, \varrho_{\max}]$ of the (Q, ϱ)-plane. Evidently, the placement of these "nodes", as we shall call them, is of utmost importance for the quality of the discretization so that it is only natural to define $\epsilon_\#$, the central parameter governing all of the numerics, in terms of the properties of this mesh: the coarser a mesh we choose, the larger $\epsilon_\#$ will be.

The locations of the nodes can, in principle, be chosen freely[3] and should be left to the corresponding parts of the program; we do, however, require the nodes' data structures to be organized in doubly linked lists roughly (*v. i.*) corresponding to Q-systems at different densities the properties of which are to be determined in parallel. As for the cut-offs Q of the nodes in such a list, we cannot assume them to coincide even though this is usually the case except for a low-density boundary at $\varrho = 0$, nor is there any reason to rule out a corresponding ϱ-dependence of Q_0 or Q_∞, the boundaries of the Q-interval considered numerically. On the other hand, as far as the densities of the nodes are concerned, implementation of the core condition *via* the truncated eqs. (2.18) and (D.11) makes anything but constant

[2] Available on the world wide web from `http://purl.oclc.org/NET/arfg/`.

[3] Consequently, when we discuss step sizes ΔQ and $\Delta\varrho$ of the FD scheme, both quantities, *viz.* the change $\Delta Q < 0$ in Q from one node to the next at the same density and the spacing $\Delta\varrho$ between adjacent densities are, in general, to be taken to depend on both Q and ϱ even though we do not explicitly show this dependence.

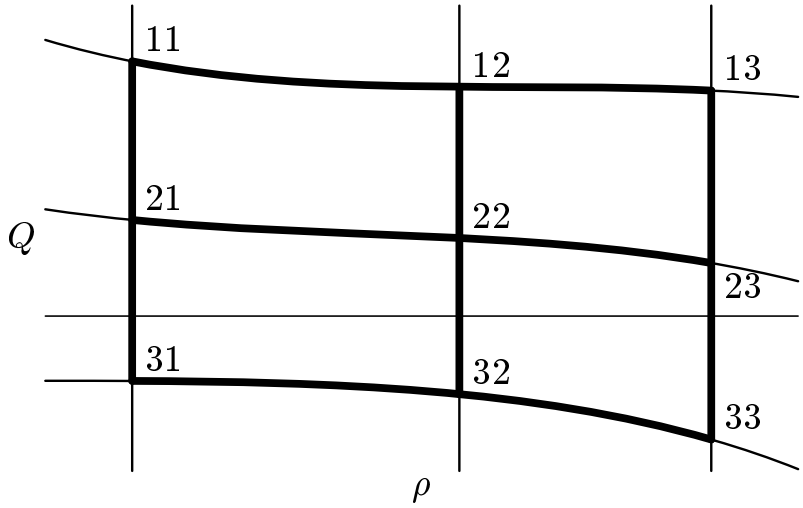

Figure 1: Schematic of the grid used in the discretization of the PDE (cf. section 4.5). Assuming use of the three-point approximation for the second derivatives in the ϱ-direction, the discretization is generated from an expansion around the intersection of the thin horizontal line with the line of constant density joining the nodes labeled ($i2$). — According to the general model of the computation discussed in section 4.2, a node list's Q-values may be ϱ-dependent, whereas the ϱ-values must coincide in all three node lists, though they need not be equispaced.

(though not necessarily equispaced) density values impractical; if the grid is to be refined for low Q, additional nodes must be inserted at the same densities in all the node lists in the calculation. After initialization of the nodes' data structures, solution of the PDE proceeds by applying a (possibly iterated) predictor-corrector scheme to generate an approximate solution for the nodes most advanced towards $Q = 0$ from the information available through the node lists at higher Q; in the interest of the code's simplicity, the number of node lists has been fixed to exactly three (*q. v.* fig. 1) which is sufficient for the determination of appropriate step sizes ΔQ by estimating selected quantities' curvatures in the Q domain. Note, however, that this choice, convenient as it is for the work we have undertaken, poses an upper limit on the order in ΔQ of the discretization and thus presents one of the hard-coded limitations of our program, *v. s.* section 4.7.

Other aspects characteristic of our software are the amount of modularity it provides and the *rôles* assigned to the program's modular constituents: indeed, most of the mutually compatible and freely exchangeable building blocks that are combined to implement a particular set of approximations to the theory outlined in chapter 2 directly correspond to the underlying physical and mathematical notions; the resulting natural organization of the code cleanly separating conceptually unrelated approximations is a direct consequence of our adoption of a meta-language and the use of automatic code generation techniques. Note, however, that it is possible only because there is no simple mapping from "main parts", as we shall call them henceforth, to `Fortran-90`'s rather inflexible modules from which they must be distinguished clearly: every main part may give rise to any number of modules and may incorporate all the information available within the code base.

In the following sections we take a closer look at some of the main parts, their physical meaning, the algorithms and approximations they implement, and at some

of the information they make available to the other parts *via* the facilities sketched in section C.1; we will, however, exclude from this discussion the program's infrastructure, *e. g.* the facilities for logging, for reading and parsing of options files, handling of node lists as well as the definition of a versatile, lossless and storage-efficient albeit platform dependent file format for the results at $Q = Q_0$. In a similar vein, we only mention the assortment of accompanying tools for reading these files and dumping their content in human-readable or `Mathematica`-usable form, for locating the critical point or calculating phase diagrams. Thus only main parts `potential`, `reference`, `ansatz` and `solver` — note that we use mono-spaced font for the main parts' names — remain to be discussed:

4.3. Main part `potential`: Properties of the interaction of the fluid's particles

First and foremost, we obviously have to provide the necessary information on the fluid's potential $v = v^{\text{ref}} + w$ and its properties: this is the purpose of main part `potential`. Just as the full potential is a sum of a reference part v^{ref} and a perturbational part w, the functions and parameters to be provided by this main part fall into two distinct categories, pertaining to either v^{ref} or w; in addition, as the temperature enters the calculation only as a pre-factor to w, *viz. via* $\phi = -\beta\, w$, the inverse temperature β is also defined here.

As far as the reference system is concerned, restriction to hard spheres (*cf.* chapter 2, *q. v.* section 4.7 below) means that only a function returning the hard sphere diameter $\sigma(\varrho)$ and a flag indicating any deviation of $\sigma(\varrho)$ from the unit of length need to be made available. — A similar parameter pertaining to the perturbational part w of the potential, *viz.* a flag indicating any density-dependence of w, also plays an important *rôle* in many parts of the program as substantial simplifications[4] and, in many cases[5], significant speed-ups by caching previous results are possible whenever $\tilde{\phi}(Q, \varrho)$ only depends on Q. In addition, at every cut-off Q the program must have access to the Fourier transforms $\tilde{w}(Q, \varrho)$ and $\tilde{\phi}(Q, \varrho)$ as well as the derivatives $\partial\tilde{\phi}(Q, \varrho)/\partial Q$ and $\partial^n \left(\tilde{\phi}(Q, \varrho)\right)^m / \partial\varrho^n$, whereas powers of the volume integral, $\tilde{\phi}(0, \varrho)^n$, and their derivatives $\partial^n \left(\tilde{\phi}(0, \varrho)\right)^m / \partial\varrho^n$ obviously do not depend on Q; here, m and n are appropriate integers known during code construction. — Even though not used by our program directly, it is customary to also implement the functions $w(r)$ and $\phi(r)$; not only do these functions allow

[4] Note that most of this simplification automatically follows from using a standardized interface for accessing the exported functions as explained in section C.1; in particular, the code has to explicitly take into account the potential's ϱ-independence only in rare circumstances, *e. g.* when installing caching or when switching to a more efficient algorithm altogether.

[5] This obviously depends on the pattern of accessing and initializing nodes, and on the computational cost of evaluating the relevant functions as opposed to mere lookup and test for equality; for a hint on the implementation of the simple one-shot cache *cf.* section C.1.

for simple tests of the internal consistency of the description of the potential, they also come in handy for additional evaluations, especially for Fourier transformations like those needed to get $g^{(Q)}(r,\varrho)$ from $\tilde{\mathcal{C}}^{(Q)}$ *via* the OZ relation (2.8), *cf.* section 5.2.

For the benefit of the PDE-solving algorithm, this main part also has to set a parameter $\lambda_{[v]}$ indicative of the potential's range and related to the maximum relative curvature of the second Q-derivative of $\tilde{\phi}(Q,\varrho)$, defined in such a way as to coincide with λ for the SW potential $v^{\mathrm{sw}[-\epsilon,\lambda,\sigma]}$ given in eq. (3.1): indeed, as discussed in chapter 3 it is this system that most of the work reported here has focused on; apart from SWs, the HCY potential $v^{\mathrm{hcy}[-\epsilon_0,-\epsilon,z,\sigma]}$ of eq. (3.2) and the multistep potentials of section 3.3 have been implemented, in the latter case automatically transforming $v^{\mathrm{st}[(-\epsilon,\lambda_1),(-\epsilon\,x_2,\lambda_2),\ldots;\sigma]}$ of eq. (3.4) into the computationally more convenient $v^{\mathrm{st}'[(\delta_1,\lambda_1),(\delta_2,\lambda_2),\ldots;\sigma]}$, *cf.* eq. (3.3). In all these cases we have implemented density-independent potentials only even though the remainder of the program is able to handle ϱ-dependent interactions just as well; also, in the calculations reported here the diameter σ of the hard-sphere reference part ($v^{\mathrm{ref}} = v^{\mathrm{hs}[\sigma]}$) and the strength ϵ of the attraction have invariably been chosen as units of length and energy, respectively.

As all of these potential types consist of an attractive tail attached to an infinitely repulsive core, the splitting of v into a reference part v^{ref} and a perturbational part w is uniquely determined outside the core; on the other hand, in the case of the HCY fluid any mismatch between ϵ_0 and ϵ dominates $\tilde{w}^{\mathrm{hcy}}(k,\varrho)$ for large k and is found to render unstable at least the numerics, and the same is also expected whenever some potential introduces a length-scale close to or even smaller than σ so that there is little room for variation of $w(r)$ inside the core, either. Also recall from sub-section 2.4.1 that an attractive potential (negative $\tilde{w}(0,\varrho)$) is a necessary though not sufficient condition for the stability of the PDE itself.

4.4. Main part `reference`: Hard-sphere reference system

Due to the specialization of v^{ref} to hard spheres, the reference system enters the expressions of chapter 2 only through the direct correlation function c_2^{ref}, implementation of which is the task set for main part **`reference`**. Not surprisingly, it turns out to be the simplest part of our program: it uses information only from main part **`potential`**, *viz.* the function $\sigma(\varrho)$ and the flag regarding the hard sphere diameter's *rôle* as unit of length, and apart from initialization code only functions for the evaluation of $\tilde{c}_2^{\mathrm{ref}}(Q,\varrho)$ and $\partial\tilde{c}_2^{\mathrm{ref}}(Q,\varrho)/\partial Q$ have to be exported.

In our program we have so far included two different versions implementing the Percus-Yevick (PY) approximation [72] and the Grundke-Henderson (GH) description[6] [73]; the latter is very similar to the widely used Verlet-Weis [74] parametriza-

[6] As [73] is more concerned with an approximation for the bridge function rather than the direct

tion of the hard sphere correlation functions in that it builds upon the PY results but is usually taken to present a superior approximation insofar as it implements consistency of both the virial EOS and the compressibility EOS with the well-known Carnahan-Starling result [75]. Note that all results reported here have been obtained using the GH-c^{ref}: in a theory relying on internal consistency conditions like eq. (2.13) as heavily as HRT, the thermodynamic inconsistency present in the PY solution seems particularly undesirable (*q. v.* section B.1).

4.5. Main part `ansatz`: Discretization, boundary conditions, and other approximations

Main part **`ansatz`** where all the approximations on the physical and mathematical level are combined to jointly define a reasonable numerical model of HRT is at the very core of the PDE-solving machinery: for the potential the perturbational and reference parts of which are described in the previous two sections, the HRT-PDE is discretized and solved according to a given set of approximations and on the mesh defined by the node-lists served by main part **`solver`** (*v. i.* section 4.6). More precisely, **`ansatz`** provides a set of facilities in the form of subroutines with standardized interfaces on the `m4`-level of **`arfg`** (*cf.* section C.1) implementing the various stages of the computation, *viz.* initialization of the node lists at $Q = Q_\infty$ and subsequent solution of the FDE in a predictor-corrector full approximation scheme. Note, however, that the code must accommodate the possibilities of both iterating the corrector step (which may allow attaining the numerical quality indicated by $\epsilon_\#$ with somewhat larger step sizes, thus speeding up the calculation) and of discarding part of the solution should $\epsilon_\#$-based criteria not be met; to aid **`solver`** in these decisions, care has to be taken to detect and signal numerical anomalies. Once a step's results have been accepted, **`ansatz`** may perform additional manipulations of the data structures: most importantly, for reasons of both simplicity of the code and efficiency of the discretization the re-scaling of all quantities affected by exponentiation of f necessary whenever f is large (*cf.* our discussion of the PDE's stiffness and the suppression of van der Waals loops in chapter 2) is adjusted only when the last corrector's result has been accepted.

Due to the eminent *rôle* the consistency condition (2.13) plays in constructing a closure to the underlying ODE (2.12), the PDE (2.23) for $f(Q, \varrho)$ is of first order in Q and of second order in ϱ; assuming the lowest possible number of nodes in the discretization (extension to higher order is straightforward) and a rectangular arrangement of the nodes we therefore need at least a 2×3 set of nodes.

correlation function we had to re-derive and to re-write the GH results in a form more suitable for the task at hand. In doing so we were led to a slightly different form of [73]'s expression (18) for the parameter m that might point to a mis-print of that equation; the results we used in our calculations can be obtained from those of [73] by changing the sign of the integral over the PY pair distribution function and by replacing the effective PY hard-sphere radius by its GH value on the left-hand side of the equation which then reads $12\,\eta\,C/m\,\sigma^2$.

According to the general model of the computation presented in section 4.2, however, we instead keep a third node list in order to allow monitoring of second Q-derivatives; this still allows us to reach a classical consistency order two in ΔQ even on a non-rectangular mesh while our discretization is of first order only in $\Delta\varrho$ due to asymmetry of the 3×3 grid schematically presenting in fig. 1 the most general constellation of nodes compatible with the general model of the computation given in section 4.2. Locally, the FDE is derived from an expansion about the midpoint of the nodes labeled (22) and (32) in the schematic 1, evaluating the second ϱ-derivative in eq. (2.23) along the line of constant Q through this point (thin horizontal line in fig. 1) by estimating the data at the intersection with the lines of constant density by interpolants defined from node triples $(i1)$ and $(i3)$, respectively; the resulting FD approximation is applied to every set of three adjacent node-triples, substituting suitable boundary conditions at $\varrho_{\min}$ and $\varrho_{\max}$.

As indicated in fig. 1, Q is not necessarily constant along a given node list, whereas the stability of the numerical scheme may impose certain geometrical constraints regarding the possible locations of the nodes, *e. g.* for ensuring that the Courant-Friedrichs-Lewy criterion [76] is met or for maintaining convexity of the remaining integration region; a suitable representation of these constraints is exported and must be taken into account by main part `solver`. If the latter decides to insert nodes at intermediate densities, the code for initializing the inserted data structures and for interpolating appropriate quantities is negotiated between the main parts, depending upon the order of the interpolation formulæ available. A further consequence of having non-constant Q is that some parts of the density range may reach $Q \approx Q_0$ earlier than others, which is regularly the case at least for the boundary condition at $\varrho_{\min} = 0$; in this case, the corresponding nodes are locked, preventing further modification, and all of the converged nodes except those necessary for providing a boundary condition for the remaining density interval (*q. v.* section 4.7) are removed from the node lists available to main part `ansatz`.

In addition to the discretization of the HRT-PDE (2.23) discussed so far, the implementation of the core condition along the lines of chapter 2 and sections D.2 and D.3 is also of interest. Relegating discussion of the choice of appropriate basis functions u_n, $1 \leq n \leq N_{\mathrm{cc}}$, to section C.2 we only point out the extremely slow convergence of the $\hat{\mathcal{I}}$-integrals (D.9) that have to be evaluated at $Q = Q_\infty$; furthermore, as the integrand is temperature dependent for $k > Q_\infty$, these integrals have to be evaluated for every isotherm — a problem that might be sidestepped by adopting the original implementation's strategy of consistently using the results for $Q \to \infty$ rather than those valid at Q_∞ for initialization even though such an approach introduces an artificial discontinuity at $Q = Q_\infty$. Also, with the usual choice of $Q_\infty \sim 10^2/\sigma$, integration merely up to $k = Q_\infty$ can hardly be deemed sufficient; an appropriate upper integration limit can instead be found by comparing the integrand's asymptotic behavior with $\epsilon_\#$.

For the benefit of the rest of the PDE solving machinery, main part `solver` (*v. i.* section 4.6) in particular, `ansatz` also has to identify quantities suitable both for monitoring convergence of the full approximation scheme and for choosing appropriate step sizes ΔQ and $\Delta\varrho$, to provide code fragments for the inspection

of nodes in various stages of the computation as well as to export a description of the boundary conditions at $\varrho_{\min}$ and $\varrho_{\max}$ including mandatory settings for either of these parameters if necessary; in particular, most implementations of `ansatz` require $\varrho_{\min} = 0$ in order to be able to use the result (A.2) brought about by the divergence of the ideal-gas term $-1/\varrho$ in $\tilde{c}_2^{\text{ref}}$ as a Q-independent boundary condition for f.

It is this main part where different approximations related to conceptually separated aspects of HRT like initial and boundary conditions, the manner of discretization, the implementation of the core condition, the formulation of the PDE or any additional approximations must be combined to jointly define a reasonable computational model of the PDE; note that a higher degree of modularization separating all of the aspects mentioned that we here decided to implement only together proves to be impractical and leads to the dreaded proliferation of largely incompatible modules known from a previous version of our program, the very experience that led us to adopt a meta-language in the first place (*cf.* section B.2). In the course of our investigations into HRT's numerical side we produced a multitude of versions (*q. v.* sections 2.4 and 5.4.1) only a selected few of which we will make use of in the remainder of this work: While mathematically inconsistent, both the re-implementation of the original program's approximations for the core and boundary conditions and the approach combining the PDE with $\alpha^{(Q)} = 0$ at all densities including $\varrho_{\max}$ retain thermodynamic consistency at least in some approximate way (*cf.* our discussion of the decoupling assumption in sub-section 2.2.2); we have also implemented the two possible approaches at least mathematically meaningful, *viz.* the thermodynamically inconsistent ODEs directly following from decoupling (*q. v.* section B.3) and the PDE resigning on the core condition for the benefit of the compressibility sum rule (2.13) with the LOGA/ORPA prescription $\gamma_0^{(Q)}(\varrho_{\max}) = 0$ as high density boundary condition.

4.6. Main part `solver`: Criteria for positioning of nodes

If main part `ansatz` is to provide a discretization on whatever mesh is handed to it, it is the task set for `solver`, the last of the main parts to be discussed in this chapter, to define this very mesh and to keep track of the numerical solution's quality. Based primarily upon the value of $\epsilon_\#$ but also taking into account other options as well as compile-time parameters (*cf.* section C.1) and respecting any restrictions exported by `ansatz`, step sizes ΔQ and $\Delta\varrho$ have to be chosen and checked for compatibility with the solution generated, iterating or discarding steps if certain criteria are not met; whenever `ansatz` signals an exception — usually an overflow in $\varepsilon(Q, \varrho)$ or numerically undefined $f(Q, \varrho)$ — the last step is discarded, accepting the data in the node list corresponding to labels $(2i)$ in fig. 1 as the best approximation to the solution for $Q \to 0$. At the same time, care has to be taken to locate and identify any problems in the solution, *i. e.* parts of the (Q, ϱ)-plane

where the solution found does not appear smooth on the scales set by the step sizes, the most basic assumption underlying any FD calculation; whenever this assumption no longer holds, the algorithm will react by locally reducing ΔQ and $\Delta\varrho$, inserting node triples (*cf.* section 4.5) in order to achieve the latter. — Once we find any nodes already holding the final results for their respective densities[7] they must be taken care of as discussed in section 4.5; integration of the PDE is ended when there is a node with $Q \leq Q_0$ for every density in the calculation, or when `ansatz` requests an end either because an error condition has occurred (*v. s.*) or because the current node list is sufficiently close to $Q = Q_0$ already. — As noted in section 4.2, the intimate link between this main part's task and the numerical quality of the solution generated makes it natural to here define $\epsilon_\#$, the central parameter governing the numerics, and it is this part of the program that relies upon $\epsilon_\#$ and the associated criteria the most; other main parts use $\epsilon_\#$ for little more than for switching between full analytic expressions and asymptotic expansions, a slightly atypical example of which is to be found in section C.2.

One last aspect of this main part common to both of the implementations discussed below regards the choice of Q_∞: As the only reasonable initial condition for the core condition assumes that the structure at Q_∞ is basically the same as that for $Q = \infty$ (so that $c_2^{(Q_\infty)} = c_2^{(\infty)} = c_2^{\mathrm{ref}}$ or, equivalently, $\gamma_n^{(Q_\infty)} = \gamma_n^{(\infty)} = 0$, $n \geq 0$) and the same set of parameters is used for the initialization of nodes at $Q = Q_\infty + |\Delta Q|$, the nodes labled $(1i)$ in fig. 1 in the first step, too, it is preferable to have $\partial\gamma_n^{(Q)}(\varrho)/\partial Q = 0$ at $Q = Q_\infty$; from eq. (2.18) one immediately concludes that this is equivalent to $\tilde{w}(Q_\infty) = 0$ whenever using the decoupling assumption. It is left to main part `ansatz` to decide whether Q_∞ should be determined in this way, thereby necessarily introducing ϱ-dependent Q_∞ when dealing with a ϱ-dependent potential; if so, provisions have been made to ensure that $Q_\infty(\varrho)$ is continuous.

4.6.1. Monitoring the solution

Of the two implementations of this main part, one has been written in the hopes of being able to avoid the problematic region of large $f(Q, \varrho)$ altogether, as is indeed possible for some similar PDEs (*q. v.* section 5.5). This implementation makes full use of $\epsilon_\#$, relying on numerous criteria to control the calculation; in the following discussion the notation $p_y^{[x]}$ refers to customization parameters that should usually be taken as real numbers of order unity. In most cases they are used as pre-factors to $\epsilon_\#$ so that increasing $p_y^{[x]}$ relaxes the constraint imposed by the corresponding criterion; the pivotal parameter $\epsilon_\#$ itself is defined *via*

$$N_\varrho = \frac{(\varrho_{\max} - \varrho_{\min})^2}{\epsilon_\# \, p_{N_\varrho}^{[\varrho]}} \,, \tag{1}$$

[7] Note that this will be the case already after the first step for the nodes at $\varrho_{\min}$ provided eq. (A.2) is used as the low-density boundary condition.

where $N_\varrho + 1$ is the number of density values spanning the range from $\varrho_{\min}$ to $\varrho_{\max}$ in the equispaced ϱ-grid we always decided to start with; the above relation reflects the importance of second ϱ-derivatives for the numerical quality of the solution of the PDE[8], the correlations of the truncation errors of the three-point FD estimator for these derivatives as well as the static nature of this set of densities due to the $\hat{\mathcal{I}}$-approach to the core-condition.

Once $\epsilon_\#$ has been fixed, the system is ready to start determining appropriate step sizes ΔQ; in particular the assumption that the potential $v(r, \varrho)$ introduces length scales only in the range from $\sigma(\varrho)$ to $\lambda_{[v]}(\varrho)\,\sigma(\varrho)$, where $\lambda_{[v]}$ is related to the second and fourth derivatives of $\tilde{v}(k, \varrho)$ with respect to k (*v. s.* section 4.3), places an upper bound on the admissible step sizes, *viz.*

$$\Delta Q \leq \frac{\sqrt{12\,\epsilon_\#\,p_{\Delta Q_{\max}}^{[\Delta Q]}}}{\lambda_{[v]}\,\sigma(\varrho)}\,.$$

On the other hand, for a FD scheme to be meaningful at least a certain number of bits must remain significant in evaluating the differences, which implies a lower bound on ΔQ proportional to Q, and the solution has to be smooth on the scales defined by the mesh, which also rules out abrupt changes in the step sizes; consequently, the ratio of two consecutive ΔQ steps at the same density is restricted to lie between $p_{\text{ratio}}^{[\Delta Q]}$ and $1/p_{\text{ratio}}^{[\Delta Q]}$. In a similar vein, considering smoothness in the ϱ-direction we have to postulate that $(Q_{(22)} + Q_{(32)})/2$ is greater than either of $Q_{(31)}$ and $Q_{(33)}$, where the labels coincide with those of the nodes of fig. 1; this condition, unlike the other rules mentioned so far, does not limit the step sizes ΔQ at any density ϱ but rather determines whether $\Delta\varrho$ should be reduced by the insertion of nodes at an additional density. But the most important criteria for choosing ΔQ come from monitoring the solution generated: for every monitored quantity x we make sure that

$$\sqrt{\frac{1}{\|x\|_Q}\left|\frac{\partial^2 x}{\partial Q^2}\right|}\,\Delta Q \leq \sqrt{\epsilon_\#\,p_x^{[\Delta Q]}}\,,$$

where

$$\|x\|_Q = \max_{k>Q} |x(k, \varrho)| \tag{2}$$

is the usual maximum-norm on the interval $]Q, \infty[$; the quantities taken for x are, of course, chosen by `ansatz` (*v. s.* section 4.5), and a usual selection is $x(Q, \varrho) \in \left\{ f(Q, \varrho), 1/\tilde{\mathcal{K}}^{(Q)}(Q, \varrho) \right\}$ so that aspects of the solution related to both thermodynamic and structural properties of the fluid are monitored. A different set of quantities y, also chosen by `ansatz` and usually comprising just $y(Q, \varrho) = f(Q, \varrho)$, is used to monitor the convergence of the predictor-corrector scheme and to determine whether or not the corrector should be iterated: denoting the absolute

[8] A conclusion based upon tests performed with the program of section B.1.

difference of consecutive approximations of y divided by $\|y\|_Q$ by Δy, iterations are performed until $\Delta y < \epsilon_\# \, p_y^{[\mathrm{conv}]}$, and the ratio of two consecutive step sizes is bounded from above by $\left(\epsilon_\# \, p_y^{[\Delta Q]}\right)^{1/\left(2+p_{N_{\mathrm{it}}}^{[\Delta Q]}\right)} / \sqrt{\Delta^{(1)} y}$, where $\Delta^{(1)} y$ is Δy evaluated after the first corrector step. According to simple heuristic arguments regarding the convergence of corrector iterations and ignoring the effect of other criteria, an average of $p_{N_{\mathrm{it}}}^{[\Delta Q]}$ calls of the corrector can be expected to solve the difference equations to within $\epsilon_\#$, and a setting of $p_{N_{\mathrm{it}}}^{[\Delta Q]} > 1$ may significantly speed up the calculation by allowing larger steps to be taken without loss of accuracy.

After finding and tentatively using a candidate ΔQ we still have to check that the assumptions leading to that particular choice for ΔQ actually hold; to this end we re-evaluate all the criteria with the obvious exception of the one involving $\Delta^{(1)} y$ after the predictor and discard the step unless a slightly smaller step size, *viz.* $\Delta Q \, p_{\mathrm{discard}}^{[\Delta Q]}$ $(0 < p_{\mathrm{discard}}^{[\Delta Q]} < 1)$, passes the tests. If no step size can be found satisfying all the constraints, the calculation is terminated.

4.6.2. Pre-determined step sizes

While the above set of prescriptions for finding suitable node locations has proved indispensible in understanding the behavior of the PDE's solution, the oscillatory nature of $f(Q, \varrho)$ invariably linked to the build-up of the isothermal compressibility's divergence for sub-critical temperatures (*cf.* sub-section 2.3.2) prevents its use for $\beta \gtrsim \beta_c$: considering even the modest value $f \sim 10^3$, $\sigma \, \Delta Q$ would have to be smaller than $e^{-10^3} \sim 10^{-430}$, which is obviously completely useless for any practical implementation. Thus, even though it means loosing control over the level of accuracy in the solution, we have also implemented a version of main part `solver` with predetermined step sizes that just happen to often be sufficient for reaching $Q = Q_0$ even well below the critical temperature while reproducing the overflow necessary for κ_T's divergence in a density interval the edges of which may then be identified with the coexisting phases' densities ϱ_v and ϱ_l. Recalling the behavior of f wherever it is large we obviously have to drastically reduce ΔQ as we approach Q_0; for this we use the very prescription introduced by the authors of [11] and evidently underlying all later published HRT calculations: at any density ϱ the Q-values are written in the form $\ln\left(1 + \exp\left(Q'_\infty - i \, \Delta Q\big|_\infty\right)\right)$ with successive integers i and a parameter Q'_∞ adjusted to yield the correct starting value $Q_\infty(\varrho)$. Apart from the determination of step sizes $\epsilon_\#$ is still very much in control of the numerical processing and plays an important *rôle* in the calculation.

4.7. Limitations inherent to our software

From the preceding superficial sketch of our implementation of HRT in conjunction

with the discussions of appendix C, section C.1 in particular, it should be clear that we have produced a rather general, flexible and extensible framework well suited to the systematic investigation of different approximations' effects in numerical calculations; also, the reader will not have failed to notice the natural separation of the code according to the underlying physical and mathematical notions that is mirrored in both the ease with which our code's capabilities can be extended by alternative implementations of the main parts and in the simplicity of the software's use (*cf.* section C.1).

On the other hand, there are a number of limitations present that prospective users should be aware of; due to the flexibility of our approach, however, some of them are related only to specific implementations of the main parts whereas others are inherent to the view of the computation underlying all our code.

The most poignant restriction on our software's range of applicability comes from the specialization to the case of a spherically symmetric pure two-body interaction with a hard-sphere reference part (*cf.* chapter 2): also taking into account rotational degrees of freedom would, of course, dramatically increase both the complexity of the program and the computing resources necessary, and while application of HRT to systems with three-body interactions has been demonstrated in [9] the necessity to include all many-body forces already in the reference part makes such an approach appear cumbersome and rather less attractive; identification of the reference fluid with pure hard spheres, a restriction not present in the original implementation of HRT, seems justified in the light of the substantial simplification it brings about. Of these extensions, only the elimination of rotational symmetry of the interaction mandates an alternative implementation of one of the main parts, *viz.* `ansatz`, only and could thus be incorporated into our implementation without much hassle; both of the other changes indicated, *viz.* three-particle potentials or non-hard-core reference system, require changes to main parts `reference` and `ansatz` and therefore cannot be accomodated within the framework laid out in the preceding sections without hampering the possibility of freely combining any of the main part versions into a reasonable computational model of some approximation to HRT as presented in chapter 2.

As noted already in section 4.2, fixing the number of node lists to exactly three certainly renders discretizations of high order in ΔQ based upon simple Taylor arguments impractical; still, not only are such an approach's merits not clear [77], it is also certainly possible to implement the handling of additional node lists without incurring too severe a performance penalty.

As far as the `solver` of sub-section 4.6.1 is concerned, we should point out that this version of the code is not ready to deal with more than one density interval where no solution has been obtained yet; still, such a situation might only arise through violation of the Courant-Friedrichs-Lewy criterion [76] and would almost certainly induce instability of the FDE, nor do we expect such a situation to arise due to the way the PDE's stiffness arises (*cf.* section 5.5).

The last class of limitations that we should mention is a number of hard-coded expansion orders: as noted, *e. g.*, in sections A.4 and C.2, in a number of circumstances evaluation of some quantities *via* the full analytical expressions is nu-

merically inappropriate except under certain conditions, and series expansions are typically applied when these are not met; with the notable exception of section C.2, while the criteria for switching between the methods of calculating an expression generally depend on $\epsilon_{\#}$, the expansion orders are typically hard-coded rather than dynamically adjusted to reflect the calculation's level of accuracy, which may cause floating-point problems for extremely small values of $\epsilon_{\#}$.

4.8. Default parameter settings

Unless otherwise noted, all of the calculations reported in this work have been performed on an equispaced density grid of $N_\varrho = 100$ density intervals spanning the range from $\varrho_{\min} = 0$ to $\varrho_{\max} = 1/\sigma^3$, corresponding to a value of $\epsilon_{\#} = 10^{-2}$; N_{cc} was usually set to 7; and the pre-determined step sizes started from $\Delta Q = -10^{-2}/\sigma$ at $Q_\infty = 80/\sigma$, plunging to a mere $-5 \cdot 10^{-6}/\sigma$ when approaching $Q_0 = 10^{-4}/\sigma$; the preferred `ansatz` inconsistently applies the decoupling assumption for $\varrho_{\min} < \varrho < \varrho_{\max}$ but consistently uses it as a boundary condition for the PDE at $\varrho_{\max}$. — When locating the binodal *via* the divergence of the isothermal compressibility $\kappa_T^{(Q_0)}$ we did not require an actual overflow to occur but instead looked for a $\kappa_T^{(Q_0)}$-ratio at neighbouring densities exceeding 10^4, which is a rather reliable indicator for the binodal's location as $\kappa_T^{(Q_0)}$ typically jumps by far less than two or by at least some twenty orders of magnitude within one $\Delta\varrho$; the reported values for ϱ_v and ϱ_l are the mid-points of the density intervals so found. In principle this allows us to locate the coexisting densities and the critical temperature and density to arbitrary precision, even though the computational cost rises sharply with falling $\epsilon_{\#}$.

V. Aspects of the numerical solution of the HRT equations for simple one-component fluids

In the preceding chapters we had to introduce a number of approximations some of which may seem rather less justified; their respective importance for and bearing on our program's predictions of structure and thermodynamics of simple liquids now remain to be assessed. As an exact solution with which to compare numerical results is lacking for non-trivial systems, for HRT in the formulation of chapter 2 as implemented by our software package (chapter 4) to be considered a reliable tool well applicable to realistic physical potentials it is necessary to demonstrate the limited effects variations in the numerical recipe have and to compare the results obtained with those available by other means for certain potentials. To this end in the sections to follow we will make use of the systems discussed at some length in chapter 3, *viz.* the HCY fluid with $z = 1.8/\sigma$ and SW systems of variable well width, varying the parameter λ from slightly above unity up to 3.6; as mentioned in section 3.2, the former of these is expected to be largely unproblematic numerically whereas the pronouncedly short-ranged SWs should bring out the difficulties inherent in HRT much more clearly.

Of course, it is to be understood that any of the deficiencies of the solutions numerically obtained or of the PDE solving process only relate to an implementation along the lines of chapters 2 and 4 and not to HRT proper; however, for reasons discussed in chapter 2 and section 4.7 alternative formulations almost certainly render the numerics far more demanding and open up a whole new suite of problems regarding the numerical implementation's soundness, especially when involving Fourier transforms of cut-off affected functions (*cf.* section D.1).

5.1. Insensitivity of the critical density

An important trait that is found for all the systems and parameter settings we considered is that the critical density ϱ_c is hardly affected by a variation of the numerical recipe and is, in fact, virtually always in good to excellent agreement with the data presented in chapter 3; consequently, in the considerations of the

sections to come ϱ_c will usually not be referred to explicitly. Insensitivity of ϱ_c is clearly illustrated by this chapter's tables 1 to 3 as well as figs. 2 and 3; furthermore, as is apparent from fig. 4, HRT is even able to reproduce the marked rise in ϱ_c predicted by [42, 48, 50] for $\lambda \to 1+$ as opposed to the rigorously constant value in [49] despite the theory's short-comings for very short-ranged potentials. The reasons for ϱ_c's insensitivity will at least partially become clear at the end of section 5.5 when we consider the effect of inappropriately large step sizes on the binodal's location.

5.2. Implementation of the core condition by coupled ODEs

Ever since application of HRT to continuous fluids started the implementation of the core condition has been a major issue; indeed, it is no coincidence that several studies [5, 8, 20, 33] primarily concerned with the RG aspect of the theory chose to completely eliminate it. When applying HRT as a regular liquid state theory, on the other hand, this is not an option: as we shall see in section 5.3, too great is the effect this may have on both correlation functions and phase behavior. As mentioned already in chapter 2, this is a likely motivation for the adoption of the closure (2.15) and variants thereof for non-hard-sphere reference systems [21] despite its known deficiencies [9, 11, 28] as it allows a computationally manageable approximate treatment of the core condition without the need to explicitly perform costly Fourier transformations (*q. v.* section D.1).

For the moment setting aside the question of thermodynamic consistency that will be considered in section 5.3 below, *i. e.* accepting any $\gamma_0^{(Q)}(\varrho)$ that decoupling or some other condition may yield (*cf.* sub-section 2.2.1), there are two important approximations that cannot be avoided in an approach based upon section D.2: truncation of the ODEs implementing the core condition to a finite number $N_{\mathrm{cc}} + 1$ of basis functions and expansion coefficients, and elimination of the non-local contribution to the slowly converging $\hat{\mathcal{I}}$-integrals' Q-dependence according to section D.3. With these we will concern ourselves in this section.

5.2.1. Inadequacy of the implementation for very short ranged potentials

For a first orientation and to demonstrate that the combination of these two approximations may, indeed, pose a problem let us shortly consider the rather artificial[1] system characterized by the potential $v^{\mathrm{core}}(r)$ defined in (3.5): as, say, the correlation functions of the exact solution of the HRT evolution equations in Q are

[1] Contrived as it may be, this type of potential could also be used for a rather stringent check on the approximations' internal consistency: as any potential $v^{\mathrm{core}}(r)$ and consequently $u_0(r)$

functionals of the total potential only, eq. (3.6) implies that $c_2^{(0)} = c_2^{(\infty)} = c_2^{\mathrm{ref}}$; taking into account the zero-loop term of eq. (2.11) and the initial condition (2.19) we easily find the expansion coefficients' limits

$$\lim_{Q\to\infty} \gamma_n^{(Q)}(\varrho) = 0\,, \qquad n \geq 0\,,$$

and

$$\lim_{Q\to 0} \sum \gamma_n^{(Q)}(\varrho)\, u_n(\varrho) = -\phi(r) = +\beta\, w(r)\,;$$

for a perturbational potential ϕ^{core} constant inside the core, *i. e.* for

$$w(r) = w^{\mathrm{core}[-\epsilon,\sigma]}(r) = \lim_{\lambda\to 1+} w^{\mathrm{sw}[-\epsilon,\lambda,\sigma]}(r) = \lim_{z\to\infty} w^{\mathrm{hcy}[-\epsilon,-\epsilon',z,\sigma]}(r)\,, \qquad (1)$$

and assuming $u_0 \propto w$ (*q. v.* section A.3) the latter relation readily reduces to[2]

$$\begin{aligned} &\lim_{Q\to 0} \gamma_0^{(Q)}(\varrho) = -\tilde{\phi}(0)\,, \\ &\lim_{Q\to 0} \gamma_n^{(Q)}(\varrho) = 0\,, \qquad n \geq 1\,. \end{aligned} \qquad (2)$$

For generic intermediate value of Q, on the other hand, none of the $\gamma_n^{(Q)}(\varrho)$, $n \geq 1$, may vanish as their evolution is driven by the projections of $w^{(Q)}(r)$ inside the core onto the basis functions $u_n(r)$, $n \geq 1$.

When testing eq. (2) numerically we cannot expect the $\gamma_n^{(Q)}$, $n \geq 1$, to vanish exactly for $Q = Q_0$, but at least their final values should be considerably smaller than their maxima in the course of the evolution from $Q = Q_\infty$ to Q_0; solving the ODEs following from the consistent imposition of the decoupling assumption (*cf.* section 4.5; $N_{\mathrm{cc}} = 5$, other parameters as in section 4.8) at some fixed density ϱ, however, clearly shows that these conditions are met not even remotely, producing a $\gamma_0^{(Q_0)}$ off by several orders of magnitude and expansion coefficients $\left|\gamma_n^{(Q_0)}\right|$, $n \geq 1$, not appreciably smaller than $\max_{Q\in[Q_0,Q_\infty]} \left|\gamma_n^{(Q)}\right|$ except for very high temperature. Note that the only approximations to the core condition that enter these calculations are truncation of eq. (2.18) to a finite value $N_{\mathrm{cc}} = 5$ of basis functions and that of neglecting the non-local contribution to eq. (D.11); such a failure to reproduce the correct behavior seems particularly troubling in view of eq. (2), and indeed do we see grave defects in the numerical solution for very short ranged SW fluids (*v. i.*).

---

have unique expansions in the basis provided by the $u_n(r)$, $n \geq 1$, with expansion coefficients v_n and u_{0n}, respectively, for any n in the range $1 \leq n \leq N_{\mathrm{cc}}$ the sum of coefficients $v_n + \gamma_0\, u_{0n} + \gamma_n^{(Q)}$ should be independent of the potential in the limit $Q \to 0$.

[2] Note that the first of the relations (2) holds despite the assumed proportionality of u_0 and w due to continuity of the limit $Q \to 0$; from a consideration of the functions for $Q = 0$ alone, on the other hand, only the limit of $\gamma_0\, u_0(0) + \gamma_1\, u_1(0)$ can be established.

There is, however, one more point that has to be addressed in this context, *viz.* the *rôle* of the decoupling assumption[3]: According to sub-section 2.2.1, the condition of vanishing $\alpha^{(Q)}(\varrho)$ in the calculations just outlined simply takes the place of thermodynamic consistency and thus should not directly affect the core condition; on the other hand, from eq. (D.10) and with the normalization of eq. (C.1) the sum $\sum_{n\geq 0}\gamma_n^{(Q)}(\varrho)$ should be independent of Q so that, strictly speaking, decoupling is incompatible with an evolution from $\gamma_n^{(Q_\infty)} = 0$, $n \geq 0$, to $\gamma_0^{(Q_0)} \neq 0$, $\gamma_n^{(Q_0)} = 0$, $n \geq 1$. Of course, from the arguments given in [6] for adopting the approximation of eq. (2.21) failure is to be expected for very short-ranged potentials (but *cf.* section 2.4); still, we think that the approximations of finite N_{cc} and of eq. (D.11) have no less a share than decoupling in causing gross violation of eq. (2), and a numerical calculation is not possible within the formulation of HRT outlined in chapter 2 except with these approximations and when eliminating either the core condition or the $\alpha^{(Q)}(\varrho)$ term in eq. (2.18): if we want to use HRT as a general tool for the study of phase transitions in simple fluids we have to gauge the severity of the restrictions brought about by this numerical necessity and to investigate their dependence on the potential's range (*v. i.*).

All in all, this sub-section's considerations at the very least demonstrate the need for further discussion of the importance of the approximations considered in this section.

5.2.2. N_{cc}-dependence of critical and phase behavior in the HCY fluid

As far as the need to replace eq. (2.18) by only a finite number of equations involving a finite number of terms each is concerned, it is important that N_{cc} should actually be rather small (as was the case in the preceding sub-section) if evaluation of the slowly-convergent $\hat{\mathcal{I}}^{(Q)}$-integrals at $Q = Q_\infty$ is not to dominate program execution time; on the other hand, for an implementation of the core condition as outlined in chapter 2 to be reasonable at all — especially as the `ansatz` consistently applying the compressibility sum-rule instead (*cf.* section 4.5) allows for much more rapid calculation of realistic phase diagrams without the need for mathematically inconsistent assumptions —, convergence of the procedure towards a solution of eq. (2.8) in the presence of a hard core, *i. e.* compliance with the core condition (2.14), must be considered and the dependence of the quality of the results on N_{cc} must be investigated.

As a first test regarding the number of basis functions to keep in the calculation let us have a look at the critical and phase behavior of the HCY system with

[3] Note that it is equally easy to solve the equations following from consistent application of the LOGA/ORPA-condition (2.22) instead of the decoupling assumption (2.21); however, as this entails a significant change in the structure of the matrices in eq. (2.18) according to sub-section 2.2.1 this, too, would provide us with only a rather tenuous link to typical numerical calculations. Still, we expect the results and conclusions to be very similar to those obtained in this section.

N_{cc}	$k_B\,T_c/\epsilon$	$\varrho_c\,\sigma^3$	$\varrho_v(\beta=0.9/\epsilon)\,\sigma^3$	$\varrho_l(\beta=0.9/\epsilon)\,\sigma^3$
—	1.20244(56)	0.325(30)	0.115(5)	0.565(5)
1	1.21847(58)	0.315(30)	0.105(5)	0.575(5)
2	1.21731(58)	0.315(10)	0.105(5)	0.565(5)
3	1.21615(58)	0.315(30)	0.105(5)	0.565(5)
4	1.21615(58)	0.315(30)	0.105(5)	0.565(5)
5	1.28740(32)	0.320(15)	0.075(5)	0.645(5)
6	1.32402(34)	0.325(30)	0.055(5)	0.685(5)
7	1.31653(34)	0.330(25)	0.065(5)	0.675(5)
8	1.29358(65)	0.320(35)	0.065(5)	0.645(5)
9	1.27300(63)	0.315(20)	0.075(5)	0.615(5)

Table 1: Dependence of the inverse critical temperature $\beta_c = 1/k_B\,T_c$, coexisting densities ϱ_v and ϱ_l at $\beta = 0.9/\epsilon$, and critical density ϱ_c of the HCY fluid with $z = 1.8/\sigma$ on the number of basis functions. The results reported have been obtained from PDEs retaining $N_{\mathrm{cc}}+1$ basis functions or (first line) not implementing the core condition at all; other parameters and main part versions were chosen as in section 4.8. We have checked that the differences summarized here cannot be explained by the N_{cc}-dependence of the upper integration limits in evaluating the $\hat{\mathcal{I}}^{(Q\,\infty)}$-integrals.

$z = 1.8/\sigma$ when varying N_{cc} in the range $N_{\mathrm{cc}} \in \{0,\ldots,9\}$ as summarized in table 1; note that the coexisting densities listed belong to the subcritical isotherm at $\beta = 0.9/\epsilon$, a temperature sufficiently far away from the critical one so that the differences in ϱ_v and ϱ_l are not merely to be attributed to the differences in β_c but not too low so that the distortion of the binodal in the boundaries' proximity (*cf.* section 5.4) is of no concern yet. — As can be seen from table 1, inclusion of the core condition is of vital importance in determining the fluid's phase behavior, and there is a considerable amount of variation in the results, the critical temperature in particular; the amount of variation seen, however, drops markedly once we eliminate the essentially constant[4] results for $1 \leq N_{\mathrm{cc}} \leq 4$, *i. e.* when we consider $N_{\mathrm{cc}} \geq 5$ only, which is a first indication for the minimum number of basis functions necessary for a suitable description of the hard cores' repulsion. Also, comparing the critical temperatures in table 1 with the literature data on the system at hand listed in table 3.3 we find that our implementation's predictions for $1 \leq N_{\mathrm{cc}} \leq 4$ fall precisely into the same range as those of that table and, for $N_{\mathrm{cc}} \in \{3,4\}$, are quite close to the MC simulation result of $T_c = 1.212(2)\epsilon/k_B$; however, as we will

[4] Note that the relative differences of the results in the parameter range $N_{\mathrm{cc}} \leq 4$ including those where the core condition is not implemented at all are compatible with the "typical accuracy" of one per-cent repeatedly claimed by the authors of the theory and their collaborators [2]. We should also point out that as of fall 1998 the original implementation was not equipped to perform any calculations with higher than fourth-order polynomials, corresponding to $N_{\mathrm{cc}} \leq 5$, and the recent calculations of [28] were performed with $N_{\mathrm{cc}} = 5$ [66]. — As for the immediate reason for the near-constancy of the results for low N_{cc}, the core condition can drive the evolution of the expansion coefficients $\gamma^{(Q)}(\varrho)$ only if the function space chosen is sufficient to accommodate a reasonable approximation to the true direct correlation function, which is the case at $N_{\mathrm{cc}} = 5$ for the first time at high densities (*v. i.*); the solution's behavior at low density, on the other hand, is dominated by the ideal gas term $-1/\varrho$ which explains why the largest change in HRT's results occurs at $N_{\mathrm{cc}} = 5$ rather than at $N_{\mathrm{cc}} = 7$.

see shortly, that very same $N_{\rm cc}$-range is characterized by gross violation of the core condition due to an insufficient number of basis functions retained in the truncated eq. (2.18). As we further increase $N_{\rm cc}$ so that the core condition is obeyed to a certain extent (*v. i.*), T_c rises dramatically to values far outside the range quoted in [28]; while the trend of decreasing T_c evident for $N_{\rm cc} \geq 7$ indicates that HRT might match the MC predictions for $N_{\rm cc} \sim 15$, we have not performed these CPU intensive calculations.

Similar but more detailed information may be gleaned directly from the final values of the expansion coefficients $\gamma_n^{(Q_0)}$: both for the expansion (2.15) to converge and for the truncation of $\mathcal{G}^{(Q)}$ to just a few terms to be admissible, the $\gamma_n^{(Q)}$ obviously have to be quite small for high enough n and indeed must tend to zero sufficiently fast for $n \to \infty$. Inspecting the $\gamma_n^{(Q_0)}$ as generated by our program with the basis functions of section C.2 and taking into account that $\max_{r\in[0,\sigma]} u_n(r) = u_n(\sigma) \propto n+2$, $n \geq 1$, not only the $\gamma_n^{(Q_0)}$ themselves but also the respective terms' contributions to the two-particle direct correlation functions markedly drop in magnitude and become rather small for $n > 5$ at high density and for $n > 7$ at low density, irrespective of the temperature used.

The real test for applicability of eq. (2.18) after truncation and of the *ad hoc* approximation (D.11) is, of course, the pair distribution function $g^{(Q_0)}(r)$ itself as obtained from the final values of the expansion coefficients $\gamma_n^{(Q_0)}$ *via* the Ornstein-Zernike equation (2.8). In order to separate these effects from other problematic aspects of HRT's numerical side we again turn to the ODEs consistently employing the decoupling assumption; the results obtained within this approach, explicitly performing the inverse Fourier transformation to get the pair correlation function $g^{(Q_0)}(r)$ from $\tilde{\mathcal{C}}^{(Q_0)}(k)$, largely confirm our earlier findings from the $\gamma_n^{(Q_0)}(\varrho)$: Inside the core, the $g^{(Q_0)}(r)$ so obtained generally takes on rather large values for small r while remaining within a few percent of the contact value $g^{(Q_0)}(\sigma+)$ for larger r up to $\sigma-$; upon increasing $N_{\rm cc}$ the magnitude of $g^{(Q_0)}(r)$ for r close to σ is hardly reduced in general but the r-range of rather small $g^{(Q_0)}(r)$ is instead extended to ever smaller r. Just as expected from the direct inspection of the final values $\gamma_n^{(Q_0)}(\varrho)$ (*v. s.*), at high density there is no substantial improvement in $g^{(Q_0)}(r,\varrho)$ within the core for $N_{\rm cc} > 5$, nor for $N_{\rm cc} > 7$ at low density; on the other hand, whenever $f(Q_0,\varrho)$ is large (corresponding to the critical region or the coexistence region in implementations relying on a PDE) the core condition is but poorly met. — As an aside we note that solving the PDE without implementing the core condition at all (first line in table 1) may, of course, result in arbitrarily large $g^{(Q_0)}(r)$ within the core: *e. g.* for $\beta = 0.7/\epsilon$ and $\varrho = 0.9/\sigma^3$, $g^{(Q_0)}(r) = -3.26$ inside the core while the contact value is $g^{(Q_0)}(\sigma+) = +1.91$.

All of these findings indicate that we needs must keep the core condition in the calculation due to its bearing on the phase behavior predicted[5], and that $N_{\rm cc}$ should probably be chosen no less than 7 (corresponding to a $6^{\rm th}$ order polynomial

[5] This is somewhat at variance with earlier findings [11] indicating only a modest influence of the core condition upon the results, a finding expressly referred to in [20].

	$\lambda = 1.5$		$\lambda = 2.0$		$\lambda = 3.0$	
$N_{\rm cc}$	$k_B\,T_c/\epsilon$	$\varrho_c\,\sigma^3$	$k_B\,T_c/\epsilon$	$\varrho_c\,\sigma^3$	$k_B\,T_c/\epsilon$	$\varrho_c\,\sigma^3$
0	1.209437(36)	0.315(15)	2.66095(13)	0.260(20)	9.89103(30)	0.260(10)
1	1.190663(35)	0.290(20)	2.68249(11)	0.255(15)	9.89994(48)	0.260(10)
2	1.203326(35)	0.295(15)	2.68629(11)	0.260(10)	9.90089(48)	0.260(10)
3	1.200152(35)	0.295(15)	2.68608(11)	0.260(10)	9.90089(48)	0.260(10)
4	1.197136(35)	0.295(15)	2.68566(11)	0.255(15)	9.90089(48)	0.260(10)
5	1.287443(40)	0.300(20)	2.52736(10)	0.250(10)	9.73708(46)	0.255(15)
6	1.098329(29)	0.280(09)	2.74240(11)	0.275(15)	9.82207(47)	0.260(10)
7	0.984757(47)	0.275(15)	2.91476(12)	0.290(20)	9.86750(48)	0.260(10)
8	1.070878(28)	0.285(15)	2.74483(11)	0.275(15)	9.77332(47)	0.255(15)
9	1.216333(36)	0.300(20)	2.74969(11)	0.275(15)	9.88751(48)	0.260(10)
10	1.207583(36)	0.300(10)	2.93759(13)	0.290(10)	9.74820(46)	0.255(15)

Table 2: Dependence of the critical temperature T_c and density ϱ_c of various square well systems on the number $N_{\rm cc}+1$ of basis functions retained in eqs. (2.15) and (D.8). For $N_{\rm cc} > 0$, the decoupling assumption was imposed as high density boundary condition, whereas the LOGA/ORPA-condition $\gamma_0^{(Q)}(\varrho_{\rm max}) = 0$ served the same purpose for $N_{\rm cc} = 0$; other parameters were chosen as indicated in section 4.8.

in r for $\mathcal{C}^{(Q)}(r)$ inside the core) even though systematic shortcomings in the pair distribution function $g^{(Q_0)}(r)$ itself cannot be avoided in an implementation relying on eqs. (2.18) and (D.11) even for higher $N_{\rm cc}$; on the other hand, $N_{\rm cc} = 5$ may still be sufficiently accurate for some applications while the near-constancy of the results for $N_{\rm cc} < 5$ listed in table 1 indicates that we cannot expect to obtain significantly better results with such a low number of basis functions than in an `ansatz` not taking into account the core condition at all, which runs much faster and at least does not rely on inconsistent assumptions (*cf.* sub-sections 2.2.1 and 4.5).

5.2.3. $N_{\rm cc}$-dependence of critical and phase behavior in the SW fluid

So far we have found that a minimum of $N_{\rm cc} + 1 = 7 + 1$ basis functions must be kept for the approximations of finite $N_{\rm cc}$ and of eq. (D.11) to yield satisfactory pair distribution functions of the fully interacting system despite residual defects. In order to assess the generality of this result we have repeated the analysis of sub-section 5.2.2 for SWS at selected values of λ; doing so provides us with a first hint on the potential range dependence of the effects found in the HCY fluid with $z = 1.8/\sigma$ before.

From table 2 where we compile the critical temperature and density for various square well potentials as functions of the number $N_{\rm cc} + 1$ of basis functions in the closure (2.15), just as in sub-section 5.2.2 we find virtually constant critical temperatures for $1 \leq N_{\rm cc} \leq 4$; on the other hand, the amount of variation seen

upon further increasing N_{cc} strongly depends on λ, which immediately carries over to the pair distribution function $g^{(Q_0)}(r,\varrho)$ and its compatibility with the core condition: For $\lambda = 3$, the longest ranged potential considered in table 2, $g^{(Q_0)}(r,\varrho) = 0$, $r < \sigma$, holds reasonably well except very close to $r = 0$ even for $N_{\mathrm{cc}} = 1$; when increasing the number of basis functions all the way to $N_{\mathrm{cc}} = 10$, the pair distribution function has to be corrected for very small r only, yielding a $|g^{(Q_0)}(r,\varrho)|$ that remains bounded by some 10^{-2} of the contact value $g^{(Q_0)}(\sigma+,\varrho)$ for all $r < \sigma$; the correspondingly only small change in $g^{(Q_0)}(r,\varrho)$ and $\mathcal{C}^{(Q_0)}(r,\varrho)$ is reflected in the near-constant predictions for β_c evident from table 2. Similarly, for $\lambda \in \{1.5, 2\}$ and within the N_{cc}-range considered, the implementation of the core condition does not convincingly improve except for supercritical temperatures and intermediate densities; this time, however, the pair distribution functions remain far from compatible with the core condition even for $N_{\mathrm{cc}} = 10$, and neither β_c nor $g^{(Q_0)}(r,\varrho)$ itself nor, for that matter, the final values of the LOGA/ORPA expansion coefficients $\gamma_n^{(Q_0)}(\varrho)$ indicate that the expansion (2.15) for $\tilde{\mathcal{C}}^{(Q)}(k,\varrho)$ might be close to convergence. But if the quality of $g^{(Q_0)}(r,\varrho)$ improves only little if at all, the remaining deficiencies are probably to be blamed on the approximation (D.11) for the poorly convergent integrals' derivative with respect to Q rather than on an insufficient number of basis functions.

As far as our results' compatibility with the literature data of tables 3.1 and 3.2 is concerned, for the λ values considered we find only marginal agreement with simulation and purely theoretical results: indeed, for $\lambda = 1.5$ not even one of the HRT values for the critical temperature falls into the range predicted by simulations, whereas the situation is clearly[6] better for higher λ. Also, it strikes as peculiar that in all three of the systems listed in table 2 it is the results for $N_{\mathrm{cc}} = 9$ that compare with literature results most favorably; on the other hand, as this does not correspond to what is found in the HCY system of sub-section 5.2.2 this seems a particularity of the SW system and has not been investigated any further.

But table 2 demonstrates not only the λ-dependence of the results' sensitivity to the number $N_{\mathrm{cc}} + 1$ of basis functions retained in the truncated eq. (D.8) when varying N_{cc} in the range $0 \leq N_{\mathrm{cc}} \leq 10$: on the one hand, the critical temperature and density predicted for $\lambda = 3$ seem trustworthy on account of the small differences apparent from table 2, the pair distribution function's compliance with the OZ relation (2.8), and its fair agreement with simulation results (*v. s.*); on the other hand, for $\lambda = 1.5$ and, to a much lesser degree, for $\lambda = 2$ the amount of variation in T_c precludes accurate determination of the critical temperature. This is a first indication of the range of potentials that the theory is able to handle: square wells with $\lambda = 3$ can be dealt with quite reliably whereas problems cannot be denied for $\lambda = 2$, and $\lambda = 1.5$ seems largely out of reach for HRT in the present formulation; this also corresponds to what we will find in section 5.6 below.

[6] Unfortunately, we have only one data point with which to compare our results for $\lambda = 3$; on the other hand, the rather small amount of variation seen here (especially when considering relative differences, which are at around one per-cent for $N_{\mathrm{cc}} > 5$ as compared to 7 and 24 per-cent for $\lambda = 2$ and 1.5, respectively) inspires some confidence in the values obtained.

5.3. Decoupling assumption and lack of thermodynamic consistency

As we have seen in sub-section 5.2.3, a likely reason for our implementation's failure to comply with the core condition for SWs with $\lambda \in \{1.5, 2\}$ is not so much the low number of basis functions but rather the approximation (D.11) for the slowly converging $\hat{\mathcal{I}}$-integral's Q-dependence; on the other hand, as stressed by the authors of [6] upon jointly introducing these two assumptions, the decoupling assumption (2.21) is on the same level of approximation as that of neglecting the non-local term in $\partial\hat{\mathcal{I}}^{(Q)}\left[\psi(k,\varrho),\varrho\right]/\partial Q$. It thus seems pertinent to also consider the effect that additional approximation may have on the results, ever more so as retaining both the core condition (the importance of which we demonstrated in section 5.2) and the compressibility sum-rule (2.13) (which is vital for HRT's ability to provide clear phase boundaries, *v. i.*) is possible only when restricting use of eq. (2.21) to the evolution equations for the expansion coefficients, *i. e.* in order to get rid of the $\hat{\mathcal{I}}$-integral on the right hand side of eq. (2.18).

But if such a procedure is to be considered harmless, the results so obtained must not differ much from those following from consistent application of eq. (2.21) to the closure (2.15) along the lines of sub-sections 2.2.1 and 2.2.2. Turning to the HCY system of section 3.2, a potential sufficiently long-ranged so that the arguments for this assumption's validity given in [6] are applicable, we have performed these calculations and summarized them in fig. 1: as is apparent from the plot, the isothermal compressibilities are very different even for super-critical temperatures so that we cannot rule out a non-negligible effect on the structural and thermodynamic properties predicted; most importantly, the ODEs cannot reproduce well-defined phase boundaries, they clearly violate thermodynamic consistency, and they even yield slightly negative inverse compressibility $1/\kappa_T$ in what would otherwise be the coexistence region. On the other hand, preserving the structure of the PDE so that thermodynamic consistency is at least partly implemented by the PDE's coefficients d_{0i} of eq. (A.5) — which is the case for three of the implementations of main part `ansatz` discussed in section 4.5, only one of which is mathematically consistent at the expense of eliminating the core condition — seems sufficient to remedy these deficiencies; at any rate, we have to accept the decoupling assumption as indispensable for the implementation of the core condition.

As far as the SW fluid is concerned, similar calculations as those summarized in fig. 1 reveal that the decoupling approximation's effects are qualitatively unchanged; furthermore, as $v^{\mathrm{sw}}(r)$ vanishes identically beyond $r = \lambda\,\sigma$ the assumptions invoked in the arguments of [6] as motivation for neglecting $\alpha^{(Q)}(\varrho)$ in eq. (2.18), *viz.* the potential's range being much larger than the hard core diameter σ, appear even less justified, and combining the analysis of sub-section 5.2.3 with the calculations summarized in fig. 1 we conclude that decoupling poses certainly no less a problem for SWs than for the HCY potential considered before.

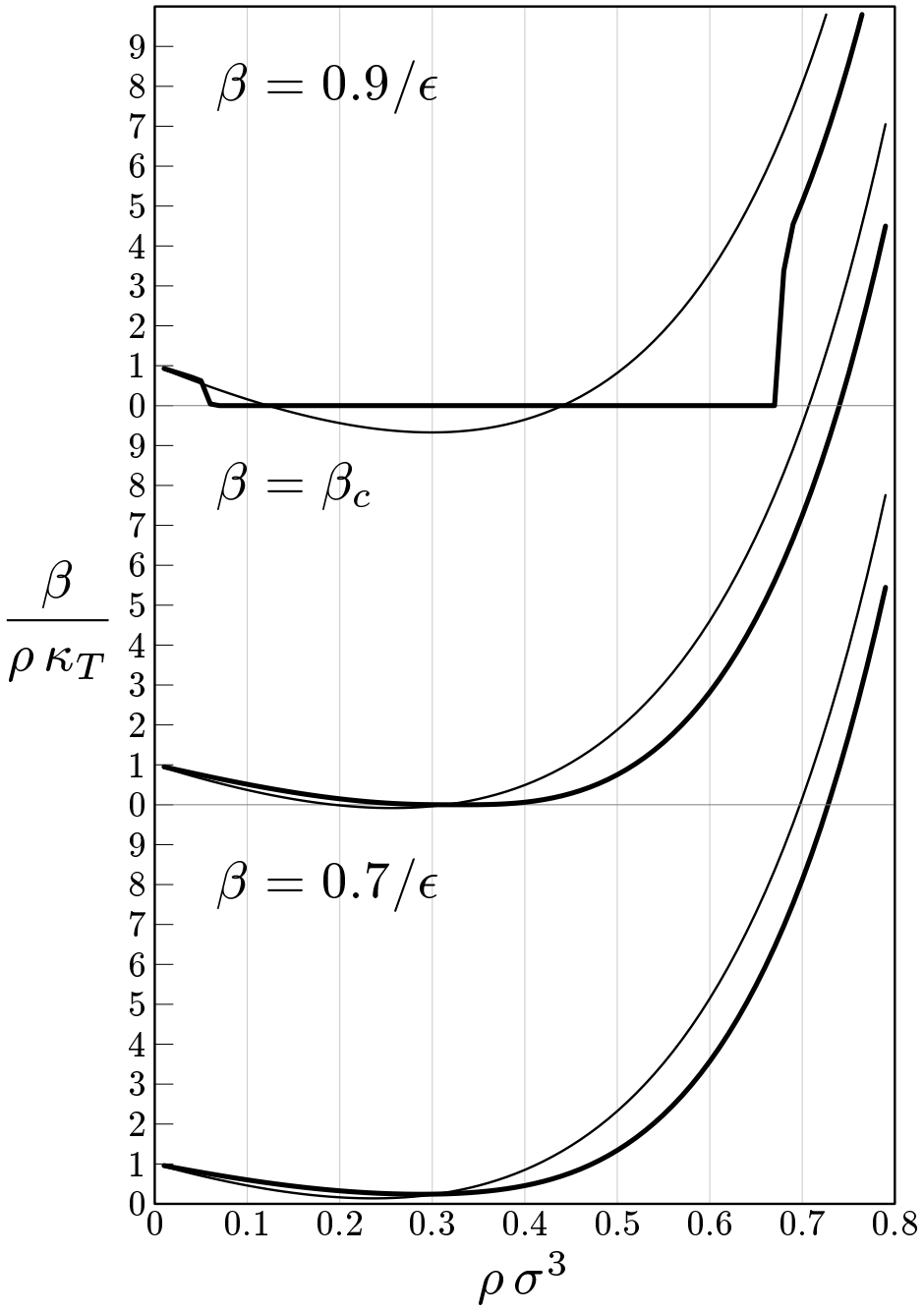

Figure 1: Comparison of the inverse compressibility of the HCY system with $z=1.8/\sigma$ as obtained from the ODEs following from the decoupling assumption $\alpha^{(Q)}(\varrho)=0$ (thin lines) and from a PDE inconsistently applying this approximation to the evolution of the core condition expansion coefficients $\gamma_n^{(Q)}$ only (thick line). The parameters of the calculation coincide with those of section 4.8, where the criterion for identifying the critical temperature $\beta_c=0.759497(24)/\epsilon$ is also documented.

5.4. Density grid and boundary conditions

As we have just seen, it is of utmost importance to retain the ϱ-derivatives char-

acteristic of a PDE in the equations or else we cannot hope to obtain clear phase boundaries; on the other hand, these differentiations have to be performed numerically as part of the FD scheme adopted, and the terms corresponding to the FD approximation to the operator $(\partial^2/\partial\varrho^2)$ have been found the primary limiting factor for the quality of the numerical solution (*cf.* sub-section 4.6.1). It is thus pertinent to shortly investigate the properties of the set of density values in the calculation, the number $N_\varrho + 1$ of densities (or, equivalently, the parameter $\epsilon_\#$ defined in eq. (4.1)), the width $\Delta\varrho$ of the density steps, and both location $\varrho_{\max}$ and nature (*cf.* section 4.5) of the high density boundary condition in particular; indeed, for any practical step size $\Delta\varrho$ the near-discontinuity of the solution close to the coexisting densities ϱ_v and ϱ_l at sub-critical temperatures and small Q is bound to render three-point formulæ inappropriate for estimating $\partial^2 f/\partial\varrho^2$; similar considerations also apply to the region of large $f(Q,\varrho)$ (*cf.* sub-section 2.3.2) and close to the boundaries (*v. i.* sub-section 5.4.1).

From fig. 1 we also readily find that ODEs substituting an approximate relation like, *e. g.*, eq. (2.21) for the compressibility sum rule (2.13) cannot reproduce the singularities characteristic of the coexistence region; on the other hand, at the boundaries of the PDE's domain the second-order ϱ-derivatives of eq. (2.13) cannot be evaluated accurately so that we have to rely on an approximate ODE of this kind at $\varrho_{\max}$ (setting $\varrho_{\min} = 0$ provides us with a convenient and numerically largely[7] unproblematic low density boundary condition, *cf.* section 4.5). But not only the solution obtained at $\varrho_{\max}$ is thus forced to lie outside the coexistence region: nearby densities are similarly bound to sport finite and, in fact, rather small $f(Q_0,\varrho)$ due to the continuity enforced by the PDE. If this is not to unduly influence the phase behavior found (*v. i.*), the coexisting densities ϱ_v and ϱ_l must maintain a separation of at least several density grid spacings $\Delta\varrho$ from the boundaries at $\varrho_{\min}$ and $\varrho_{\max}$; consequently, β should never exceed some maximum value, $\beta < \beta_{\max}$, and for the systems considered here and the typical choices for $\varrho_{\min}$ and $\varrho_{\max}$ the binodal's proximity to the low density boundary renders $\beta_{\max}$ largely density grid- and $\epsilon_\#$-independent. — Not to be confused with $\beta_{\max}$ is the lowest temperature $k_B/\beta_{\max,\#}$ numerically accessible to the program with pre-determined step sizes: this is the temperature below which the program of chapter 4 never reaches $Q \approx Q_0$ (*cf.* section 4.6) or produces abnormal results (*v. i.*); note that $\beta_{\max,\#}$ may be larger or smaller than $\beta_{\max}$, depending on the chosen combination of physical potential, approximations in the formulation used (the boundary conditions in particular), and the choice of parameters affecting the numerical work.

[7] Care has to be taken when evaluating some of the ϱ-derivatives of eq. (A.5) for $\varrho \to 0$; in particular, only inverse powers of direct correlation functions are amenable to numerical differentiation without incurring substantial truncation error.

5.4.1. The boundary condition's significance for the square well fluid

Not surprisingly, the problems of the numerical procedure related to the density grid chosen again show up much more clearly in SWs than in the comparatively long-ranged HCY system with $z = 1.8/\sigma$, so that we discuss the related effects in the context of SWs only, highlighting any differences found in the HCY fluid in sub-section 5.4.2 below.

Numerically, there are two ways for the implementation of chapter 4 to fail in progressing to $Q = Q_0$, both, of course, easily detected by the "monitoring" variant of our code as described in sub-section 4.6.1, *viz.* due to the solution's pathological behavior wherever $f(Q, \varrho)$ is large (*v. i.* section 5.5) or because of inappropriate boundary conditions at high density; as for the latter — an issue intimately linked to the decoupling assumption (*v. s.*) —, the immediate reason for the program's failure is a near-discontinuity in the numerical solution close to the boundary.

5.4.1.1. Mismatch at the high-density boundary

Both[8] to understand how such a solution betraying the most basic assumption underlying any FD scheme may arise and to put into perspective the different boundary conditions routinely used in the original implementation and in our software let us for the moment set aside the decoupling assumption or any other approximations; we also demand that the low density boundary be located at $\varrho_{\min} = 0$ so that the boundary condition there reads $f(Q_0, \varrho) = 0$ (*cf.* eq. (A.2)). Applying HRT with the closure (2.15) to some model potential $v(r)$, at any point (Q, ϱ) in the interior of the PDE's domain the core condition uniquely determines the $\gamma_n^{(Q)}(\varrho)$, $n \geq 1$, for given $\gamma_0^{(Q)}(\varrho)$; for $\varrho < \varrho_{\max}$ this expansion coefficient is then determined by imposing thermodynamic consistency[9] as embodied in the compressibility sum-rule (2.13). For $\varrho = \varrho_{\max}$, on the other hand, we are in principle free to use any suitable approximation for the structural and thermodynamic properties of the Q-system and to calculate $f(Q, \varrho_{\max})$ from said approximation *via* the defining relation (A.1) and eq. (2.12), thereby providing the necessary boundary condition for the PDE (2.23); for practical reasons, however, it is desirable to use the same LOGA/ORPA-form for the Q-system's direct correlation function at $\varrho_{\max}$ as in the rest of the problem's domain so that, in particular, the LOGA/ORPA prescription (2.22) is a natural choice of boundary condition. In general, however, due to the PDE's diffusion-like character any condition imposed at $\varrho_{\max}$ that is

[8] In addition to the effects of the boundary condition to be discussed in this sub-section and present at any Q, note that according to eq. (A.3) $\tilde{\phi}(Q, \varrho) = 0$ implies $\bar{\varepsilon}(Q, \varrho) = 0$; thus, from the explicit expression for the PDE's coefficient d_{02} given in eq. (A.5) both for $Q \to 0$ and at a root of the Fourier transform of the perturbational part of the potential the parabolic PDE degenerates into a hyperbolic one and is of mixed type for small $\bar{\varepsilon}(Q, \varrho)$ — a situation almost certainly characterized by non-differentiable solutions [77].

[9] This is the conceptual basis of the decoupling assumption (2.21).

incompatible with the solution for $\varrho < \varrho_{\max}$ by necessity induces a corresponding near-discontinuity in $f(Q, \varrho)$ close to the boundary; within the framework of an FD scheme this is reflected in a mismatch of $f(Q, \varrho_{\max})$ and the solution at densities close by, *i. e.* $f(Q, \varrho_{\max} - i\,\Delta\varrho)$ for small $i \geq 1$, and the mismatch's severity may serve as a natural measure for the inappropriateness of the boundary condition at $\varrho_{\max}$ in relation to the approximations applied at densities in $]\varrho_{\min}, \varrho_{\max}[$.

In a numerical realization of this scheme, however, at least the approximations discussed in section 5.2, *viz.* truncation of eq. (2.18) to a small number of basis functions and elimination of some integrals according to eq. (D.11), have to be adopted; but even for rather high λ (and for the HCY fluid just as well) the structural changes in the matrices of eq. (2.18) brought about by the condition of vanishing $\gamma_0^{(Q)}(\varrho_{\max})$ at the high density boundary give rise to a rapidly growing mismatch[10], and the calculation founders after only a few steps when Q is still close to Q_∞. In an attempt to remedy this situation without incurring the disadvantages adoption of the decoupling assumption in the interior of the PDE's domain brings about we also studied numerous variations of main part `ansatz` (and the analogous program parts of the implementation sketched in section B.2) imposing, *e. g.*, vanishing first- or second-order ϱ-derivatives of various components of the solution vector at $\varrho_{\max}$; none of these, however, succeeded in reducing the mismatch to the point of allowing us to advance the solution to cut-offs significantly lower than Q_∞, which once more illustrates the severity of the approximations discussed in section 5.2.

Unless we are ready to abandon the core condition altogether we thus have no choice but to adopt the decoupling assumption (2.21); but according to subsection 2.2.1 the condition of vanishing $\alpha^{(Q)}(\varrho)$, when applied consistently, decouples the HRT-PDE to a set of ODEs at fixed density only, which, unfortunately, removes all traces of thermodynamic consistency from the equations and thereby precludes obtaining clear phase boundaries (*v. s.* section 5.3). Together with the large amount of mismatch whenever $\alpha^{(Q)}(\varrho)$ is not taken to vanish identically in the interior of the PDE's domain (*v. s.*), this is the reason for restricting application of the decoupling assumption to the implementation of the core condition only while retaining the structure of a PDE so that the compressibility sum rule (2.13) is still partially implemented for $\varrho_{\min} < \varrho < \varrho_{\max}$ *via* the expressions (A.5) for the PDE's coefficients d_{0i} despite its incompatibility with decoupling; at $\varrho_{\max}$, however, again any approximation allowing calculation of $f(Q, \varrho_{\max})$ may be used so that it is tempting to once again resort to the LOGA/ORPA-condition of vanishing $\gamma_0^{(Q)}(\varrho_{\max})$ or variants thereof as in the original implementation.

But due to the decoupling assumption's possibly large effect (*v. s.* section 5.3), any boundary condition that does not incorporate $\alpha^{(Q)}(\varrho_{\max}) = 0$ — and bear in mind that $\gamma_0^{(Q)}(\varrho_{\max})$ and $\alpha^{(Q)}(\varrho_{\max})$ cannot both vanish at the same time for generic cut-off Q — will once again incur a fatally large mismatch; if, however, we must resort to decoupling anyway, it seems preferable to consistently apply it at

[10] Except, of course, for extremely high temperatures like $\beta\,\epsilon \sim 10^{-20}$ that will be excluded from further considerations.

$\varrho = \varrho_{\max}$, too, rather than to inconsistently combine it with a condition alien to the theory, especially as this has the added advantage of allowing matrices of the same structure to be used both within the PDE's domain and at the boundary: after all, a discontinuity in the terms of eq. (2.18) is likely to introduce an additional mismatch in the numerical solution. In the original implementation, it should be noted, uniform structure of the matrices is achieved in a manner involving an even greater number of inconsistent assumptions, *viz.* by invoking decoupling for all densities including $\varrho_{\max}$ for the core condition only while using the LOGA/ ORPA condition $\gamma_0^{(Q)}(\varrho_{\max}) = 0$ to determine $f(Q, \varrho_{\max})$; in addition, it retains the compressibility sum-rule (2.13) incompatible with any of these conditions in the interior of the PDE's domain. On the other hand, as our implementation of main part `ansatz` combining the core condition with decoupling as high-density boundary condition to the PDE (2.23) does not make use of eq. (2.22), only two conflicting assumptions enter calculations adhering to the choices of section 4.8..

In the numerical work we find that a mismatch of the kind just outlined is present whenever the calculation proceeds *via* mathematically inconsistent or conflicting approximations; as we shall see in section 5.6 below, in the case of square wells with their comparatively short potential range the associated problems are so severe as to render $\beta_{\max,\#}$ rather small and to make it drop even below β_c for most of the λ interval from 1 to 2 (*cf.* section 5.6). At intermediate to large Q, and not considering peculiarities brought about by the PDE's stiffness for $Q < 10/\sigma$ and low enough temperatures, the mismatch of some component of the solution vector[11] is an oscillating function of Q the amplitudes of which are largely constant or growing as Q decreases, depending both on the quantity considered and the potential used in the calculations; in particular, $f(Q, \varrho_{\max})$ is always found to oscillate out of phase with respect to f at densities close by, which immediately carries over to other components of the solution as well.

Considering the fully interacting system, *i. e.* $Q = Q_0$, and thus obviously restricting ourselves to $\beta < \beta_{\max,\#}$, the final mismatch is typically reflected in an increase by one order of magnitude in the three-point FD estimate of, *e. g.*,

[11] Specifically, for several quantities $x(Q, \varrho)$ (the approximation of which obtained in the numerical process we denote by $\mathtt{x}(Q, \varrho)$) and small non-negative integers o and s we defined ${}_{o,s}\delta^{(Q)}_{\#,x}$ as the relative difference of the solution obtained at the boundary and an o-th order extrapolation from results at adjacent densities, skipping the first s ones, *i. e.* by

$$
\begin{aligned}
{}_{o,s}\delta^{(Q)}_{\#,x} &= \frac{\mathtt{x}(Q, \varrho_{\max})}{{}_{o,s}x(Q, \varrho_{\max})} - 1\,, \\
{}_{o,s}x(Q, \varrho) &= \sum_{i=0}^{o} {}_{o,s}x_i(Q)\, \varrho^i\,, \\
{}_{o,s}x(Q, \varrho_{\max} - i\,\Delta\varrho) &= \mathtt{x}(Q, \varrho_{\max} - i\,\Delta\varrho), \qquad s \le i - 1 \le s + o\,;
\end{aligned}
$$

we analyzed ${}_{o,s}\delta^{(Q)}_{\#,x}$ for $o \in \{1, 2\}$, $s \in \{0, 1\}$, and identifying $x(Q, \varrho)$ with $f(Q, \varrho)$, $\tilde{\mathcal{K}}^{(Q)}(Q, \varrho)$ and $\ln \varepsilon(Q, \varrho)$ in turn for several settings of $\epsilon_\#$, different boundary conditions, and both sub- and super-critical temperatures.

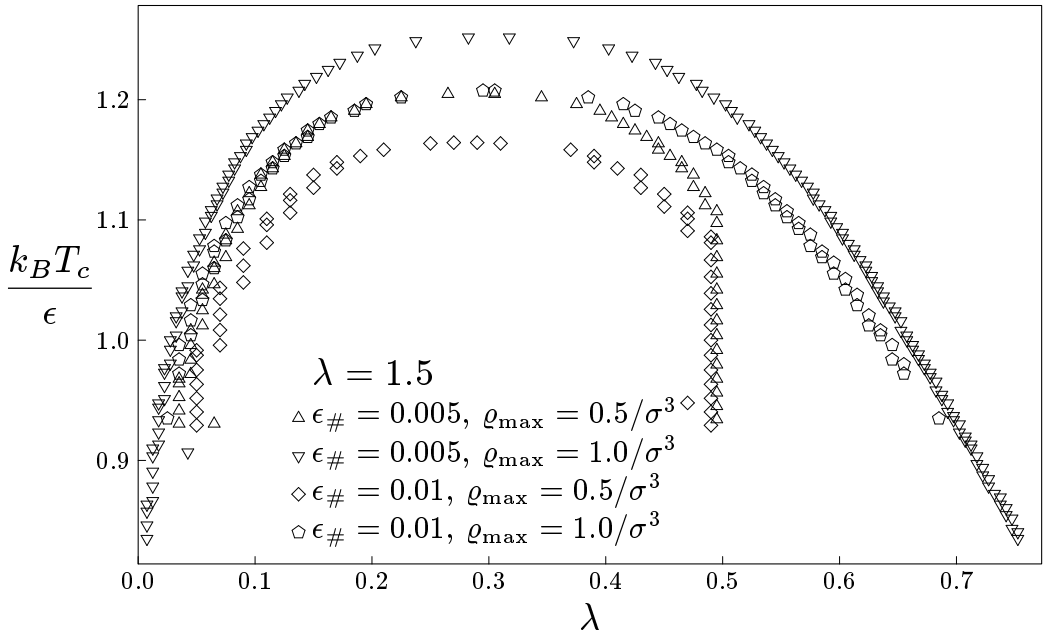

Figure 2: The binodal of the square well system with λ=1.5 as obtained for different values of $\epsilon_\#$ and $\varrho_{\max}$, *cf.* the discussion in sub-section 5.4.1. Most strikingly, there are large differences in the binodals (including the critical temperatures and, to a lesser degree, even the critical densities) under variation of these parameters. Note that, for clarity's sake, only a selection of the calculated isotherms is shown.

$|\partial^2 f(Q_0, \varrho)/\partial \varrho^2|$ right at the boundary over the near-constant values at slightly lower densities; apart from a positive correlation with $\epsilon_\#$, the mismatch's severity is qualitatively unaffected by a change in parameters of the numerical procedure or the choice and location of the boundary condition as long as sufficient separation of the boundaries and the binodal is maintained, while changing the model potential may significantly alter the picture (*v. i.* sub-section 5.4.2). At least part of the reason for the almost uniform amount of mismatch in $f(Q_0, \varrho)$ close to the high density boundary, furthermore corroborated by the finding of smaller mismatches upon decreasing $\epsilon_\#$, is the obvious precondition of the isotherm's calculation actually having reached $Q = Q_0$: indeed, if the mismatch ever gets too large, the numerical procedure will founder one way or another (*cf.* section 4.6) already at $Q \gg Q_0$. Note that an implementation insisting on some level of convergence of the FDEs will never accept even the small mismatch seen for square wells at Q only slightly less than Q_∞; on the other hand, when resigning on control of the numerical scheme's convergence (*cf.* sub-section 4.6.2), the PDE's stiffness is the limiting factor for $\beta_{\max,\#}$ as evidenced by the distribution of the last Q values in the calculation (*v. i.* section 5.5).

5.4.1.2. Location of the high-density boundary

Another effect worth mentioning in connection with the boundaries is the influence their locations, *viz.* $\varrho_{\min}$ and $\varrho_{\max}$, may have on the results, the binodal and the

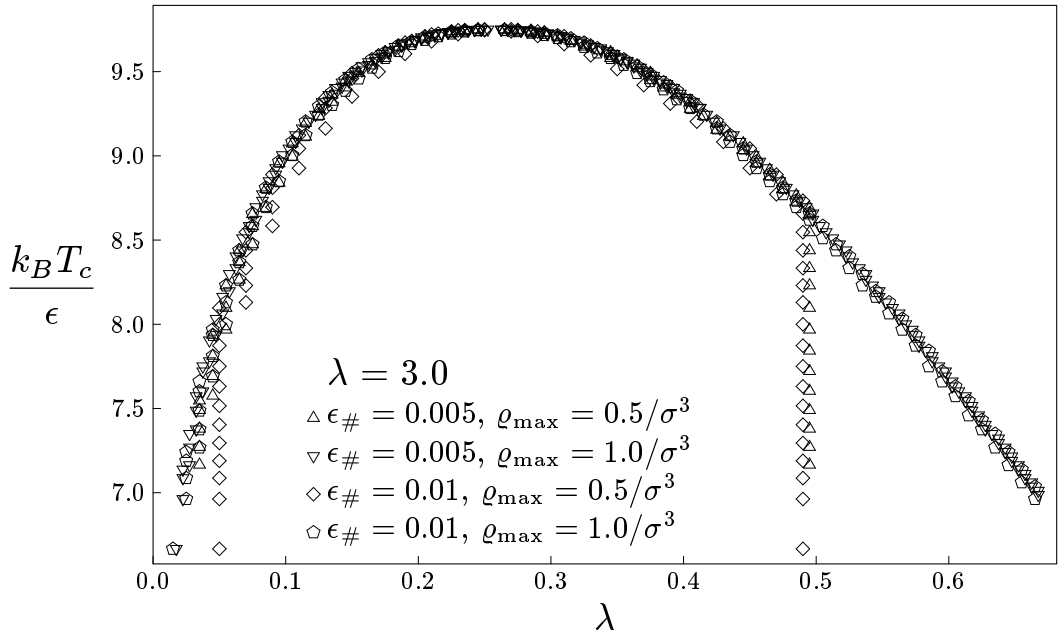

Figure 3: The binodal of the square well system with λ=3 as obtained for different values of $\epsilon_\#$ and $\varrho_{\max}$, *cf.* the discussion in sub-section 5.4.1. Note that for this rather long-ranged system (unlike fig. 2) the critical point's location is virtually unaffected by variation of these parameters. Also, imposing the boundary condition at $\varrho_{\max}=0.5/\sigma^3$ clearly induces a shift in ϱ_v to higher and, to a lesser degree, in ϱ_l to lower values even well above the temperature where ϱ_l gets close to $\varrho_{\max}$, which is readily interpreted as an effect brought about by stiffness (*cf.* section 5.5), and the shift in the binodal's vapor branch decreases somewhat as $\epsilon_\#$ is lowered from 0.01 to 0.005. Again, for clarity's sake, only a selection of the calculated isotherms is shown.

critical point predicted in particular: as mentioned earlier, the need of resorting to an ODE at the boundaries prevents nearby densities from entering the coexistence region, which may considerably distort the binodal; furthermore, very small $\varrho_{\max}$ may also allow one to reach $Q = Q_0$ at higher β, thus effectively raising $\beta_{\max,\#}$ while lowering $\beta_{\max}$. From the results for SWs with $\lambda = 1.5$ displayed in fig. 2 we immediately conclude that, indeed, the amount of distortion seen in the binodal may be considerable, and furthermore there is nothing in the theory or the numerical solution that helps us single out any one of the four curves displayed as most trustworthy. On the other hand, the much longer ranged potential used for fig. 3, *viz.* SWs with $\lambda = 3$, leads to binodals in fair agreement at least as regards the critical point's location, just as expected on the basis of table 2; imposition of the boundary condition at the rather low value of $\varrho_{\max} = 0.5/\sigma^3$, however, induces shifts in the coexisting densities ϱ_v and, to a lesser degree, ϱ_l towards smaller phase separation at temperatures only slightly below T_c, *i. e.* at temperatures where the binodal still keeps considerable distance from the boundaries. In this case, the results' apparent stability under variation of $\epsilon_\#$ for $\varrho_{\max} = 1/\sigma^3$ clearly inspires some confidence in those curves representing the "true" HRT binodal of the system at hand. — Taken together, the data of figs. 2 and 3 further corroborate sub-section 5.2.3's preliminary conclusions on the λ range accessible to HRT in the formulation of chapter 2; they also illustrate the importance of always combining several related calculations if reliable information is to be extracted from numerical

N_{cc}	boundary condition	$k_B\,T_c/\epsilon$	$\varrho_c\,\sigma^3$	$\beta = 0.9/\epsilon$ $\varrho_v\,\sigma^3$	$\varrho_l\,\sigma^3$
–	$\gamma_0^{(Q)}(\varrho_{\mathrm{max}}) = 0$	1.20254(13)	0.330(20)	0.115(5)	0.565(5)
7	$\gamma_0^{(Q)}(\varrho_{\mathrm{max}}) = 0$	1.31678(15)	0.325(15)	0.055(5)	0.675(5)
7	$\alpha^{(Q)}(\varrho_{\mathrm{max}}) = 0$	1.31678(15)	0.325(15)	0.055(5)	0.675(5)

Table 3: Critical temperature T_c and density ϱ_c as well as the coexisting densities ϱ_v and ϱ_l at $\beta = 0.9/\epsilon$, for a HCY potential with $z = 1.8/\sigma$ as predicted by various combinations of approximations and boundary conditions at $\varrho_{\mathrm{max}} = 1/\sigma^3$; again, the results reported have been obtained from PDEs retaining $N_{\mathrm{cc}} + 1$ basis functions or (first line) not implementing the core condition at all.

application of HRT.

We should also point out that sometimes the expectation of the binodal keeping a separation from the boundary of several $\Delta\varrho$ at least does not hold, and a preposterous two-phase region appears very close to ϱ_{max} or, very rarely, close to ϱ_{min}; *e. g.*, for $\lambda = 1.88$ and $\beta = 0.392/\epsilon$ the equations can be solved all the way down to $Q = Q_0 = 10^{-4}/\sigma$, predicting an unrealistic two-phase region extending from $0.845/\sigma^3$ to $0.995/\sigma^3$, and two examples can also be seen at rather low temperatures from the binodals obtained by setting $\varrho_{\mathrm{max}} = 0.5/\sigma^3$ for $\lambda = 1.5$ as displayed in fig. 2. It is again by varying parameters in the numerical procedure and by looking at isotherms at slightly different temperatures that such results can be rejected as unphysical without taking recourse to, *e. g.*, simulation results; the mechanism responsible for large $f(Q_0, \varrho)$ close to the boundary is, of course, easily clarified: combining the abnormally large second ϱ-derivatives following from a mismatch at the boundary with the PDE (2.23), the d_{02}-term in $\partial f(Q, \varrho)/\partial Q$ will also be large, and depending on the signs of the coefficients we may well be able to enter the region of large $f(Q, \varrho)$ at low enough Q so that the reasoning of sub-section 2.3.1 applies.

5.4.2. Hard-core Yukawa fluid

Let us now shortly outline the differences seen when going from SWs to the HCY fluid with $z = 1.8/\sigma$; not surprisingly, the numerical problems are much smaller here, and $\beta_{\mathrm{max},\#}$ exceeds β_{max} by far: for some parameter settings and with the `ansatz` not implementing the core condition the mismatch's severity is so small that even the monitoring variant of main part `solver` (*cf.* sub-section 4.6.1) can successfully be used in a large part of the PDE's domain. Similarly, limiting ourselves to $\epsilon_{\#} \leq 0.02$ and with the same `ansatz` we find that neither the critical point nor the binodal predicted appreciably depend upon N_ϱ, nor does $f(Q_0, \varrho)$ some $3\Delta\varrho$ outside the coexistence region; also, the results are largely independent of the location ϱ_{max} of the high-density boundary as well as of the boundary condition chosen there ($\gamma_0^{(Q)} = 0$ *vs.* $\alpha^{(Q)} = 0$) provided ϱ_{max} is well above ϱ_l, as evidenced by the data collected in table 3.

Just as expected from our lengthy discussion of the choice of boundary condition for SWs in sub-section 5.4.1, if we do not adopt the decoupling assumption of vanishing $\alpha^{(Q)}(\varrho)$ the mismatch at the boundaries is again so severe as to prevent the numerical calculation from going significantly below Q_∞; but inspection of the solution at high Q as generated when choosing the same high-density boundary condition as the original implementation, *viz.* the LOGA/ORPA relation $\gamma_0^{(Q)}(\varrho_{\max}) = 0$, as opposed to decoupling itself clearly shows the latter approach's preferability: inconvenient as the mismatch discussed in this section may be, it once more turns out a sensitive indicator of the assumptions' inconsistency.

5.5. Thermodynamic states of high compressibility: the region of large $f(Q, \varrho)$, stiffness, and pre-determined step sizes

As evidenced by the data presented in the preceding section and in keeping with section 5.1, HRT's estimates for the critical density present little to no difficulties for both of the model systems considered, nor is there any mention of such difficulties in any of the other publications on this topic that we are aware of; indeed, apart from the solution's defects close to the boundaries just discussed, the theory's numerical problems primarily lie in the solution's pathological small-Q behavior for close-to-critical and sub-critical temperatures that we will summarily refer to as the PDE's stiffness in the following; we now turn to the corresponding features of the solution numerically obtained, which will provide us with a signature of the problem readily detected by the monitoring variant of our code (*cf.* sub-section 4.6.1); we also note in passing that the effects of stiffness will be evident from section 5.6's application of HRT in its current formulation to SWs of quasi-continually varying range parameter λ.

From sub-section 2.3.2 it should be clear that the HRT-PDE's true solution eludes reliable numerical realization for high compressibility states, *i. e.* for sub-critical or close-to-critical temperatures and densities close to ϱ_c or the interval $[\varrho_v, \varrho_l]$; in particular, while $\epsilon_\#$ still characterizes the level of accuracy in auxiliary calculations, the same can no longer be true for the accuracy of the PDE's discretization as this would require step sizes ΔQ so small as to cause floating point underflow upon evaluating, *e. g.*, $Q - (Q - \Delta Q)$, thus rendering FDs numerically insignificant. In this respect we thus have to give up our strategy of controlling the numerical procedure so as to locally ensure a quality of $\epsilon_\#$ at least, turning to pre-determined step sizes ΔQ (*cf.* sub-section 4.6.2) in addition to fixed $\Delta\varrho$ (to which similar concerns apply, *cf.* sub-section 2.3.2) instead; on such a coarse mesh of (Q, ϱ)-points, however, the PDE's true solution cannot be represented adequately, and the numerical approximation for $f(Q, \varrho)$ obtained from the FDE the PDE is mapped onto cannot be trusted to faithfully represent even the average behavior of $f(Q, \varrho)$.

$\varrho\,\sigma^3$	$f\big\vert_{\Delta Q\vert_\infty = 0.002/\sigma}$	$r^{0.002}_{0.005}$	$r^{0.002}_{0.01}$	$r^{0.002}_{0.02}$	$r^{0.002}_{0.05}$
0.06	$1.046\,10^4$	7.092	1.083	2.185	5.317
0.15	$4.361\,10^4$	7.100	1.083	2.186	5.321
0.25	$6.311\,10^4$	7.102	1.083	2.186	5.322
0.34	$6.822\,10^4$	7.103	1.083	2.186	5.322
0.45	$5.870\,10^4$	7.103	1.083	2.186	5.321
0.61	$0.960\,10^4$	7.092	1.083	2.185	5.316

Table 4: The final values of the auxiliary function $f(Q,\varrho)$ for various densities in the coexistence region as obtained with different sets of step sizes ΔQ for the isotherm at $\beta = 1/\epsilon$ of the SW system with $\lambda = 1.5$ in an implementation of main part `ansatz` not implementing the core condition (other parameters as in section 4.8); here, the symbol r^a_b is used to denote the ratio $(f(Q_0,\varrho)\vert_{\Delta Q\vert_\infty = -a/\sigma})/(f(Q_0,\varrho)\vert_{\Delta Q\vert_\infty = -b/\sigma})$. With these settings, the coexisting densities are $\varrho_v = 0.05(1)/\sigma$ and $\varrho_l = 0.62(1)/\sigma$, and $f(Q_0,\varrho)$ takes on its maximum at $\varrho = 0.34/\sigma$. Most strikingly, the ratios displayed are close to constant except right next to the binodal; if the $f(Q,\varrho)$ numerically obtained were to represent an average over the true solution's oscillations these ratios should all be unity. Also note that $\partial^2 f(Q_0,\varrho)/\partial\varrho^2$ is rather small, just as expected from, and assumed at somewhat higher cut-off Q in, sub-section 2.3.1.

This inadequacy of the step sizes is reflected in various peculiarities of the solution obtained in the numerical procedure; indeed, when monitoring the evolution of $f(Q,\varrho)$ and the core condition coefficients $\gamma_n^{(Q)}(\varrho)$, our code readily detects the plummeting step sizes necessary and, when forced to use pre-determined step sizes, signals the incompatibility of the behavior seen with the assumption of smoothness underlying FD schemes. Another telltale sign is iterated corrector steps' failure to converge when $f(Q,\varrho)$ is large: even though implicit schemes like the one we employ are the standard treatment for stiff systems, the rapid growth of the oscillations' amplitudes (*cf.* our estimates in sub-section 2.3.2) renders the non-linear FDEs themselves unstable under iteration; only when resigning on any control of the numerical error and refraining[12] from iterations of the corrector step do the step sizes ΔQ chosen allow one to force advancing Q all the way to Q_0 in remarkably many cases.

Considering the FDE's solution in that part of the (Q,ϱ)-plane where the isothermal compressibility's divergence builds up, we always find smooth functions of Q and ϱ that are in gross violation of the behavior of the PDE's solution demonstrated in sub-section 2.3.2; one might therefore hope that the function obtained numerically presents an average over oscillations. It is, however, easy to see that this is not so, or else the solution obtained at any fixed value of the cut-off Q would have to be largely independent of the step sizes used in obtaining them; numerically, however, we find that, say, $f(Q_0,\varrho)$ not only sensitively depends on the step sizes inside the coexistence region, it does so in a very distinct pattern, too: With the version of main part `solver` discussed in sub-section 4.6.2, for any Q the step sizes ΔQ are fully determined by the Q_∞ and the step size for infinite cut-off, $\Delta Q\vert_\infty$;

[12] Or, for that matter, when fixing the number of iterations beforehand, without taking heed of questions of convergence; on the other hand, in this case the standard argument against iteration of the corrector step applies [78].

considering the final values of f as a function of $\Delta Q|_\infty$ and ϱ, while f typically varies by half an order of magnitude between the center and the boundaries ϱ_v and ϱ_l of the region of large f, it markedly depends on the initial step sizes $\Delta Q|_\infty$, and the ratios of the f values obtained with different $\Delta Q|_\infty$ are virtually independent of[13] ϱ. Such a behavior, illustrated for a particular isotherm of the SW fluid with $\lambda = 1.5$ in table 4, is readily explained in a two-tier model of the computation: as stiffness typically sets in only for $Q \lesssim 8/\sigma$, in any of the cases considered in the table the step sizes chosen are viable for most of the Q-interval $[Q_0, Q_\infty]$, *i. e.* for Q down to, say, some cut-off Q_1 that should not depend too sensitively on $\Delta Q|_\infty$ due to the oscillatory nature of f and the still rather large cut-off; however, as the solution is forced to proceed beyond Q_1 the FDE's solution can no longer serve as an appropriate approximation for the HRT-PDE, and the following evolution is driven by the number of steps[14] and the corresponding Q values, with the largely $\Delta Q|_\infty$-independent $f(Q_1, \varrho)$ as starting value. Note that this model is also able to explain a small ΔQ-dependence of the critical temperature like the one of the data of fig. 3 (not to be seen on the scale of the plot), whereas the tremendous differences in the critical point's locations in fig. 2 are due to other effects to be discussed in section 5.6 below.

So far we only discussed the relation of the FDE's solution to that of the underlying PDE in the region of large $f(Q, \varrho)$; on the other hand, due to the d_{01}- and d_{02}-terms in eq. (2.23), the PDE's stiffness and the related problems in that region have a direct bearing on the solution outside the coexistence region. Unfortunately, the influence of the fundamental discrepancy of the solutions of the PDE and the FDE, respectively, whereever $\kappa_T^{(Q)}(\varrho)$ is large on the data produced outside the coexistence region is not assessed easily; and even though the numerical predictions there turn out rather insensitive to variation of parameters of the numerical procedure we expect a gradual but non-negligible distortion[15] of the binodal, increasing with falling temperature. But if the solutions for $\varrho \notin [\varrho_v, \varrho_l]$ are hardly affected by the vastly differing numerical approximations for $f(Q_0, \varrho)$ within the coexistence region, this is indicative of effective boundary conditions arising at the coexisting densities due to the very large second-order ϱ-derivative in eq. (2.23) there; consequently, it should in principle be possible to avoid entering the region of large $f(Q, \varrho)$ altogether even though the PDE's characteristics are the lines of constant Q and such an approach must therefore be at variance

[13] Note that these calculations cannot directly be repeated for the ODEs obtained by imposing some constraint like, *e. g.*, the decoupling assumption or the LOGA/ORPA condition on the solution as discussed in sub-section 2.2.1: not only $\bar{\varepsilon}(Q_0, \varrho)$ becomes negative in what would otherwise be identified as the coexistence region as can be seen from fig. 1, even $\varepsilon(Q_0, \varrho)$ does so that $f(Q_0, \varrho)$ and, consequently, the free energy cannot be real for these states. This also precludes any use of this peculiar $\Delta Q|_\infty$-dependence, an otherwise quite sensitive indicator for the onset of stiffness, as a means of extracting information on the system's phase behavior from calculations *via* ODEs.

[14] Also, the numerical estimates for $\partial^2 f(Q, \varrho)/\partial Q^2$ in the region of large $f(Q, \varrho)$ are found to roughly correlate to $1/(\Delta Q|_\infty)^2$, which corresponds to an essentially exponential growth with the number of steps.

[15] In addition to the effects of numerical differentiation *via* three-point formulæ close to the solution's near-discontinuities at the coexisting densities.

with the Courant-Friedrichs-Lewy criterion (*cf.* sub-section 4.6.1). An immediate consequence of this effective-boundary-condition interpretation is that the two branches of the binodal are numerically decoupled, which is borne out by the preliminary[16] finding of differing pressures at the coexisting densities; of course, both branches of the binodal must meet, and the corresponding limits of the pressure along the branches must coincide, for $\beta \to \beta_c$; note that this irregularity of the pressures provides further evidence for a distortion of the HRT-binodal of the kind just indicated.

As a corollary we note that the effective phase decoupling scenario just developed also casts some doubt on HRT's ability to deal with systems exhibiting more than one liquid-vapor transition, *i. e.* where the region of large f consists of two or more lobes in the (Q, ϱ)-plane: For one, if we try to avoid the region of the PDE's stiffness, the corresponding loss of convexity of the remaining integration region almost certainly induces instability in the FDE. On the other hand, if we adopt a rectangular grid and force the solution to advance to smaller Q as in most of the applications of HRT presented in this study it seems likely that the same mechanism sets in that we find to give rise to the situation postulated in sub-section 2.3.1 in the first place: for the systems with only one critical point and intermediate Q we typically find several small patches of the PDE's domain where f is rather large (one of which will often be located close to the high density boundary due to the mismatch discussed in sub-section 5.4.1); as Q decreases there is a clear tendency for these patches to either die out or to shift, spread and join until for sub-critical temperatures we are left with exactly one density interval of high isothermal compressibility. In this context we should also mention that we were unable to apply even the `ansatz` not implementing the core condition to the multi-step potential v^{st} with parameters $\epsilon_1 = -\epsilon$, $0 < \epsilon_2 \leq \epsilon$, $\epsilon > 0$, $\lambda_1 = 1.25$, $\lambda_2 = 1.5$ [79].

Returning to the theme of the step sizes' inappropriateness, given the sheer numbers — according to section 4.8, for Q close to Q_0 we have $|\Delta Q| \sim 10^{-6}/\sigma$ whereas table 4's data and the estimates of sub-section 2.3.2 demand step sizes much smaller by some 10^3 to 10^4 orders of magnitude — it is certainly astonishing that we are able to reach rather small Q in so many calculations even though implicit FD schemes' stability properties are generally considered excellent; on the other hand, while the re-scaling of quantities affected by exponentiation of f certainly allows us to deal with the tremendous magnitudes that have to be considered in the calculation, according to section 4.5 the scaling factors are adjusted only after the last corrector step, and they are the same for all three node lists.

[16] These calculations were performed with version 2 of our software (*cf.* section B.2) for SWs with $\lambda = 1.5$ and $N_{\mathrm{cc}} = 5$, and the pressure was calculated by differentiation of the free energy; these results await confirmation and further investigation in other model systems with the more advanced possibilities the program of chapter 4 provides. Also note that the difficulties associated with the core condition (*v. s.* section 5.2) preclude accurate determination of the pressure from the virial route. Of course, in an implementation like the one discussed in section B.1 not relying on the re-writing of appendix A the pressure obtained by differentiating $\mathcal{A}^{(Q_0)}(\varrho)$ cannot differ, but then again that version does not allow one to force the solution to advance towards $Q = Q_0$ so that sub-critical temperatures are not accessible, $\beta_{\mathrm{max},\#} \lesssim \beta_c$.

While obviously justified for any appropriate step size ΔQ, for the pre-determined step sizes we employ this smoothness- and regularity-assumption is certainly not met and it will come as no surprise that overflows or numerically undefined values sometimes occur at $Q > Q_0$; as discussed in conjunction with main parts `ansatz` and `solver` (sections 4.5 and 4.6, respectively), the calculation is then terminated and the data at the last Q before the numerical exception occurred are taken as the final results for the isotherm at hand. If, indeed, stiffness is the limiting factor for the numerical procedure's ability to reach $Q = Q_0$, the lowest Q values in the calculation must be sufficiently small so that we are already in the region of large f, the maximum of $f(Q, \varrho)$ should be at intermediate densities rather than close to the boundaries, and we will generally see the program halt at higher cut-off for lower temperature; taken together these criteria allow us to distinguish between the mismatch discussed in sub-section 5.4.1 and the effects of stiffness as the immediate reason for the program's halt (*v. s.*).

In concluding this section we should point out that stiffness' effects are qualitatively very much the same for both SWs and for the HCY fluid considered earlier; quantitatively, however, the numerical problems associated with the PDE's stiffness are much more severe for narrow wells so that $\beta_{\max,\#} < \beta$ for many SW systems with $\lambda < 2$; these effects, however, cannot be discussed without reference to the *rôle* discontinuities of $w(r)$ play.

5.6. Discontinuities in the potential's perturbational part

For the case of HCY fluids with variable inverse potential range parameter z, the authors of [28] found a systematic degradation of HRT's performance comparable to that of GMSA with growing z, *i. e.* when going to ever narrower potentials; in particular, they studied $z\,\sigma \in \{1.8, 4, 7, 9\}$, and for all these systems except the longest ranged one, *viz.* the one with $z = 1.8/\sigma$ also considered in the present study, the critical temperature predicted by HRT was consistently found to be too high. It may therefore, and in view of some of the limitations of the theory expected for genuinely short-ranged potentials (*cf.* chapter 1, *q. v.* section 2.4), be interesting to also consider SWs of varying range parameter λ, which furthermore will serve to illuminate the decisive *rôle* played in the numerical process by discontinuities.

For a first orientation, let us look at the results summarized in fig. 4 (*q. v.* section E.1), where the critical temperature T_c and density ϱ_c are shown as functions of λ; the underlying calculations have been obtained with the parameters chosen as indicated in section 4.8. With the exception of some spurious results at $\lambda \sim 1.10$, wherever $\beta_c < \beta_{\max,\#}$ the critical temperature generally compares quite favorably with the data of tables 3.1 and 3.2; from the calculations we have performed for a large number of systems in the range $1 < \lambda \leq 3.6$ and ignoring some isolated results, a critical point is found for $1.06 \leq \lambda \leq 1.24$, for $1.45 \leq \lambda \leq 1.53$, and for

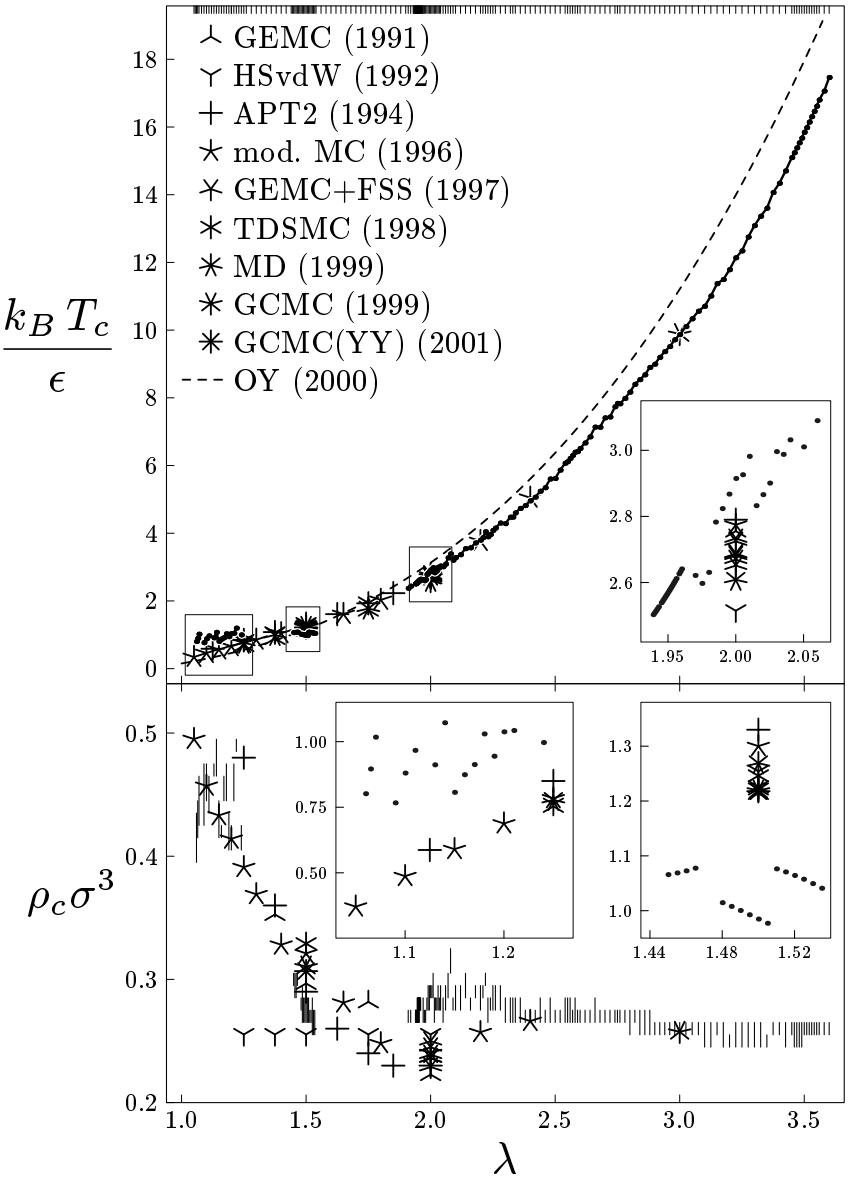

Figure 4: The critical temperature T_c (upper panel) and critical density ϱ_c (lower panel) of square well systems for λ ranging from close to unity up to 3.6 as obtained from calculations with the parameter settings of section 4.8; also included are the non-HRT predictions listed in tables 3.1 and 3.2, labeled by the acronyms introduced in sub-section 3.1.1 and already used in those tables. *q. v.* appendix F. The ticks on the top border of the figure's frame indicate the λ values considered; of the 200-odd systems we studied, $\beta_{\max,\#}$ exceeds β_c only in the λ ranges indicated in section 5.6 or for some isolated λ values outside those ranges. To facilitate comparison, both HRT and literature results on the critical temperature for λ close to 1.1, 1.5, and 2 are shown at larger scale in insets. In the lower panel, the bars show the coexisting densities found according to the prescriptions of section 4.8 for the highest-temperature sub-critical isotherm calculated in locating the critical temperature; this explains the apparent differences in ϱ_c's accuracy. The smallest ϱ_c intervals shown coincide with the spacing $\Delta\varrho{=}10^{-2}/\sigma^3$ of the density grid. The HRT-results used in this plot are given in section E.1.

$\lambda \geq 1.939$; calculations with $N_{\rm cc} = 5$ (summarized in section E.2) yield analogous results, with $\beta_c < \beta_{\max,\#}$ in a somewhat larger part of the parameter range, *viz.* for $1.09 \leq \lambda \leq 1.58$ and for $\lambda \geq 1.896$, but will not be considered in the following

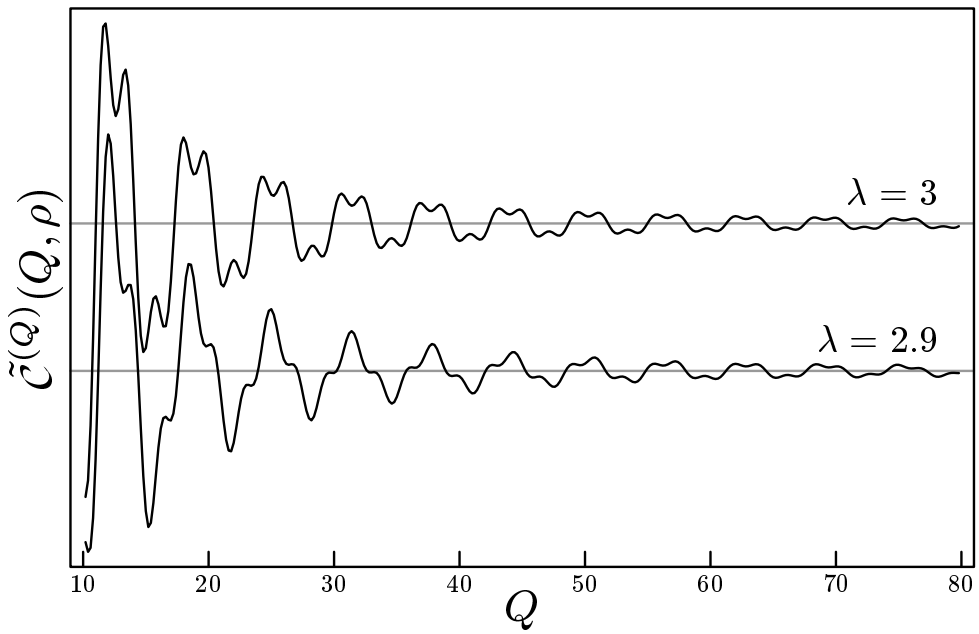

Figure 5: The core-condition function $\tilde{\mathcal{C}}^{(Q)}(Q,\varrho)$ for ϱ=0.3/σ^3, β=0.2/ϵ and for two different ranges λ of the square well potential, on arbitrary scales; the horizontal lines correspond to the ideal gas value $-1/\varrho$. Note that for λ=3 (upper curve) the peak of every single one of the function's swings is partially reduced, just as expected for a superposition of terms involving periodic functions of $Q\,\sigma$ and $3\,Q\sigma$, respectively; the same happens less than half the time — and at rather high Q only — for λ=2.9 (lower curve). We have excluded the data for $Q<10/\sigma$ so that the effects of the PDE's stiffness are still negligible; the underlying calculations have been performed by solving the ODEs corresponding to consistent application of the decoupling assumption at the density indicated.

in view of the considerations of section 5.2 and of other defects that turn out to be larger than for $N_{\rm cc} = 7$, the amount of variation in the critical temperature for narrow wells in particular.

For the moment setting aside the data for $\lambda < 1.939$, HRT's predictions for the critical temperature are in generally satisfactory agreement with the $\beta_c(\lambda)$-curve expected from the simulation-based and purely theoretical results presented in sub-section sub-section 3.1.1. Embedded into this regular overall behavior of β_c as a function of λ, however, we find a number of depressions and elevations of β_c, some of which cannot be seen on the scale of the plot fig. 4 but from the numeric results only; others, however, are so strong as to render the critical temperature a non-monotonic function of λ, which is certainly not expected on the grounds of the literature presented in sub-section 3.1.1, the data of [48–50] in particular.

In the light of section 5.5 it is of course tempting to simply attribute this behavior to the difficulties previously discussed, especially since the critical point is located in the region of large $f(Q_0, \varrho)$ by definition; the peculiar distribution of λ-values affected, however, suggests that these problems of the numerical procedure are triggered or modulated by a special mechanism. Indeed, a closer look at the core condition function $\tilde{\mathcal{C}}^{(Q)}(Q, \varrho)$ for fixed density ϱ reveals, for every single one of the λ values implicated that we checked, that the combination of terms pertaining to $w(r)$ or $v^{\rm hs}(r)$ alone (of ranges $\lambda\,\sigma$ and σ, respectively) regularly and quite

frequently reduces the amplitude of this function's swings about the ideal gas value of $-1/\varrho$; the same happens only occasionally for λ-values removed from these irregularities, a pattern consistent to the point of allowing one to quite reliably determine whether or not a given λ is affected by these shifts of β_c from a plot of $\tilde{\mathcal{C}}^{(Q)}(Q,\varrho)$ for $\varrho \sim \varrho_c$ alone; two typical examples at similar λ values illustrating this point are shown in fig. 5. In that plot's curve corresponding to $\lambda = 3$ it is very clear that every oscillation of the reference-system part corresponds to three oscillations of the perturbational part of $\tilde{\mathcal{C}}^{(Q)}$ that partly cancel where the former would otherwise have its maximum; the regularity with which this occurs is, of course, a direct consequence of λ, the ratio of the two characteristic lengths present in the model, being integer. Slightly generalizing this reasoning, it will come as no surprise that most of the irregularities occur when λ is close to a simple fraction: among the shifts in T_c most obvious in the plot 4 are those where λ is close to 2, $2\frac{1}{4}$, $2\frac{1}{7}$, $2\frac{1}{9}$ and $2\frac{1}{12}$, and in retrospect it seems justified to also include the small parameter range around $\lambda = 1\frac{1}{2}$ in this list, *v. i.*; the effect is less obvious from fig. 4 but still discernible at $2\frac{1}{2}$, $2\frac{1}{3}$ and $2\frac{2}{3}$, whereas for $2\frac{1}{4}$ and $2\frac{3}{4}$ it is so small as to make the plot of $\beta_c(\lambda)$ appear smooth while the irregularities are still evident from the numerical values; also note that, once again, ϱ_c is hardly affected.

Taken together all these observations seem to point to the interplay of the two different lengths special to the model and the resulting partial oppression of a significant portion of the extrema of $\tilde{\mathcal{C}}^{(Q)}(Q,\varrho)$ that cause the discrepancy of HRT and literature results for the critical temperature around certain λ values; this interpretation is corroborated by the finding that an interpolation of HRT's predictions from λ values nearby is usually well compatible with the data presented in sub-section 3.1.1. Even though we currently cannot pinpoint the precise mechanism by which this unphysical behavior of HRT arises and, in particular, cannot distinguish between the closure's inadequacy and the PDE's stiffness as the main culprit — though the latter is certainly implicated to some degree[17] —, two conclusions may be drawn quite safely: for one, these shifts in the critical temperature are not an issue as long as we stay clear of values of $\lambda \gtrsim 2$ that are close to simple fractions or other special values (a condition to be checked by considering the effect of varying λ in a narrow range around the value of interest), or else as long as we restrict ourselves to $\lambda \gtrsim 2.7$ where the effects are rather small; and secondly, it is only in the presence of discontinuities in the potential's perturbational part that certain lengths feature prominently[18] in the relevant functions' Fourier transforms and can so give rise to problems of the kind outlined above. In any case, however, the numerical effects discussed in sections 5.2 to 5.5 above are, in principle, always present; the special mechanism outlined in this section only highlights these effects' severity and thus acts as a magnifying glass of sorts for the

[17] Take into account that, from eq. (A.3) in appendix A, $\bar{\varepsilon}(Q,\varrho) = -\tilde{\phi}(Q,\varrho)/\tilde{\mathcal{C}}^{(Q)}(Q,\varrho)$ so that a reduction of $|\tilde{\mathcal{C}}^{(Q)}(Q,\varrho) + 1/\varrho|$ can conceivably modulate both the cut-off for the onset of the growth of $f(Q,\varrho)$ following from the discrepancy of the PDE and the FDE as well as that function's starting value, denoted Q_1 and $f(Q_1,\varrho)$, respectively, in section 5.5.

[18] Recall that the cut-off procedure (2.4) only affects the potential's continuous component, as shortly discussed in chapter 3.

uncertainty in the results brought about by the corresponding difficulties of the numerical procedure. In order to avoid at least this mechanism from setting in it is thus preferable to avoid systems with discontinuities in $w(r)$ like, *e. g.*, SWs or the multi-step potential defined in section 3.3; fortunately this still leaves most of the potentials popular in liquid state physics like the HCY fluid or Lennard-Jones systems, to both of which HRT has been applied in the original implementation [5, 6, 11, 13, 19, 21, 28, 80, 81].

VI. Concluding remarks

In the course of the last few chapters we have mainly been concerned with a rather detailed study of a number of traits characteristic of the application of HRT to one-component fluids, both in a general setting (*cf.* chapter 2) and in the numerical treatment of selected model systems (*cf.* chapter 5). As this study draws to an end, however, it is only fitting to pause for a moment and once more contemplate the major points we raised. We then see a theory, rich in promise and attractive in its generality but still not in wide-spread use, that presents itself as a unified framework for the description of thermodynamic systems throughout their phase diagrams; its key ingredient is the combination of perturbation- and integral equation theory with RG-theoretical ideas *via* a sequence of renormalized potentials.

In order to allow application to specific physical models and to extract both universal and non-universal information from the theory it is, of course, necessary to close the formally exact but non-terminating hierarchy of ODEs underlying all of HRT at some order of the perturbational expansion; in principle there are many suitable approximations, and when combined with thermodynamic consistency as expressed in the compressibility sum-rule (2.13) they typically give rise to partial integro-differential equations. In the case that we concern ourselves with, *viz.* that of simple one-component fluids interacting *via* purely additive, spherically symmetric pair potentials with infinitely repulsive cores, there is one such *ansatz* that has been used almost exclusively, *viz.* the LOGA/ORPA-style closure of eq. (2.15) that we, too, decided to adopt in our work. The formulation we rely on is thus largely the same as that of earlier applications, but we take care in motivating the introduction of the various approximations and discuss their relative merits. Among the most important of our analytical and semi-analytical results on the resulting equations — all of which are borne out by the numerics — are those regarding the PDE's stability and the build-up of divergences of the isothermal compressibility: in particular, HRT is found unable to deal with predominantly repulsive potentials in the formulation of chapter 2, and the mechanism leading to a suppression of van der Waals loops is shown to be linked to the PDE's stiffness in the critical region or when describing phase coexistence; furthermore, grave problems are shown to be likely to arise for very short-ranged interactions.

In order to put into perspective and to gauge the relevance of these rather general concerns regarding the theory's applicability we turned to two types of model potentials, *viz.* the HCY potential with inverse screening length $z = 1.8/\sigma$ as well as a large number of SW systems with range parameter λ varying from extremely narrow wells up to $\lambda = 3.6$. By way of experimentation we were then able to identify three major issues affecting the computational realization of HRT in its standard formulation: An important one that should not be taken lightly without at least checking its implications for a particular system is the necessarily approximate treatment of the core condition by ODEs coupled to the HRT-PDE at every density ϱ; in addition to some systematic shortcomings in the pair distribution functions that we found in all the systems we looked at, the numerical problems associated with adoption of eq. (D.11) alone are so severe as to necessitate elimination of other terms related to third-order partial derivatives of the free energy. While this so-called decoupling assumption provides a partial remedy for some of the problems linked to the core condition, decoupling by necessity introduces both mathematical and thermodynamical inconsistency into the equations; in particular, well-defined phase boundaries are strictly incompatible with a full implementation of decoupling, and imposition of a boundary condition at the highest density $\varrho_{\max}$ in the calculation gives rise to an unphysical near-discontinuity of the solution there reflecting the lack of internal consistency in the approximations made and the condition imposed at $\varrho_{\max}$. Other than these two problems that are likely to be linked both to the closure adopted and the continuous (*i. e.*, non-discrete) nature of the physical systems considered, the equations' stiffness for high-compressibility states seems deeply rooted in HRT; in the one-component fluids under consideration here this leads to a pathological behavior of the solution wherever the auxiliary quantity $f(Q, \varrho)$ is large and the RG-theoretical cut-off Q sufficiently small, a behavior that cannot be matched with practical step sizes in an FD scheme and brings about considerable uncertainty regarding the results obtained numerically and their validity. Not the least, even if the data outside the coexistence region turn out rather stable under variation of the computational strategy or the parameters it depends upon we still have to anticipate the possibility of a systematic distortion of the binodal and other defects, in addition to what problems an inappropriate choice and location of the high-density boundary condition may bring about. Interestingly enough, the presence of discontinuities in the potential's perturbational part makes for some peculiar effects in, *e. g.*, the critical point's location that might be used as a diagnostic tool for the level of confidence that should be attributed to numerical results in view of the unavoidable stiffness of the PDE and the corresponding FDE in part of the phase diagram. — All these effects, it should be noted, to some degree depend on the potential's range, *i. e.* on the parameters z and λ for the HCY and the SW case, respectively.

From the preceding remarks we find that HRT, a theory successfully applied to a number of different systems by various authors, clearly has its share of numerical difficulties; as a consequence, every single calculation must be regarded as of uncertain standing, and it is only through the combination of meticulous scrutiny

of a set of related calculations that meaningful and reliable information can be extracted from HRT calculations.

Such a program is, of course, greatly facilitated by the availability of a fully modular implementation of HRT in several variants of its usual formulation like the one we have written. In doing so we have gone to great lengths to ensure the numerical soundness of each and every step in the calculation except where this is not compatible with the PDE's nature; as secondary design goals we have also striven for efficiency, ease of use, and a natural organization of the program, which has only been possible through the adoption of a simple meta-language and code construction techniques. Not only should our software provide the liquid physics community with a versatile tool for the systematic exploration and application of HRT to a variety of systems, it has also proved essential in understanding both numerical and analytical properties of the equations at hand; indeed, several of the issues mentioned above were first found in the numerical work when monitoring and assessing the evolution of the solution throughout the numerical process. As discussed in some detail in the text, the same approach also provides us with distinct signatures for the problems we found as well as with a means of detecting them.

All in all this puts us into a position where we are confident of our ability to apply HRT in a numerically meaningful way to a variety of physically significant systems and to use the tools and techniques we developed to extract relevant information from these calculations; the possibilities here range from the rapid determination of approximate binodals including the liquid-vapor critical points in an *ansatz* not implementing the core condition all the way to extensive numerical work employing several variations of the theory's formulation as well as a host of checks to gauge the the level of confidence to be attributed to the results obtained. Despite the considerable computational challenges encountered we thus find that HRT is, indeed, capable of providing reliable structural and thermodynamic information on liquid-vapor transitions in simple one-component fluids even in the immediate vicinity of the critical point.

Appendix

A. Rewriting the partial differential equation in not-quite quasi-linear form

In order to facilitate the numerical treatment of the PDE implied by eqs. (2.13) and (2.12), it is advantageous to adopt a re-formulation in terms of an auxiliary quantity $f(Q, \varrho)$ rather than the modified free energy $\mathcal{A}^{(Q)}(\varrho)$: the resulting PDE (2.23) superficially resembling a quasi-linear one (cf. section A.1) allows implementation of an implicit finite-difference scheme by simple inversion of a tri-diagonal matrix instead of more cumbersome and slower iterative procedures; also note that, despite complete mathematical equivalence, the PDE's formulation plays a *rôle* in the numerical algorithm's ability to enter the region of the PDE's stiffness with pre-determined step sizes.

This re-writing, leading up to eq. (2.23) and to be detailed here, is characterized by a certain amount of arbitrariness that can be used to optimize the final expressions with regard to their numerical properties at the cost of repeatedly performing the time-consuming calculations for various *ansatzes* for $f(Q, \varrho)$; and even though the calculations themselves are straightforward, intermediate results soon become unwieldy, making experimentation with different definitions for f rather cumbersome. It is precisely in a situation like this that computer algebra systems (CASs) may be put to particularly good use: not only is it much more convenient to check the validity of high-level commands for the symbolic manipulation of the complicated expressions arising than to actually follow these steps, but the necessary experimentation reduces to mere re-evaluation of the re-writing procedure starting with a modified initial definition of f. Considering these advantages, much of the re-formulation's presentation in this appendix is devoted to the use of the popular CAS `Mathematica` [82] for implementing and analyzing the steps leading to eq. (2.23); the reader should, however, keep in mind that the code given here is not meant to be optimally efficient but favors clarity over speed; the experienced user will no doubt easily spot unnecessarily slow calculations. — In this appendix's remainder, input into `Mathematica` is given in mono-spaced font whereas the program's output (as obtained with version 4) is shown in slanted mono-spaced font.

Mathematica	arguments	symbol
`c`	3	$\tilde{\mathcal{C}}$
`c`ij	–	c_{ij}
`cR0`	1	$\tilde{c}^{\mathrm{ref}}\vert_{k=0}$
`cRef`	2	$\tilde{c}^{\mathrm{ref}}$
`d`ij	–	d_{ij}
`eny`	2	$\mathcal{A}$
`eps`	2	ε
`f`	2	f
`g`	3	$\tilde{\mathcal{G}}$
`g0`	2	$\tilde{\mathcal{G}}_0$
`gamma0`	2	γ_0
`phi`	2	$\tilde{\phi}$
`phi0`	1	$\tilde{\phi}_0$
`u0`	2	$\tilde{u}_0$
`u0divphi`	2	$\tilde{u}_0/\tilde{\phi}$

Table 1: Correspondence of identifiers used in `Mathematica` code and the symbols used in conventional notation (eq. (3) in this appendix; *q. v.* appendix F); in the above table, i and j are to be replaced by suitable one-digit integers. The number of arguments the `Mathematica` symbols listed expect is indicated in the second column; these functions enter the calculations with either the density ϱ alone, with both Q and ϱ, or with the full triple of (Q,Q,ϱ) as arguments; also note that the distinction of superscripts (Q), indicating quantities to be evaluated for the Q-system, and of function arguments Q, where Q plays the more general *rôle* of a wave number coinciding with the cut-off, is inappropriate in the `Mathematica` code due to the peculiar behavior of `D[]` when operating on expressions of the form `x[Q][Q,rho]`. — In addition to the `Mathematica` symbols listed above, we also use variables with names of the form `dQ`n`Rho`m`x` to indicate the partial derivative $\partial^{n+m}x/\partial^n Q\partial^m\varrho$ of x, suppressing `Q0` or `Rho0` as well as the digit `1` after `Q`.

A.1. Basic relations and introduction of auxiliary function $f(Q,\varrho)$

Much of the following exposition is vastly facilitated by introduction of various rules implementing trnasformations corresponding to the basic relations underlying HRT in the formulation chosen; among these, and with the notational correspondences listed in table 1, the LOGA/ORPA-*ansatz* (2.15) for $\tilde{\mathcal{C}}^{(Q)}(k,\varrho)$ is written as:

```
rC = c[Q_,k_,rho_] :> cRef[k,rho] + phi[k,rho] +
     gamma0[Q,rho] u0[k,rho] + g[Q,k,rho];
```

As the all-important compressibility sum rule (2.13) involves $\tilde{\mathcal{C}}^{(Q)}(0,\varrho)$ and setting a wave number to zero means loosing one argument, we introduce some additional symbols for Fourier transforms evaluated at zero momentum; note that the only condition imposed upon basis function $u_0(r,\varrho)$ at this point is the normalization condition $\tilde{u}_0(0,\varrho)=1$, *cf.* eq. (2.16):

```
g[Q_,0,rho_] := g0[Q,rho];
phi[0, rho_] := phi0[rho];
u0[0, rho_] := 1 (* Four[u_0](k=0) == 1 *) ;
cRef[0, rho] := cR0[rho];
```

Also, arithmetic with derivatives is facilitated by introduction of special symbols named according to the rules given in conjunction with table 1:

```
Derivative[1,0][phi] := dQphi;
Derivative[0,1][phi] := dRho1phi;
Derivative[0,1][dRho1phi] := dRho2phi;
Derivative[0,2][phi] := dRho2phi;
Derivative[1,0][cRef] := dQcRef;
Derivative[0,1][cRef] := dRho1cRef;
Derivative[0,1][dRho1cRef] := dRho2cRef;
Derivative[0,2][cRef] := dRho2cRef;
Derivative[1,0][u0] := dQu0;
Derivative[0,1][u0] := dRho1u0;
Derivative[0,1][dRho1u0] := dRho2u0;
Derivative[0,2][u0] := dRho2u0;
```

The list `eqs` is now defined to hold the fundamental relations that our re-writing is based upon: definition of $\tilde{\mathcal{C}}^{(Q)}(Q,\varrho)$ according to eq. (2.15), the HRT result (2.12) for $\partial\mathcal{A}^{(Q)}(\varrho)/\partial Q$, and the compressibility sum-rule (2.13):

```
eqs = {
  c[Q,Q,rho] == (c[Q,Q,rho] /. rC),
  Derivative[1,0][eny][Q,rho] ==
     Q^2/(4 Pi^2) Log[1-phi[Q,rho]/c[Q,Q,rho]],
  Derivative[0,2][eny][Q,rho] == -(c[Q,0,rho]/. rC) }
{c[Q, Q, rho] == cRef[Q, rho] + g[Q, Q, rho] + phi[Q, rho] +

>      gamma0[Q, rho] u0[Q, rho],

                          2          phi[Q, rho]
                         Q  Log[1 - ------------]
        (1,0)                       c[Q, Q, rho]
>    eny     [Q, rho] == ------------------------,
                                     2
                                  4 Pi

        (0,2)
>    eny     [Q, rho] == -cR0[rho] - g0[Q, rho] - gamma0[Q, rho] - phi0[rho]}
```

In order to make the transition from the PDE as implied by the above relations into a form numerically more tractable (falsely labeled "quasi-linear" in the literature [11], *v. i.*), it might seem most natural to define $f(Q,\varrho)$ as equal to the logarithm in eq. (2.12); however, to avoid spurious singularities at roots of $\tilde{\phi}$, f has to be multiplied by a term of order $\mathcal{O}(\tilde{\phi}^2)$ at least, and an extra term must be added. As for the factor, note that our choice of $\tilde{u}_0^2 \propto \tilde{\phi}^2$ allows for a reduction of the number of floating point operations necessary when evaluating the final expressions (5) for the coefficients d_{0i} when compared to the factor $\tilde{\phi}^2$ adopted by [11], the first reference to acknowledge the necessity to adopt such a re-writing.

(Previous work re-cast the PDE as a flux-conserving one but was unable to enter the critical region [6].) The term to be added is still largely undetermined but is written as a product of $\tilde{\phi}$ and a regular function `extra[]` of $\tilde{c}^{\mathrm{ref}}(Q,\varrho)$ and $\tilde{\mathcal{G}}^{(Q)}(Q,\varrho)$ alone, the simplest choice possible; note that the final result for the the additional term is largely determined by the choice of the pre-factor for f. — As stated before, experimentation with more general definitions of $f(Q,\varrho)$ is possible by mere modification of the following statement and subsequent re-evaluation of the remaining steps.

```
ansatz =
  Log[1-phi[Q,rho]/c[Q,Q,rho]] ==
     f[Q,rho] u0[Q,rho]^2 + phi[Q,rho] extra[cRef[Q,rho], g[Q,Q,rho]];
(rAnsatz = Simplify[Solve[ansatz, c[Q,Q,rho]][[1,1]]]) // InputForm
c[Q, Q, rho] ->
 -(phi[Q, rho]/(-1 + E^(extra[cRef[Q, rho], g[Q, Q, rho]]*phi[Q, rho] +
      f[Q, rho]*u0[Q, rho]^2)))
```

This *ansatz* must, of course, be inserted into into the set of equations considered earlier; furthermore, it is convenient to define $\varepsilon(Q,\varrho)$ as the exponential appearing in the expression for $\tilde{\mathcal{C}}^{(Q)}(Q,\varrho)$:

```
(eqsAnsatz = (eqs /. rAnsatz // Simplify) /. Log[Power[E,x_]] -> x) // InputForm
{0 == cRef[Q, rho] + g[Q, Q, rho] + phi[Q, rho] +
   phi[Q, rho]/(-1 + E^(extra[cRef[Q, rho], g[Q, Q, rho]]*phi[Q, rho] +
       f[Q, rho]*u0[Q, rho]^2)) + gamma0[Q, rho]*u0[Q, rho],
 Derivative[1, 0][eny][Q, rho] ==
  (Q^2*(extra[cRef[Q, rho], g[Q, Q, rho]]*phi[Q, rho] +
     f[Q, rho]*u0[Q, rho]^2))/(4*Pi^2),
 cR0[rho] + g0[Q, rho] + gamma0[Q, rho] + phi0[rho] +
   Derivative[0, 2][eny][Q, rho] == 0}
rEps = E^(b_. Evaluate[Cases[rAnsatz, E^a_ -> a, Infinity] [[1]]]) :>
  eps[Q,rho]^b;
rrEps = RuleDelayed @@ {eps[Q_, rho_], rEps[[1]] /. _Optional -> 1};
```

In order to make the transition from two equations, *viz.* eqs. (2.12) and (2.13), to a single PDE of the form of eq. (2.23), the compressibility sum-rule (2.13) is used to eliminate the LOGA/ORPA-coefficient $\gamma_0^{(Q)}(\varrho)$:

```
rElim = Solve[Select[eqsAnsatz, !FreeQ[#,Derivative[0,2]]&],
    gamma0[Q,rho]][[1,1]]
eqsElim = Simplify[eqsAnsatz /. rElim]
gamma0[Q, rho] ->

                                              (0,2)
>    -cR0[rho] - g0[Q, rho] - phi0[rho] - eny     [Q, rho]
```

The PDE is now obtained by postulating interchangeability of partial derivatives acting on $\mathcal{A}^{(Q)}$, *i. e.* by equating the expressions $\partial\left(\partial^2\mathcal{A}^{(Q)}(\varrho)/\partial^2\varrho\right)/\partial Q$ and $\partial^2\left(\partial\mathcal{A}^{(Q)}(\varrho)/\partial Q\right)/\partial^2\varrho$ for eq. (2.17)'s $\alpha^{(Q)}(\varrho)$; after the following commands defining `quasilin` as the difference of these expressions, the PDE is equivalent to the condition of vanishing `quasilin`:

```
dQeny = Solve[Select[eqsElim, !FreeQ[#,Derivative[1,0]]&],
  Derivative[1,0][eny][Q,rho]][[1,1,2]];
dRho2eny = (Solve[Select[eqsElim, !FreeQ[#,Derivative[0,2]]&],
  Derivative[0,2][eny][Q,rho]][[1,1,2]]) // Simplify;
quasilin = Expand[(D[dQeny, {rho, 2}] - D[dRho2eny, Q])
      /. rEps];
```

With the last step, the modified free energy $\mathcal{A}^{(Q)}(\varrho)$ has been eliminated from the PDE and replaced by $f(Q, \varrho)$; the new formulation involves the following derivatives of f:

```
Union[Cases[quasilin, Derivative[__][f][__], Infinity]]
  (0,1)          (0,2)          (1,0)
{f     [Q, rho], f     [Q, rho], f     [Q, rho]}
```

All in all, the following derivatives are present in the new formulation of the PDE:

```
Union[Cases[quasilin, Derivative[__][_][__], Infinity]] /.
  f_[Q,rho] :> f /. f_[Q,Q,rho] :> f /. f_[cRef,g] :> f
      (0,1)   (0,1)       (0,2)   (0,2)       (1,0)   (1,0)
{extra     , f     , extra     , f     , extra     , f     ,

       (1,0)       (1,1)       (2,0)   (0,0,1)   (0,0,2)   (0,1,0)   (1,0,0)
>    g0     , extra     , extra     , g       , g       , g       , g       }
```

Presence of second-order ϱ-derivatives on functions other than f clearly makes the PDE in this formulation, just as the form used in [11], *not* fall into the quasi-linear class despite reiterated claims to the contrary; fortunately this is an issue of little practical relevance.

A.2. Coefficients of the PDE

With the representation of the PDE obtained so far, we can easily extract from `quasilin` the explicit expressions for the coefficients c_{ij} for writing the PDE in the form $\sum_{ij} c_{ij} \left(\partial^{i+j} f / \partial^i Q \partial^j \varrho\right) = 0$:

```
c02 = Coefficient[quasilin, Derivative[0,2][f][Q,rho]];
c01 = Coefficient[quasilin, Derivative[0,1][f][Q,rho]];
c10 = Coefficient[quasilin, Derivative[1,0][f][Q,rho]] // Together;
c00 = Select[quasilin, FreeQ[#,Derivative[__][f]]&];
```

These expressions, c_{00} in particular, are rather unwieldy; may it suffice to demonstrate that they, indeed, represent the full PDE:

```
Expand[quasilin - (
  c02 Derivative[0,2][f][Q,rho] +
```

```
  c01 Derivative[0,1][f][Q,rho] +
  c00 +
  c10 Derivative[1,0][f][Q,rho])] // Simplify
0
```

In the numerical implementaton, however, the PDE is more useful when $\partial f/\partial Q$ is isolated; the coefficients d_{0i} for expressing the PDE as $\partial f/\partial Q = \sum_i d_{0i} \left(\partial^i f/\partial \varrho^i\right)$ are, of course, related to c_{10} and the c_{0i} in a straightforward way:

```
d02 = Together[-c02/c10];
d01 = Together[-c01/c10];
d00 = Together[-c00/c10];
```

Note that this simplistic approach to the re-writing, though well suitable for d_{02} and d_{01}, can be used for d_{00} only in fairly recent versions of `Mathematica` and on sufficiently fast hardware; a more efficient way of performing the necessary calculation and simplification should be obvious.

A.3. Coefficients d_{0i} for small $\tilde{\phi}$

In order to fix the still unknown function `extra[]`, we now analyze the coefficients d_{0i} just found for small $\tilde{\phi}(Q, \varrho)$; it is this analysis, performed for various *ansatzes* for f, that leads to the requirements quoted earlier. The following series expansion (including terms only up to order $\mathcal{O}(\tilde{\phi}^0)$) for extracting the coefficients' singularities is one of the most demanding calculations in this re-writing of the HRT-PDE:

```
ser = (Normal[Series[#, {phi[Q,rho],0,0}]]& /@
(Simplify[
  {d02, d01, d00} /. rrEps /.
  u0 :> (phi[##] u0divphi[##]&)
])) /. Exp[b_. extra[__]] :> ExpExtra^b;
```

While the first two coefficients, *i. e.* d_{02} and d_{01} actually vanish for $\tilde{\phi} \to 0$, the limit of d_{00} is a complicated expression depending on `extra[]` and still containing $\tilde{\phi}$ with exponents -2 and -1:

```
ser[[{1,2}]]
{0, 0}
s = ser[[3]];
Cases[s, phi[Q,rho]^b_. -> b, Infinity]
```

```
{1, -2, 1, -1}
```

Now the reason for introducing the function `extra[]` becomes clear: together with the pre-factors quoted earlier, it allows the removal of any singularities in d_{00}. — There are two candidates for `extra[]` that eliminate terms of order $\mathcal{O}(\tilde{\phi}^{-2})$:

```
sol2 = (RuleDelayed @@ {#[[1,1,0]], Function @@ ({List@@(#[[1,1]]),
   Evaluate[#[[1,1]]/.#]} /.
    f_[Q,rho]:>f /. f_[Q,Q,rho] :> f)})& /@
Solve[Coefficient[s, phi[Q,rho], -2] == 0,
  extra[cRef[Q,rho],g[Q,Q,rho]]]
{extra :> Function[{cRef, g}, 0],

                                          1
>    extra :> Function[{cRef, g}, ---------]}
                                    -cRef - g
```

The first of these, *i. e.* vanishing `extra[]`, is, however, not sufficient to also remove the first-order pole:

```
Coefficient[s, phi[Q,rho], -1] /. sol2[[1]]
(-12 Pi  dQu0[Q, rho] f[Q, rho] u0divphi[Q, rho]  +

           2                                          3
>      4 Pi  dQphi[Q, rho] f[Q, rho] u0divphi[Q, rho] ) /

          2                  3
>    (4 Pi  u0divphi[Q, rho] )
```

Unless the *ansatz* for f was not sufficiently general in the first place, we thus have to accept the second solution for `extra[]`; this, however, entails a further restriction, in addition to the normalization condition $\tilde{u}_0(0,\varrho) = 1$ given earlier, of the basis functions $u_0(r,\varrho)$ admissible:

```
(Coefficient[s, phi[Q,rho], -1] /. sol2[[2]] // Simplify)
((-dQu0[Q, rho] + dQphi[Q, rho] u0divphi[Q, rho])

                          2                                  2
>      (1 + 2 cRef[Q, rho]  f[Q, rho] u0divphi[Q, rho]  +

                                                            2
>        4 cRef[Q, rho] f[Q, rho] g[Q, Q, rho] u0divphi[Q, rho]  +

                                  2                  2
>        2 f[Q, rho] g[Q, Q, rho]  u0divphi[Q, rho] )) /

                                      2                  3
>    (2 (cRef[Q, rho] + g[Q, Q, rho])  u0divphi[Q, rho] )
```

Of the three solutions for the ratio `u0divphi[Q,rho]` of $\tilde{u}_0(Q,\varrho)$ and $\tilde{\phi}(Q,\varrho)$, two have non-vanishing imaginary part and still depend on $f(Q,\varrho)$, while the third one yields:

```
Select[
  Solve[(Coefficient[s, phi[Q,rho], -1] /. sol2[[2]] // Simplify)==0,
        u0divphi[Q,rho]],
  FreeQ[#,f]&]
                        dQu0[Q, rho]
{{u0divphi[Q, rho] -> -------------}}
                        dQphi[Q, rho]
```

Note that this result, easily re-written as

$$\frac{1}{\tilde{u}_0(Q,\varrho)}\,\frac{\partial\tilde{u}_0(Q,\varrho)}{\partial Q} = \frac{1}{\tilde{\phi}(Q,\varrho)}\,\frac{\partial\tilde{\phi}(Q,\varrho)}{\partial Q} \qquad \left(\tilde{\phi}\to 0\right),$$

in conventional notation, does not imply strict proportionality of $\tilde{u}_0$ and $\tilde{\phi}$; rather, $\tilde{u}_0 \propto \tilde{\phi}$ must hold only up to terms of order $\mathcal{O}(\tilde{\phi})$. This freedom might, of course, be exploited to arrive at basis functions $u_0(r,\varrho)$, and, by virtue of eq. (2.15), of direct correlation functions $\mathcal{C}^{(Q)}(r,\varrho)$, of longer range than $\phi(r,\varrho)$; it is, however, hardly conceivable that such a strategy might advantageously by applied without introducing an additional, computationally unattractive ϱ-dependence, not to mention the basis functions' Q dependence one would naturally want to introduce in such a more general closure. Thus, in our work we fix u_0 as strictly proportional to ϕ so that $\tilde{u}_0/\tilde{\phi}$ is a constant, *viz.* $-1/\tilde{\phi}(0,\varrho)$:

```
rU0 = {u0 -> (phi[#1,#2] / phi0[#2]&),
       dQu0 -> (dQphi[#1,#2] / phi0[#2]&),
       u0divphi -> (1/phi0[#2]&)};
rExtra = sol2[[2]]
                                  1
extra :> Function[{cRef, g}, ---------]
                             -cRef - g
(Coefficient[s, phi[Q,rho], -1] /. sol2[[2]] /. rU0 // Simplify)
0
```

The last of these command confirms that the terms of order $\mathcal{O}(\tilde{\phi}^{-1})$ do, indeed, cancel; consequently, the *ansatz* by which we introduced f is sufficient to avoid spurious singularities in the PDE's coefficients d_{0i}. With these results, the definition of $f(Q,\varrho)$ reads

$$\ln\left(1-\frac{\tilde{\phi}(Q,\varrho)}{\tilde{\mathcal{C}}^{(Q)}(Q,\varrho)}\right) = f(Q,\varrho)\,\tilde{u}_0^2(Q,\varrho) - \frac{\tilde{\phi}(Q,\varrho)}{\tilde{\mathcal{K}}^{(Q)}(Q,\varrho)}\,, \tag{1}$$

a result very similar to that of [11]. Taking the ideal gas limit and considering the divergence of the term $-1/\varrho$ in $\tilde{c}^{\mathrm{ref}}$ we readily find that both f and its derivative with respect to ϱ vanish,

$$f(Q,0) = \left.\frac{\partial f(Q,\varrho)}{\partial\varrho}\right|_{\varrho=0} = 0\,, \tag{2}$$

the former of which is a convenient low-density boundary condition most versions of our program rely on; indeed, as eq. (2) provides us with two conditions this in principle already suffices to determine the PDE's solution up to high density, even though such a use is computationally clearly unattractive. Introducing the short-hand notations (with the obvious superscripts and arguments omitted)

$$\begin{aligned} \varepsilon = 1 - \frac{\tilde{\phi}}{\tilde{\mathcal{C}}^{(Q)}} = e^{f\,\tilde{u}_0^2 + x_\phi} \qquad \bar{\varepsilon} = \varepsilon - 1 \\ x_\phi = -\frac{\tilde{\phi}}{\tilde{\mathcal{K}}^{(Q)}} \qquad x_f = -\frac{f\,\left(\tilde{\mathcal{K}}^{(Q)}\right)^2}{\tilde{\phi}_0^2} \\ \tilde{\phi}_0 = \tilde{\phi}(0,\varrho) \qquad \tilde{\mathcal{G}}_0 = \tilde{\mathcal{G}}^{(Q)}(0,\varrho)\,, \end{aligned} \tag{3}$$

eqs. (2.12) and (1) can be written more succinctly as

$$\begin{aligned} \frac{\mathrm{d}}{\mathrm{d}Q}\left(\frac{\beta\mathcal{A}^{(Q)}(\varrho)}{V}\right) &= \frac{Q^2}{4\pi^2}\ln\varepsilon(Q,\varrho)\,, \\ \frac{\tilde{\phi}(Q,\varrho)}{\tilde{\mathcal{C}}^{(Q)}(Q,\varrho)} &= -\bar{\varepsilon}(Q,\varrho)\,. \end{aligned}$$

Restricting ourselves to the fully interacting system, *i. e.* to the limit $Q \to 0$ so that $\mathcal{C}^{(Q)} \to c_2$ and $\mathcal{A}^{(Q)} \to A$, and taking into account the OZ relation (2.8), the isothermal compressibility κ_T is easily found to be

$$\begin{aligned} \frac{1}{\kappa_T^{(0)}} &= \frac{\varrho^2}{\beta}\,\frac{\partial^2}{\partial\varrho^2}\left(\frac{\beta\mathcal{A}^{(0)}}{V}\right) \\ &= \frac{\varrho/\beta}{1+\varrho\,\tilde{h}^{(0)}(0,\varrho)} \\ &= \frac{\varrho^2\,\tilde{\phi}(0,\varrho)}{\beta\,\bar{\varepsilon}(0,\varrho)}\,; \end{aligned} \tag{4}$$

note that a divergence of $\kappa_T^{(Q)}$ in the limit $Q \to 0$ is thus only possible if accompanied by a corresponding divergence of $f(Q,\varrho)$ in the same limit.

A.4. Final results

Even though the PDE's coefficients are now fully determined, they — and d_{00} in particular — are still not in a form usable but demand further simplification. This straightforward but rather tedious process will not be detailed here; suffice it to say that CASs again prove very helpful in manipulating the complex expression trees representing the coefficient functions. — Reverting to conventional notation

and dropping the obvious arguments and superscripts, our final results for the d_{0i} are

$$\begin{aligned} d_{00} = &+ \frac{\partial\tilde\phi}{\partial Q}\left(\frac{\tilde\phi_0^2}{\tilde{\mathcal{K}}^{(Q)}\,\tilde\phi^2} - \frac{\tilde{\mathcal{K}}^{(Q)}\,\bar\varepsilon^2\,\tilde\phi_0^2}{\varepsilon\,\tilde\phi^4} - \frac{2f}{\tilde\phi}\right) + \frac{\partial\tilde{\mathcal{K}}^{(Q)}}{\partial Q}\left(\frac{\bar\varepsilon^2\,\tilde\phi_0^2}{\varepsilon\,\tilde\phi^3} - \frac{\tilde\phi_0^2}{\left(\tilde{\mathcal{K}}^{(Q)}\right)^2\tilde\phi}\right) \\ &- \frac{\partial^2\tilde u_0^2}{\partial\varrho^2}\,\frac{Q^2\,\bar\varepsilon^2\,f\,\tilde\phi_0}{4\pi^2\,\varepsilon\,\tilde\phi^2} - \frac{\partial^2 x_\phi}{\partial\varrho^2}\,\frac{Q^2\,\bar\varepsilon^2\,\tilde\phi_0}{4\pi^2\,\varepsilon\,\tilde\phi^2} - \frac{\partial\tilde{\mathcal{G}}_0^{(Q)}}{\partial Q}\,\frac{\bar\varepsilon^2\,\tilde\phi_0}{\varepsilon\,\tilde\phi^2}\,, \\ d_{01} = &- \frac{\partial\tilde u_0}{\partial\varrho}\,\frac{Q^2\,\bar\varepsilon^2}{\pi^2\,\varepsilon\,\tilde\phi}\,, \qquad d_{02} = -\frac{Q^2\,\bar\varepsilon^2}{4\pi^2\,\varepsilon\,\tilde\phi_0}\,. \end{aligned} \tag{5}$$

In the light of our previous analysis of these coefficients' behavior in the limit $\tilde\phi \to 0$, great care must be exercised when evaluating the d_{0i} for small $\tilde\phi$; noting that $(\bar\varepsilon^2\,\tilde\phi_0^2/\varepsilon\tilde\phi^3) - (\tilde\phi_0^2/(\tilde{\mathcal{K}}^{(Q)})^2\,\tilde\phi)$, the coefficient of $\partial\tilde{\mathcal{K}}^{(Q)}/\partial Q$ in d_{00}, can be written in terms of the $(\partial\phi/\partial Q)$-coefficient, in the numerical implementation the calculation of these terms proceeds *via* the fifth-order Taylor expansion

$$\begin{aligned} &\frac{\tilde\phi_0^2}{\tilde{\mathcal{K}}^{(Q)}\,\tilde\phi^2} - \frac{\tilde{\mathcal{K}}^{(Q)}\,\bar\varepsilon^2\,\tilde\phi_0^2}{\varepsilon\,\tilde\phi^4} - \frac{2f}{\tilde\phi} \\ &\quad = -\frac{1}{\left(\tilde{\mathcal{K}}^{(Q)}\right)^3}\left(\tilde\phi_0^2\left(\tfrac{1}{12} + x_f^2\right) + x_\phi\left(\tilde{\mathcal{K}}^{(Q)}\right)^2 f\,\tfrac{1}{3}\right. \\ &\qquad\qquad + x_\phi^2\,\tilde\phi_0^2\left(\tfrac{1}{360} + \tfrac{1}{2}\,x_f^2\right) + x_\phi^3\left(\tilde{\mathcal{K}}^{(Q)}\right)^2 f\left(\tfrac{1}{60} + \tfrac{1}{3}\,x_f^2\right) \\ &\qquad\qquad + x_\phi^4\,\tilde\phi_0^2\left(\tfrac{1}{20160} + \tfrac{1}{24}\,x_f^2 + \tfrac{1}{12}\,x_f^4\right) \\ &\qquad\qquad \left. + x_\phi^5\left(\tilde{\mathcal{K}}^{(Q)}\right)^2 f\left(\tfrac{1}{2520} + \tfrac{1}{18}\,x_f^2\right)\right) + \mathcal{O}(x_\phi^6)\,, \end{aligned}$$

and $\bar\varepsilon/\tilde\phi$, another quantity of order $\mathcal{O}(\tilde\phi^0)$, is evaluated as

$$\begin{aligned} \frac{\bar\varepsilon}{\tilde\phi} = &- \frac{1}{\tilde{\mathcal{K}}^{(Q)}}\left(1 + x_\phi\left(\tfrac{1}{2} + x_f\right) + x_\phi^2\left(\tfrac{1}{6} + x_f\right) + x_\phi^3\left(\tfrac{1}{24} + \tfrac{1}{2}\,x_f + \tfrac{1}{2}\,x_f^2\right)\right. \\ &\left. + x_\phi^4\left(\tfrac{1}{120} + \tfrac{1}{6}\,x_f + \tfrac{1}{2}\,x_f^2\right) + x_\phi^5\left(\tfrac{1}{720} + \tfrac{1}{24}\,x_f + \tfrac{1}{4}\,x_f + \tfrac{1}{6}\,x_f^2\right)\right) \\ &+ \mathcal{O}(x_\phi^6)\,. \end{aligned}$$

Note that even though the criteria for switching between the full analytic expressions and said expansions depend on $\epsilon_\#$, the expansion orders are not increased for very small values of $\epsilon_\#$, which is one of the few hard-coded limitations of our program (*cf.* section 4.7).

In this appendix we have shown some details of the transition from the combination of eqs. (2.12) and (2.13) to the PDE (2.23) superficially resembling a quasi-linear one; only use of the CAS `Mathematica` allowed us to focus the presentation of the PDE's re-writing on the general procedure and to emphasize the deliberate choices made as opposed to mere conclusions following from them; in particular, it should be clear that there is ample room for variation of the precise

form of the *ansatz* (1), and we have given our reasons for the specific choices we made. The final results (3) for the coefficients clearly show that in the case of ϱ-independent potentials — and only these have been considered in this work despite our program's ability to deal with ϱ-dependent potential — substantial simplification ensues, resulting in significant speed-ups of the numerical procedure: in that case, none of the basis functions depend on the density, which allows for simpler data structures and for caching of intermediate results.

B. Overview of previous versions of the implementation of HRT for simple one-component fluids

Most of the calculations presented in this work have been performed within the framework provided by the implementation of chapter 4, *i. e.* with version 4 of our program; occasionally, however, we will also reference results obtained, or conclusions reached, with earlier versions. Therefore it is pertinent to give a short overview of these programs, their main characteristics and differences, as well as their relation to the software's final form.

As a general note regarding all three of the versions sketched in this appendix, the implementations touched upon here differ from that of chapter 4 in the basis functions they use (*cf.* section C.2), and their inflexible and unnecessarily complicated code-structure (most obvious in version 2) betrays the programmer's former object-oriented background [83] (*cf.* the discussion of our adoption of a meta-language in chapter 4); other than the implementation of chapter 4, there is no intent to make the ones discussed in this appendix generally available. All versions (including version 4) are written in `Fortran-90`, striving for full standards [69] compliance.

B.1. Version 1: Non-linear PDE for the modified free energy

This initial implementation of HRT differs from its successors (as well as from what is referred to as the original implementation in chapter 4) in that it does not rely on the re-writing of the PDE in the form (2.23) superficially resembling a quasi-linear one (*cf.* appendix A); instead, eqs. (2.12) and (2.13) were subject to discretization in a straight-forward way, with the core condition implemented along the lines of section D.2 with the approximations of section D.3. Due to the markedly non-linear character of this PDE for the modified free energy $\mathcal{A}^{(Q)}(\varrho)$, convergence of an implicit finite-difference full-approximation scheme can only be ensured by

iteration of the corrector step; the need to keep the number of corrector iterations as low as possible without compromising the numerical procedure's convergence first led to the introduction of the central parameter $\epsilon_{\#}$ and early versions of a number of the criteria summarized in section 4.6. The PDE's numerical treatment relied on a second-order three-level predictor-corrector scheme similar to that of the original implementation: in particular, in the step leading from Q to $Q - \Delta Q$, the predictor produced an estimate for the solution at cut-off $Q - \frac{1}{2}\Delta Q$ only; as this is obviously inconvenient in iterations of the corrector step, later versions switched to a two-level algorithm, where the predictor step estimates the solution at $Q - \Delta Q$ directly.

As far as the reference system's description is concerned, in this version of the program only the PY approximation was implemented; there was some numerical evidence of this resulting in a smooth additional contribution to the isothermal compressibility κ_T as evaluated by differentiation of $\mathcal{A}^{(Q)}(\varrho)$ while the binodal (or ϱ_l at least) could still be made out from κ_T's near-discontinuity.

Incidentally, this first version was already fully capable of handling square wells with $\lambda = 1.5$, the primary test case for all the programs presented in this appendix, for super-critical temperatures, even though the computational cost was prohibitive (typically on the order of one hour of CPU time per isotherm for low-precision calculations on an alpha workstation). Upon increasing β beyond its critical value β_c, then estimated at around 0.85, however, the $\epsilon_{\#}$-based criteria led to dramatically falling step sizes ΔQ, which is a clear indication of the PDE's stiffness not being an artifact of the rewriting of appendix A; other than in the formulation first adopted in version 2 and used ever since, an attempt to force the solution's advancement towards Q_0 *via* pre-determined step sizes produced numerically undefined results only, *i. e.* the IEEE floating-point standard's special values of `NaN` or $\pm$`Inf` [70]. It was also with this implementation that the core-condition function $\mathcal{C}^{(Q)}(Q, \varrho)$ was first considered, *cf.* section 5.6.

B.2. Version 2: Not-quite quasi-linear PDE for an auxiliary quantity

Version 2 differs from its predecessor mainly in the adoption of the re-writing of appendix A (although in a somewhat simpler form considering density-independent potentials only) and the corresponding transition from the modified free energy $\mathcal{A}^{(Q)}(\varrho)$ to the auxiliary function $f(Q, \varrho)$; it was within the framework provided by this implementation that some of the problems discussed in chapter 5 were first uncovered and partly understood [84]. Just as version 1, this version, too, made use of `Fortran-90`'s built-in module system to enhance re-usability and flexibility of the program; but as experimentation with different approximations and re-factoring of some of the program's functionality continued, the need to accomodate

vastly different data structures became obvious, prompting the proliferation of a large number of partly incompatible module versions.

The discretization of the PDE again relied on an iterated predictor-corrector full-approximation scheme; despite the PDE's being of first order in Q and the use of a rectangular (Q, ϱ)-grid in a two-level scheme, in order to be able to apply $\epsilon_{\#}$-based criteria for assessing or choosing the step sizes in the $-Q$ direction from second-order derivatives we had to retain the solution at a third Q value in the calculation; by way of contrast, version 4 needs three node-lists in order to accomodate the possibility of a more general grid underlying the numerical calculation (*cf.* section 4.2).

The main conclusions drawn from experimentation with version 2 concern the problematic nature of the decoupling assumption (*cf.* section B.3) and of the boundary conditions as well as the numerical inaccessibility of the true solution in the region of large $f(Q, \varrho)$ in the PDE's domain. On the other hand, this program first allowed us to generate some solution all the way down to $Q = Q_0$ even below the critical temperature, albeit only when imposing the decoupling assumption and resigning on the local error's boundedness in the finite difference scheme; as can be seen from [84], it also became apparent that square wells could be treated for some λ values only [84].

B.3. Version 3: ODEs following from consistent application of the decoupling assumption

Other than versions 1, 2, and 4, version 3 of the program was never meant to implement HRT in a generally usable form; rather, its only point was to investigate the decoupling assumption's effects and to demonstrate its importance. To this end we implemented the solution of the ODEs following from consistent application of the decoupling assumption (2.21), *cf.* sub-section 2.2.2. Apart from minor changes concerning some of the $\epsilon_{\#}$-based criteria and the choice of basis functions (*cf.* section C.2), this version is fully equivalent to, and superseded by, one of the *ansatzes* discussed in section 4.5.

C. Implementational Details

In this appendix we want to shortly discuss some specialized aspects of the implementation of HRT presented in chapter 4; in particular, we highlight the *rôle* of the meta-language in our software and some of the facilities this offers for its potential users, and we give the explicit expressions for the set of basis functions u_n, $n \geq 1$, we use in the computations and compare it to some alternatives.

C.1. The `arfg` meta-language

As shortly mentioned in section 4.1, some of the most attractive features of our software have become possible only by our adoption of the simple meta-language `arfg`[1] constructed from readily available text-processing and scripting tools: In particular, this allows us to code in a manner not unlike the "literate programming" style pioneered by Knuth [85], although the pipelined nature of the system we use, originally inspired by Engelschall's `wml` system[2], more closely resembles Ramsey's `noweb` [86]. But where the traditional literate programming tools emphasize the production of high-quality documentation ("weaving") and constructing the code ("tangling") is seen as a rather trivial task, for `arfg` the focus is on flexible construction of code customized to the chosen combination of approximations and the physical system at hand instead; the resulting `Fortran-90` code is not meant for human inspection, and no pretty printing is performed.

As expected from this similarity to literate programming, the overall effect of adopting a meta-language is to enhance readability and maintainability of the source, at the same time encouraging modularization while providing us with enough flexibility to generate efficient and reliable `Fortran-90` code that takes into account as much information about the properties of the physical system as is feasible; furthermore, the free flow of information and the self-configuring nature of the code (*v. i.*) make it much easier to maintain consistency within the code base

[1] Available on the world wide web from `http://purl.oclc.org/NET/arfg/`. More precisely, `arfg` is a framework for the definition of a customized meta-language that co-evolved with the implementation of chapter 4 into its current state.

[2] Available from `http://www.engelschall.com/sw/wml/`.

and to introduce non-trivial changes[3]. As an added bonus, the expressive power of more modern programming or scripting languages provides a means of overcoming some of the limitations inherent to `Fortran-90`, mitigating its austerity to a certain extent.

The meta-language `arfg` itself is just a simple script written in `Perl` that does little more than feed the current source file, together with appropriate definitions, to a UNIX pipeline consisting of an arbitrary re-writing filter, GNU's `m4` macro processor, a diversion filter for accumulation and re-ordering of text blocks, and the `eperl` interpreter for embedded commands in the `Perl` language; the latter relies on the budding CAS `yacas`[4] for simple auxiliary calculations. With these tools, code construction usually proceeds by repeated application of the `arfg`-script to all source files until the output files — typically `Fortran-90`-code, interfacing information, include files, and customized scripts for compiling of the resulting program — no longer change; re-configuration of the software thus only means selection of the desired components followed by re-construction and re-compilation of the `Fortran-90` code. As a consequence of this organization none of the main parts can make any assumptions about the internal workings of any other main part, and the code produced must be generic with respect to any information not available *via* either the program's general design as sketched in section 4.2 or the interface provided by the code, usually in the form of `m4` definitions. This also means that optimizations valid only for special combinations of main parts have not been implemented; such a situation might arise, *e. g.*, for an `ansatz` (*cf.* section 4.5) implementing the core condition *via* the truncated eq. (2.18) if the $\hat{\mathcal{I}}$-integrals turn out to allow an analytical short-cut only for a certain choice of `potential` (*cf.* section 4.3; *v. i.* section C.2).

In order to provide a solution to this problem we have introduced a hook-mechanism reminiscent of that found in other programs but resolved during code construction rather than at run-time: wherever a hook has been declared in the `arfg`-source, arbitrary replacement text may be inserted at the `m4` step. In combination with automatic declaration of hooks during the initial re-writing step and with `arfg`'s subsequent filters, they provide an extremely powerful and versatile tool, opening up a wide range of possibilities: most obviously, already quite simple hook definitions allow for, *e. g.*, insertion of test code, additional evaluations and logging of selected quantities as well as the implementation of installation- and site-specifics, which allows one to deal, *e. g.*, with non fully standards compliant, inefficient or otherwise deficient `Fortran-90` compilers; slightly more advanced definitions may result in small-scale program transformations like the introduction of explicit caching of numerical results or the transformation of loop bodies into internal subroutines to prompt timely garbage collection should this be necessary.

In addition to the far-reaching code manipulation facilities offered by hooks, there are numerous parameters, usually endowed with reasonable default values, that may be used to customize specific aspects of the program; these fall into

[3] In this context the ability to maintain test code in the same source file as the implementation it is to act on proves particularly valuable.

[4] Available from `http://www.xs4all.nl/~apinkus/yacas.html`.

two groups: the "compile-time parameters" — *e. g.* the number $N_{\mathrm{cc}} + 1$ of basis functions u_n in eq. (2.18) or settings that are unlikely to be changed once a satisfactory value has been found — are specified as `m4` definitions and thus have to be processed during code construction, whereas the "options" — most prominently the temperature, $\epsilon_{\#}$, and the potential's parameters — are read from files at run-time. — Especially in a setting as variable as the one afforded by the `arfg`-approach to our implementation the main parts of which may freely be combined, anything less but thorough documentation is bound to render any results unusable in the long term; consequently, a suitable description of the program including both compile-time parameters and relevant options is generated automatically and stored together with the isotherm data produced. In a similar vein, it is important to assist the user in dealing with this system, in particular as far as selection of appropriate options and interpretation of error messages is concerned: to this end, well-documented templates for the options files are produced, and any run-time error messages include both the `Fortran-90` program unit and the `arfg` source file where it occurred.

C.2. The basis functions

According to section D.2 there is ample freedom in choosing the basis functions u_n, $n \geq 1$; in particular, there is no use for orthogonality properties *per se*, and regularity considerations in r space are of only minor interest — they play a *rôle* only for assessing convergence of the expansion (2.15) of $\mathcal{C}^{(Q)}(r, \varrho)$. All this amounts to the impression that the original implementation's choice of affine transforms of the Legendre polynomials might not be a particularly fortunate one.

As long as we deal with hard-sphere reference systems only, in view of the considerations of section D.2 it is natural to ask for the set $\{u_1(r), \ldots, u_{N_{\mathrm{cc}}}(r)\}$ to span the space of polynomials of order up to $N_{\mathrm{cc}} - 1$ so that $u_n(r)$ will generally be a polynomial or order $n - 1$ in r; but whereas different sets of polynomials do not alter the function space, their choice has implications for the numerical properties of the matrix equations implementing the core condition (*cf.* sections D.2 and D.3), as well as, to a certain extent, for the convergence of the $\hat{\mathcal{I}}$-integrals to be evaluated at $Q = Q_\infty$ (*cf.* section 4.5).

In our work we considered two different definitions of the u_n, $n \geq 1$: in the program's versions summarized in appendix B as well as in some very early implementations of version 4's main part `ansatz` not considered in section 4.5 we adopted basis functions orthonormalized in $]0, \sigma[$ with respect to the weighting function r^2; according to simple heuristic arguments this enhances the diagonal elements of the matrices in the truncated eq. (2.18) relative to the off-diagonal elements which might help in ensuring existence of a solution. Unfortunately, however, this choice of basis functions turns out to be insufficient to render the

matrices diagonally dominant due to the $(\tilde{u}_0(k,\varrho)\,\tilde{u}_n(0,\varrho))$-term in eq. (2.18); furthermore, the matrices' entries vary by several orders of magnitude which brings about additional numerical problems.

Based upon these experiences, in the software of chapter 4 we adopted a different and computationally more convenient set of basis functions instead, choosing $u_n(r,\varrho)$ simply proportional to r^{n-1} and normalizing it to $\tilde{u}_n(0,\varrho) = 1$. These functions are easily evaluated in r space, and the normalization condition renders evaluation of $\tilde{\mathcal{G}}^{(Q)}(0,\varrho)$, a term in the coefficients d_{0i} of eq. (A.5), particularly simple; also, all the entries of the matrices of eq. (2.18) are usually of the same order of magnitude, allowing Gaussian elimination with full pivoting to be used without the need for a re-scaling of the equations. — Dropping the obvious argument ϱ, with the *ansatz*

$$\begin{aligned} u_n(r) &= u_n(\sigma)\,\left(\frac{r}{\sigma}\right)^{n-1}\,\Theta(\sigma-r)\,, \\ \tilde{u}_n(0) &= 1\,, \end{aligned} \tag{1}$$

a simple calculation based upon eq. (F.1) and using eq. (2.633.1) of [87] easily yields[5] $u_n(\sigma) = (n+2)/4\pi\sigma^3$ as well as the Fourier transform

$$\tilde{u}_n(k) = \frac{n+2}{(\sigma k)^{n+2}}\,\left[n!\,\cos\frac{n\pi}{2} - \sum_{j=0}^{n}\frac{n!}{(n-j)!}\,(\sigma k)^{n-j}\,\cos\left(\sigma k + \frac{j\pi}{2}\right)\right]\,,$$

an expression used for $\sigma k > n$ only for numerical reasons. For smaller k, we rely on the expansion

$$\tilde{u}_n(k) = (n+2)\,\sum_{j=0}^{\infty}\frac{(-1)^j}{(n+2j+2)\,(2j+1)!}\,(\sigma k)^{2j}\,,$$

truncating the series to N_n terms, where N_n is the smallest number such that

$$\frac{n+2}{n+2N_n+4}\,\frac{n^{2N_n+2}}{(2N_n+3)!} \leq \epsilon_{\#}\,p_{N_n}^{[u_n]}$$

with a customization factor $p_{N_n}^{[u_n]}$ of order unity. Of course, analogous results may be derived for the basis functions' derivatives with respect to k. Note that the asymptotic behavior of the $\tilde{u}_n(k)$ for large k allows an analytic short-cut in the $\hat{\mathcal{I}}$-integrations of eq. (2.18) for certain forms of the Fourier transform of the perturbational part of the potential for $k \to \infty$ (*q. v.* section C.1); *e. g.* for SWS we can replace the large-k part of such an integration by a single evaluation of the sine-integral $\mathrm{si}(k)$ at finite k only (*cf.*, *e. g.*, eq. (2.642.7) of [87]; for the numerical evaluation of $\mathrm{si}(k)$ by continued fractions *cf.*, *e. g.*, [78]).

[5] Note that $\max_{r\in[0,\sigma]} u_n(r) = u_n(\sigma) \propto n+2$, which must be taken into account when using the maximum norm for discussing convergence of the expansion (2.15) for the direct correlation function.

D. Mathematical Supplement

In this appendix we spell out in detail some auxiliary calculations that would only hinder the flow of arguments in the main text, the presence of which nevertheless seems desirable for completeness' sake. The sections are given in no particular order.

D.1. The Q-potential in r-space

Much of the motivation for using the closure (2.15) despite its known and frequently referred-to short-comings is related to the artificial shape, and long-ranged nature, of the Q-potential defined in eq. (2.4). In order to see how this long-rangedness arises, for an arbitrary function $\psi(r)$ in real space we ask for the function $\psi^{(Q)}(r)$ obtained by this cut-off procedure. Taking into account eq. (F.1) in applying eq. (2.4), we obviously have

$$\begin{aligned} \tilde{\psi}(k) &= \frac{4\pi}{k} \int_0^\infty \mathrm{d}r\, r\, \psi(r)\, \sin kr\,, \\ \tilde{\psi}^{(Q)}(k) &= \tilde{\psi}(k)\, \Theta(k-Q)\,, \\ \psi^{(Q)}(r) &= \frac{1}{2\pi^2 r} \int_0^\infty \mathrm{d}k\, k\, \tilde{\psi}^{(Q)}(k)\, \sin kr\,. \end{aligned} \tag{1}$$

With Fourier's theorem and the identity $\Theta(k-Q) = 1-\Theta(Q-k)$, the last integral becomes

$$\begin{aligned} \psi^{(Q)}(r) &= \frac{1}{2\pi^2 r} \left(\int_0^\infty \mathrm{d}k\, k\, \tilde{\psi}(k)\, \sin kr - \int_0^Q \mathrm{d}k\, k\, \tilde{\psi}(k)\, \sin kr \right) \\ &= \psi(r) - \frac{1}{2\pi^2 r} \int_0^Q \mathrm{d}k\, k\, \tilde{\psi}(k)\, \sin kr\,; \end{aligned}$$

inserting the expression (1) for $\tilde{\psi}(k)$ in the last expression and assuming interchangeability of the integrations, we then obtain

$$\begin{aligned}
\psi^{(Q)}(r) - \psi(r) &= -\frac{4\pi}{2\pi^2 r} \int_0^Q \mathrm{d}k \int_0^\infty \mathrm{d}r'\, r'\, \psi(r') \sin kr \sin kr' \\
&= -\frac{2}{\pi r} \int_0^\infty \mathrm{d}r'\, r'\, \psi(r') \int_0^Q \mathrm{d}k \sin kr \sin kr' \\
&= -\frac{1}{\pi r} \int_0^\infty \mathrm{d}r'\, r'\, \psi(r') \int_0^Q \mathrm{d}k \left(\cos k(r'-r) - \cos k(r'+r)\right) \\
&= -\frac{1}{\pi r} \int_0^\infty \mathrm{d}r' r' \psi(r') \Bigg(\underbrace{\frac{\sin Q(r'-r)}{r'-r}}_{\text{“peak”}} - \underbrace{\frac{\sin Q(r'+r)}{r'+r}}_{\text{“regular”}} \Bigg)
\end{aligned} \tag{2}$$

where we have used the trigonometric relation $2 \sin a \sin b = \cos(a-b) - \cos(a+b)$. (Eq. (2.6) is obtained by replacing the general function ψ by the perturbation part w of the potential in the last expression.)

From eq. (2) the limits of eq. (2.3) are apparent: for $Q \to 0$, both sines obviously vanish, whereas for $Q \to \infty$ the first of these (labeled “peak”) reproduces the δ-function necessary for vanishing $\psi^{(\infty)}$ while the second one (“regular”) vanishes again. For an intermediate value of Q, however, it should be clear that the peak of width $\sim 1/Q$ coming from $\sin(Q\,(r'-r))/(r'-r)$ makes $\psi^{(Q)}(r)$ a long-ranged function in r space, rendering Fourier transformations unattractive at least for very small Q, *i. e.* in that part of the HRT evolution where criticality is recovered; on the other hand, due to the peak's height's proportionality to Q, in an approach relying on boundedness of relative errors by some small constant $\epsilon_\#$ we can expect to be able to restrict calculations in r space to a finite interval even in the limit $Q \to 0$.

To make this expectation somewhat more explicit, in the following we look at the contribution $\psi^{(Q)}_{\text{peak}}$ coming from the “peak” term for a function $\psi(r)$ of range R, *i. e.* for a function $\psi(r)$ that may be neglected for $r > R$ without incurring a relative error larger than $\epsilon_\#$; our aim is to estimate the range $R^{(Q)}$ of $\psi^{(Q)}(r)$ so that $\psi^{(Q)}(r)$ must be considered on the grounds of $\epsilon_\#$ only for $r < R^{(Q)}$. To this end, in the convolution integral eq. (2) we neglect the “regular” term as well as the contributions coming from the “peak” term outside of the main maximum, and we make the simple approximation of replacing the main peak of $\sin(Q\,(r'-r))/(r'-r)$ by a rectangle of equal width and area:

$$\frac{\sin Q(r'-r)}{r'-r} \Longrightarrow \frac{Q}{2}\,\Theta\left(|r'-r| - \frac{\pi}{Q}\right) \tag{3}$$

With this and restricting integration to ψ's domain, *viz.* $r < R$, only, we have

$$\begin{aligned}\psi^{(Q)}_{\text{peak}} &= -\frac{1}{\pi r}\int_0^R \mathrm{d}r'\,\psi(r')\,\frac{Q}{2}\,\Theta\left(|r'-r|-\frac{\pi}{Q}\right)\\ &= -\frac{Q}{2\pi\,r}\int_{\max(0,r-\frac{\pi}{Q})}^{\min(R,r+\frac{\pi}{Q})}\mathrm{d}r'\,r'\,\psi(r')\end{aligned} \tag{4}$$

where the integral is taken to vanish if $r-(\pi/Q) > R$; again, for $Q \to \infty$ we readily find $\psi^{(Q)}_{\text{peak}} \to -f$. For very small Q, on the other hand, the integral's bounds are, of course, 0 and R; assuming that ψ does not differ wildly from its mean value for $r \in [0, R]$, neglecting $\psi^{(Q)}(r)$ is compatible with $\epsilon_\#$ for $r > R^{(Q)}$, where $R^{(Q)} \propto Q$ is obtained from

$$\frac{Q}{2\pi\,R^{(Q)}}\int_0^R \mathrm{d}r'\,r' = \frac{Q\,R^2}{4\pi\,R^{(Q)}} = \epsilon_\# \qquad (Q \to 0) \tag{5}$$

(but note that the neglected terms, the "regular" contribution to $\psi^{(Q)}(r)$ in particular, enforce $R^{(Q)} \geq R$).

The behavior for intermediate values of Q is, of course, more complicated; shortly before the integration region of eq. (4) spans the whole of $[0, R]$, however, we must have $r-(\pi/Q) > 0$ and $r+(\pi/Q) > R$ for $r \geq R^{(Q)}$. Inserting this into eq. (4), by a reasoning analogous to that leading to eq. (5) we immediately find

$$\frac{Q}{2\pi\,R^{(Q)}}\int_{R^{(Q)}-\frac{\pi}{Q}}^R \mathrm{d}r'\,r' = \frac{Q}{4\pi\,R^{(Q)}}\left(Q^2-\left(R^{(Q)}-\frac{\pi}{Q}\right)^2\right) = \epsilon_\#\,. \tag{6}$$

This is a quadratic equation for $R^{(Q)}$ in terms of R and $\epsilon_\#$; ignoring terms of order $\mathcal{O}(\sqrt{\epsilon_\#})$ and depending on the value of Q, the $R^{(Q)}$ so found lies between $R+(\pi/Q)$ and π/Q, where the latter applies to very small Q.

With these approximate results for $\psi^{(Q)}_{\text{peak}}$ we are now in a position to find an explicit estimate for the maximum value of $R^{(Q)}$ as Q is varied from $+\infty$ to 0: the transition from intermediate Q, where eq. (6) applies, to the regime of eq. (5) takes place when the integration's lower bound in eq. (4) for evaluating $\psi^{(Q)}(R^{(Q)})$ first becomes 0, and the estimates for $R^{(Q)}$ as obtained from eq. (5) or from eq. (6) will then coincide. We thus have

$$\max_{0<Q<\infty} R^{(Q)} = \frac{\pi}{Q} = \frac{Q\,R^2}{4\pi\,\epsilon_\#}\,,$$

which is easily evaluated to[1]

$$\max_{0<Q<\infty} R^{(Q)} = \frac{R}{2\sqrt{\epsilon_\#}}. \tag{7}$$

Taking into account that $\epsilon_\#$ is supposed to be a small quantity hardly greater than 10^{-2} in typical calculations, we thus see that $\psi^{(Q)}(r)$ is indeed not only much longer ranged than $\psi(r)$ but has to be considered over an r range much larger than the domain of $\psi(r)$ if numerical errors resulting from the truncation of Fourier transformations in r space are not to render the results' accuracy incompatible with $\epsilon_\#$.

Thus it seems that an implementation of HRT in a formulation relying on Fourier transforms to implement the core condition might well be feasible, at least for modest values of $\epsilon_\#$; but in such an approach not only the cut off potential $w^{(Q)}$ but also more complicated functionals of $w^{(Q)}$ must be accomodated, and some of these are by necessity affected by at least partial cancellation[2]; this makes it impossible to determine the domain of integration in Fourier transformations beforehand in a way analogous to the estimates leading up to eq. (7). If, indeed, such an approach were to be used in HRT, it is not obvious how one might ensure local errors to remain bounded by $\epsilon_\#$ without providing for potentially repeated adjustment of the parameters of the Fourier transform in accordance with the results of monitoring the behavior of appropriate functions for large r, thereby rendering Fast Fourier Transform libraries, and the excellent `FFTW` code [88] in particular, largely useless. Furthermore, as the properties of the full potential on length scales comparable to σ must not be lost, the step size Δr remains fixed throughout the calculation so that a change in the r range considered is invariably accompanied by a corresponding change in the number of function values in the calculation, a procedure not necessarily unproblematic; also, the question of an appropriate choice for the grid for representing $\tilde{\psi}^{(Q)}(k)$ in Fourier space has not been addressed so far.

Thus, while a formulation of HRT with a closure depending on quantities both in real space and in Fourier space can conceivably be implemented, the long-rangedness introduced by the cut-off procedure defined in eq. (2.4) certainly renders the numerics much more involved and opens up a whole new suite of problems regarding Fourier transformations of cut-off affected quantities; at present, and in the light of the limitations of HRT in its current formulation as highlighted in section 2.4 and chapter 5, it is not clear that the improvements from the more appropriate closure relations then possible can be expected to justify the implementational effort.

[1] In eq. (7), the factor 1/2 is, of course, completely insignificant and a mere artifact of the crude approximation of eq. (3).

[2] Consider, *e. g.*, the modified direct correlation function in the critical region.

D.2. Implementation of the core condition and thermodynamic consistency by ordinary differential equations

With the *ansatz* of eq. (2.15), implementation of both the core condition (2.14) and thermodynamic consistency as embodied in the compressibility sum-rule (2.13) reduces to the correct choice of the expansion coefficients $\gamma_n^{(Q)}$, $n \geq 0$; as was first shown in [6], for the LOGA/ORPA-like closure this can be achieved without relying on costly and precarious Fourier transformations (*cf.* section D.1). In this section we present an analogous scheme, closely following but somewhat extending the calculations first reported in [6] and later generalized to non-hard sphere reference systems [2, 29]; just as [6] we start by assuming that both conditions, *viz.* eqs. (2.14) and (2.13), already hold for the reference system; furthermore, in the following we take convergence of sums and integrals as granted so that we may freely change the order of these operations as well as of any derivatives; infinite sums are interpreted in the obvious way; and the space spanned by the basis functions $u_n(r, \varrho)$, $|\{u_n\}| = \aleph_0$, is required to be sufficiently general (*v. i.*); note that the general result is not compatible with only a finite number N_{cc} of these basis functions.

As the core condition must be met for $Q = \infty$ (or, numerically, for $Q = Q_\infty$), this will also be the case if, and only if, the pair distribution function's derivative with respect to Q also vanishes for all $r \in [0, \sigma(\varrho)[$; with the OZ relation (2.8) in the form $\tilde{h}^{(Q)} = -(1/\varrho) - (1/\varrho^2\, \tilde{c}_2^{(Q)})$ and swapping the integration from the inverse Fourier transform and the differentiation with respect to Q this readily yields

$$
\begin{aligned}
0 = \frac{\partial\, g^{(Q)}(r,\varrho)}{\partial Q} &\propto \frac{\partial}{\partial Q} \int_0^\infty \mathrm{d}k \frac{k \,\sin kr}{c_2^{(Q)}(k,\varrho)} \\
&= \int_0^\infty \mathrm{d}k\, k \,\sin kr\, \frac{\partial}{\partial Q} \left(c_2^{(Q)}(k,\varrho) \right)^{-1}, \qquad r < \sigma(\varrho)\,;
\end{aligned}
$$

as the above involves the derivative of a term affected by the discontinuity of $\tilde{c}_2^{(Q)}$ (*cf.* the definition (2.11) of $\mathcal{C}^{(Q)}$), we have to distinguish two parts of the integration domain:

$$
\tilde{c}_2^{(Q)}(k,\varrho) = \begin{cases} \tilde{\mathcal{C}}^{(Q)}(k,\varrho) - \tilde{\phi}(k,\varrho) : k < Q \\ \tilde{\mathcal{C}}^{(Q)}(k,\varrho) : k > Q\,, \end{cases}
$$

so that

$$\begin{aligned}\frac{\partial}{\partial Q}\big(c_2^{(Q)}(k,\varrho)\big)^{-1} &= -\left(\frac{\Theta(Q-k)}{\big(\tilde{\mathcal{C}}^{(Q)}(k,\varrho)-\tilde{\phi}(k,\varrho)\big)^2}+\frac{\Theta(k-Q)}{\big(\tilde{\mathcal{C}}^{(Q)}(k,\varrho)\big)^2}\right)\frac{\partial\tilde{\mathcal{C}}^{(Q)}(k,\varrho)}{\partial Q}\\ &\quad+\frac{\tilde{\phi}(Q,\varrho)}{\tilde{\mathcal{C}}^{(Q)}(Q,\varrho)\big(\tilde{\mathcal{C}}^{(Q)}(Q,\varrho)-\tilde{\phi}(Q,\varrho)\big)}\,\delta(k-Q)\\ &= -\frac{1}{\big(\tilde{c}_2^{(Q)}(k,\varrho)\big)^2}\,\frac{\partial\tilde{\mathcal{C}}^{(Q)}(k,\varrho)}{\partial Q}\\ &\quad+\frac{\tilde{\phi}(Q,\varrho)}{\tilde{\mathcal{C}}^{(Q)}(Q,\varrho)\big(\tilde{\mathcal{C}}^{(Q)}(Q,\varrho)-\tilde{\phi}(Q,\varrho)\big)}\,\delta(k-Q)\,.\end{aligned}$$

From eq. (2.15), however, the Q-derivative of $\tilde{\mathcal{C}}^{(Q)}$ is easily evaluated to

$$\frac{\partial\tilde{\mathcal{C}}^{(Q)}(k,\varrho)}{\partial Q}=\sum_{n=0}^{\infty}\tilde{u}_n(k,\varrho)\,\frac{\partial\gamma_n^{(Q)}(\varrho)}{\partial Q}\,,\qquad r<\sigma(\varrho)\,,$$

and combining all these expressions and interchanging integration and summation we obtain

$$\begin{aligned}&\sum_{n=0}^{\infty}\frac{\partial\gamma_n^{(Q)}(\varrho)}{\partial Q}\int_0^{\infty}\mathrm{d}k\,\frac{k\,\tilde{u}_n(k,\varrho)}{\big(\tilde{c}_2^{(Q)}(k,\varrho)\big)^2}\,\sin kr\\ &\qquad=\frac{Q\,\tilde{\phi}(Q,\varrho)}{\tilde{\mathcal{C}}^{(Q)}(Q,\varrho)\big(\tilde{\mathcal{C}}^{(Q)}(Q,\varrho)-\tilde{\phi}(Q,\varrho)\big)}\,\sin Qr\,,\qquad r<\sigma(\varrho)\,.\end{aligned}$$

In this equation, the free variable r appears as $\sin Qr$ on the right hand side but under the integral, as $\sin kr$, on the left hand side; in order to extract the ODEs for the expansion coefficients $\gamma_n^{(Q)}(\varrho)$, we now multiply both sides by[3] $4\pi\,r\,u_j(r)$, $j\geq 1$, and integrate over $0<r<\sigma(\varrho)$; by once more changing the order of the integrations and taking into account eq. (F.2) we immediately recover the Fourier transform of u_j:

$$\begin{aligned}&\sum_{n=0}\frac{\partial\gamma_n^{(Q)}(\varrho)}{\partial Q}\int_0^{\infty}\mathrm{d}k\,\frac{k^2\,\tilde{u}_j(k,\varrho)\,\tilde{u}_n(k,\varrho)}{\big(\tilde{c}_2^{(Q)}(k,\varrho)\big)^2}\\ &\qquad=\frac{Q^2\,\tilde{\phi}(Q,\varrho)\,\tilde{u}_j(Q,\varrho)}{\tilde{\mathcal{C}}^{(Q)}(Q,\varrho)\big(\tilde{\mathcal{C}}^{(Q)}(Q,\varrho)-\tilde{\phi}(Q,\varrho)\big)}\,,\qquad j\geq 1.\end{aligned}$$

[3] Note that, in the limit of short potential range, *i. e.* for the potential $v^{\mathrm{core}}(r)$ considered in sub-section 5.2.1, with the usual choice of $u_0\propto w$ the following considerations are valid also for $j=0$.

Thus we arrive at the result that the core condition is completely equivalent to the combination of

$$\begin{aligned} & g^{\mathrm{ref}}(r,\varrho) = 0 \text{ for } r < \sigma(\varrho) \qquad \text{and} \\ & \sum_{n=0}^{\infty} \hat{\mathcal{I}}^{(Q)}[\tilde{u}_j(k,\varrho)\,\tilde{u}_n(k,\varrho),\varrho]\,\frac{\partial\gamma_n^{(Q)}(\varrho)}{\partial Q} \\ & \qquad = \frac{Q^2}{2\pi^2}\,\frac{\tilde{\phi}(Q,\varrho)\,\tilde{u}_j(Q,\varrho)}{\tilde{\mathcal{C}}^{(Q)}(Q,\varrho)\left(\tilde{\mathcal{C}}^{(Q)}(Q,\varrho)-\tilde{\phi}(Q,\varrho)\right)}\,, \qquad j \geq 1\,; \end{aligned} \tag{8}$$

the symbol $\hat{\mathcal{I}}$ so introduced — a convenient notation we will heavily rely on in section D.3 — we define as

$$\hat{\mathcal{I}}^{(Q)}[\psi(k,\varrho),\varrho] = \frac{1}{2\pi^2}\int_0^\infty \mathrm{d}k\,k^2\,\frac{\psi(k,\varrho)}{\left(\tilde{c}_2^{(Q)}(k,\varrho)\right)^2}\,, \tag{9}$$

where $\psi(k,\varrho)$ is an arbitrary spherically symmetric function (extension to non-rotationally invariant $\psi(\vec{k},\varrho)$ is straightforward [26, 27] but will not be considered here; note the discontinuity at $k = Q$ in the $\hat{\mathcal{I}}^{(Q)}$-integrand due to the presence of $\tilde{c}_2^{(Q)}$ rather than the continuous $\tilde{\mathcal{C}}^{(Q)}$, *v. i.* section D.3).

So far we have only made use of the core condition, and only r values inside the core have entered the derivation of eq. (8); however, under the assumptions stated at the beginning of this section $u_0(r,\varrho)$ has an expansion inside the core in terms of the $u_j(r,\varrho)$, $j \geq 1$, and the generalized matrix equation just derived (or its truncation to $N_{\mathrm{cc}}+1$ basis functions) cannot be invertible. On the other hand, the one additional real parameter can easily be fixed by imposing an additional constraint on the expansion coefficients $\gamma_n^{(Q)}(\varrho)$, $n \geq 0$; for the HRT-PDE with the closure (2.15) it is, of course, the compressibility sum-rule (2.13) itself that provides the information necessary to uniquely determine all the $\gamma_n^{(Q)}(\varrho)$, $n \geq 0$, provided the $u_n(r)$, $n \geq 1$, are linearly independent in $]0,\sigma(\varrho)[$; inserting the definition (2.11) into eq. (2.13) we find

$$\tilde{\mathcal{C}}^{(Q)}(0,\varrho) = \tilde{c}_2^{\mathrm{ref}}(0,\varrho) + \tilde{\phi}(0,\varrho) + \sum_{n=0}^{\infty}\gamma_n^{(Q)}(\varrho)\,\tilde{u}_n(0,\varrho) = -\frac{\partial^2\mathcal{A}^{(Q)}(\varrho)}{\partial\varrho^2}\,,$$

and again assuming that this already holds for the reference system it is sufficient to consider the above relation's derivative with respect to Q. Thus the compressibility sum-rule (2.13) turns out completely equivalent to

$$\begin{aligned} & \tilde{\mathcal{C}}^{\mathrm{ref}}(0,\varrho) = -\frac{\partial^2\mathcal{A}^{\mathrm{ref}}(\varrho)}{\partial\varrho^2} \qquad \text{and} \\ & \frac{\partial\gamma_0^{(Q)}(\varrho)}{\partial Q} = -\alpha^{(Q)}(\varrho) - \sum_{n=1}^{\infty}\frac{\partial\gamma_n^{(Q)}(\varrho)}{\partial Q}\,\tilde{u}_n(0,\varrho)\,, \end{aligned} \tag{10}$$

where we have made use of the normalization (2.16) and the symbol $\alpha^{(Q)}(\varrho)$ of eq. (2.17). — Eq. (10) now allows us to eliminate $\gamma_0^{(Q)}(\varrho)$ from the core condition (8), which directly leads to eq. (2.18), while the initial condition (2.19) merely expresses the equivalence of the reference system with the system at infinite cut-off, *i. e.* $c_2^{(\infty)} = c_2^{\mathrm{ref}}$.

By following the derivation of eqs. (8), (10) and (2.18), we also find what properties the set of basis functions must have in addition to the $u_j(r,\varrho)$ vanishing for $r > \sigma(\varrho)$ and $j \geq 1$; these requirements turn out to be remarkably moderate: indeed, for the combination of eqs. (8) and (10) to uniquely determine all the expansion coefficients it is sufficient that the $u_j(r,\varrho)$, $j \geq 1$, be linearly independent on $]0,\sigma(\varrho)[$; neither normalization nor orthogonality are required, and the latter concept is not even defined so far as we have not cared to introduce an inner product in the function space at hand. On the other hand we need a metric if we want to speak of convergence of the expansion (2.15) for $\mathcal{C}^{(Q)}(r,\varrho)$, and for its validity the space spanned by the $u_j(r,\varrho)$, $j \geq 1$, must lie dense in some appropriate Banach space over $]0,\sigma(\varrho)[$, a natural choice being $L_2([0,\sigma(\varrho)])$. It is thus sufficient to let $u_j(r,\varrho)$, $j \geq 1$, be a polynomial of degree $j-1$ within the core; the remaining considerable amount of freedom can still be used to optimize the basis functions' numerical properties, *cf.* section C.2.

Another point worth making concerns the way a description of the reference system that is not thermodynamically self-consistent may be used in HRT: While approximations like, *e. g.*, the Percus-Yevick one do yield vanishing $g^{(Q)}(r,\varrho)$ for $r < \sigma(\varrho)$ as called for by eq. (8), they fail to also meet the requirements of eq. (10); on the other hand, as the derivation of the matrix equation (2.18) detailed in this section hinges on the compressibility sum-rule's validity for the reference system we immediately conclude that the free energy for infinite cut-off Q (or at finite $Q = Q_\infty$, for that matter, taking into account the zero-loop terms of eq. (2.11)) should be obtained by the compressibility route so that the pre-condition of eq. (10) holds again.

D.3. Approximation for Q-dependence of core-condition integrals

Considering the ideal-gas term $-1/\varrho$ in $\tilde{c}_2^{(Q)}$ and large k only it is evident that the oscillatory nature of the basis functions' Fourier transforms $\tilde{u}_n$ will immediately carry over to the integrands of the $\hat{\mathcal{I}}^{(Q)}$-terms in eqs. (2.18) and (8), rendering these integrations slowly convergent and certainly no less problematic than the Fourier transformations they allow to avoid. In this section we want to discuss an approximation that makes an implementation along the lines of section D.2 feasible by bringing the number of $\hat{\mathcal{I}}^{(Q)}$-integrations necessary down to only one per density; that even the remaining initial integration still takes up a considerable

fraction of the program's execution time in a typical application of the implementation sketched in chapter 4 (unless an analytical short-cut is taken, *v. i.*, *q. v.* section C.2) dramatically underlines the practical importance of adopting such an approximation.

This approximation is simple enough: rather than re-evaluating the $\hat{\mathcal{I}}^{(Q)}$-integrals for every Q, it is sufficient to calculate only the derivative with respect to Q and integrate the resulting ODEs alongside the HRT-PDE; assuming interchangeability of differentiation and integration and taking into account the integrand's discontinuity at $k = Q$ due to the appearance of $\tilde{c}_2^{(Q)}$ instead of the continuous $\tilde{\mathcal{C}}^{(Q)}$, from eq. (9) we easily find

$$\begin{aligned}
&\frac{\partial\,\hat{\mathcal{I}}^{(Q)}[\psi(k,\varrho),\varrho]}{\partial Q} \\
&\quad= \int_0^\infty \mathrm{d}k\,\frac{k^2\,\psi(k,\varrho)}{2\pi^2}\,\frac{\partial}{\partial Q}\left(\frac{\Theta(Q-k)}{\left(\tilde{\mathcal{C}}^{(Q)}(k,\varrho)-\tilde{\phi}(k,\varrho)\right)^2}+\frac{\Theta(k-Q)}{\left(\tilde{\mathcal{C}}^{(Q)}(k,\varrho)\right)^2}\right) \\
&\quad= \int_0^\infty \mathrm{d}k\,\frac{k^2\,\psi(k,\varrho)}{2\pi^2}\left(\frac{-2\,\Theta(Q-k)}{\left(\tilde{\mathcal{C}}^{(Q)}(k,\varrho)-\tilde{\phi}(k,\varrho)\right)^3}+\frac{-2\,\Theta(k-Q)}{\left(\tilde{\mathcal{C}}^{(Q)}(k,\varrho)\right)^3}\right)\frac{\partial\tilde{\mathcal{C}}^{(Q)}(k,\varrho)}{\partial Q} \\
&\qquad+ \int_0^\infty \mathrm{d}k\,\frac{k^2\,\psi(k,\varrho)}{2\pi^2}\left(\frac{1}{\left(\tilde{\mathcal{C}}^{(Q)}(k,\varrho)-\tilde{\phi}(k,\varrho)\right)^2}-\frac{1}{\left(\tilde{\mathcal{C}}^{(Q)}(k,\varrho)\right)^2}\right)\delta(k-Q) \\
&\quad= -2\sum_{n=0}^{\infty}\hat{\mathcal{I}}^{(Q)}\left[\frac{\psi(k,\varrho)\,\tilde{u}_n(k,\varrho)}{\tilde{c}_2^{(Q)}(k,\varrho)},\varrho\right]\frac{\partial\gamma_n^{(Q)}(\varrho)}{\partial Q} \\
&\qquad+ \psi(Q)\,\frac{Q^2}{2\pi^2}\,\frac{2\,\tilde{\mathcal{C}}^{(Q)}(Q,\varrho)\,\tilde{\phi}(Q,\varrho)-\left(\tilde{\phi}(Q,\varrho)\right)^2}{\left(\tilde{\mathcal{C}}^{(Q)}(Q,\varrho)\right)^2\left(\tilde{\mathcal{C}}^{(Q)}(Q,\varrho)-\tilde{\phi}(Q,\varrho)\right)^2}
\end{aligned}$$

where $\psi(k,\varrho)$ once more plays the *rôle* of an arbitrary spherically symmetric function and we have used eq. (2.11) to evaluate the Q-derivative of $\tilde{\mathcal{C}}^{(Q)}$ in the last step. Of these terms, the one stemming from the change in the discontinuity's location, dubbed the 'local' contribution in [6], is easily evaluated at any Q as it involves functions evaluated at $k = Q$ only; by way of contrast, the 'non-local' term related to the expansion coefficients' change again involves an integral of the same type as before. Note that the latter will, in fact, converge somewhat more readily than $\hat{\mathcal{I}}^{(Q)}[\psi,\varrho]$ itself due to the large-k behavior of the factor $\tilde{u}_n(k,\varrho)$ in the integrand; still, its evaluation will just the same be plagued by near-cancellation of the integrand's oscillations' contributions, and performing the integrations at every Q would incur prohibitive computational cost. — Even though it is far from clear that the $\hat{\mathcal{I}}^{(Q)}$-term's magnitude is small when compared to that of the local term, it is convenient to adopt the strategy first introduced in [6] and seemingly unvaryingly used ever since when implementing the core condition and thermodynamic consistency along the lines of section D.2, *i. e.*, to simply drop the non-local

term with its numerically expensive and cumbersome integrations, leading to the approximation

$$\frac{\partial}{\partial Q}\hat{\mathcal{I}}^{(Q)}[\psi(k,\varrho),\varrho] \Longrightarrow \psi(Q,\varrho)\,\frac{Q^2}{2\pi^2}\,\frac{2\,\tilde{\mathcal{C}}^{(Q)}(Q,\varrho)\,\tilde{\phi}(Q,\varrho) - \left(\tilde{\phi}(Q,\varrho)\right)^2}{\left(\tilde{\mathcal{C}}^{(Q)}(Q,\varrho)\right)^2\,\left(\tilde{\mathcal{C}}^{(Q)}(Q,\varrho) - \tilde{\phi}(Q,\varrho)\right)^2}\,. \tag{11}$$

Of course, eq. (11) is not well justified *a priori*; as pointed out in [6], it is only by checking that the resulting pair distribution function $g^{(Q)}(r,\varrho)$ remains small within the core — which is feasible only in the limits of eq. (2.3) due to the long-rangedness of the $\phi^{(Q)}(r,\varrho)$ for intermediate Q (*cf.* section D.1) — and by independently verifying thermodynamic consistency that the above approximation may be found admissible (*q. v.* section 5.2).

In the above calculation we have used an arbitrary function $\psi(k,\varrho)$ for $\hat{\mathcal{I}}^{(Q)}$ to operate on, whereas only certain combinations of the basis functions' Fourier transforms are considered in eqs. (2.18) and (8); it is well conceivable that these integrals may be amenable to an analytical short-cut so that the numerical integration has to be extended over only a small k-range. *E. g.*, for the basis functions of section C.2 this is the case whenever the leading term in $\tilde{w}(k,\varrho)$ (and thus, of basis function $\tilde{u}_0(k,\varrho)$) is of the form $\sin(ak+b)/k^2$; replacing $\tilde{c}_2^{(Q)}(k,\varrho)$ by $-1/\varrho$ and considering leading terms only, for large k the integral can formally solved and evaluated numerically by the use of a continued-fractions series for the sine integral function. Still, such an approach obviously depends on the potential chosen (which has certain implications for the implementation of chapter 4, *cf.* section C.1), and even where the analytical short-cut is available, its applicability only for large k renders this mode of evaluation still too costly to repeat at every step in Q and ϱ.

Also we should point out that, with the usual choice of $Q_\infty \sim 10^2/\sigma$, extending the initial integration only up to $k = Q_\infty$ is completely unsatisfactory and cannot be expected to lead to an acceptable implementation of core condition and thermodynamic consistency.

E. Tables

On the pages to follow we collect some of the numerical results we obtained in tabular form.

E.1. Critical temperature and density for square wells of variable range with $7+1$ basis functions

In this section we present the critical temperature T_c and critical density ϱ_c of square well systems for various values of λ as predicted by HRT with $N_{\mathrm{cc}} = 7$ (other parameters as in section 4.8). These are the data underlying fig. 5.4, *cf.* the discussion in section 5.6.

λ	$k_B\,T_c/\epsilon$	$\varrho_c\,\sigma^3$
1.06	1.247607(49)	0.415(25)
1.065	1.116157(22)	0.430(20)
1.07	0.983168(38)	0.445(25)
1.09	1.304243(35)	0.450(30)
1.1	1.1359488(47)	0.460(20)
1.11	1.0342880(46)	0.450(20)
1.13	1.0969009(50)	0.470(10)
1.14	0.9328253(47)	0.480(20)
1.15	1.239469(31)	0.430(20)
1.16	1.1441553(49)	0.420(10)
1.17	1.095618(37)	0.455(15)
1.18	0.971344(31)	0.460(20)
1.19	1.058746(31)	0.420(20)
1.2	0.9638977(44)	0.415(15)
1.21	0.959198(31)	0.460(20)
1.22	0.8355684(43)	0.490(10)
1.24	1.003369(49)	0.415(15)

(contd.)

λ	$k_B\,T_c/\epsilon$	$\varrho_c\,\sigma^3$
1.45	0.938257(24)	0.300(10)
1.455	0.935561(50)	0.295(15)
1.46	0.932264(29)	0.295(15)
1.465	0.9280290(47)	0.300(10)
1.48	0.985574(46)	0.280(10)
1.485	0.99222(25)	0.280(20)
1.49	0.999573(37)	0.275(15)
1.495	1.007487(46)	0.275(15)
1.5	1.015479(49)	0.275(15)
1.505	1.023449(50)	0.275(15)
1.51	0.929114(37)	0.275(15)
1.515	0.933961(50)	0.270(10)
1.52	0.939642(25)	0.270(10)
1.525	0.94567(25)	0.270(20)
1.53	0.952911(31)	0.265(15)
1.535	0.960687(50)	0.265(15)
1.91	0.421395(11)	0.270(10)
1.92	0.410502(11)	0.270(10)
1.939	0.399557(11)	0.270(10)
1.94	0.398622(11)	0.270(10)
1.941	0.397687(11)	0.270(10)
1.942	0.396741(11)	0.270(10)
1.943	0.395785(11)	0.270(10)
1.945	0.393867(11)	0.270(10)
1.946	0.392913(11)	0.275(15)
1.947	0.391933(11)	0.270(10)
1.948	0.390958(11)	0.275(15)
1.949	0.389981(11)	0.275(15)
1.95	0.388988(11)	0.275(15)
1.951	0.387993(11)	0.275(15)
1.952	0.386980(11)	0.275(15)
1.953	0.385967(11)	0.275(15)
1.954	0.384935(11)	0.275(15)
1.955	0.383903(10)	0.280(10)
1.956	0.382871(10)	0.280(10)
1.958	0.380773(10)	0.280(10)
1.959	0.379705(12)	0.280(10)
1.96	0.378640(10)	0.280(10)
1.97	0.381476(10)	0.275(15)
1.975	0.385001(10)	0.270(10)
1.98	0.380143(10)	0.270(10)
1.985	0.359343(10)	0.280(10)
1.99	0.3541496(99)	0.285(15)

(contd.)

λ	$k_B\,T_c/\epsilon$	$\varrho_c\,\sigma^3$
1.995	0.3487383(98)	0.285(15)
2.0	0.3430749(97)	0.290(10)
2.005	0.3417560(97)	0.290(10)
2.01	0.3353786(96)	0.295(15)
2.015	0.3530471(95)	0.275(15)
2.02	0.3489358(94)	0.280(10)
2.025	0.3447285(94)	0.280(10)
2.03	0.3337710(93)	0.285(15)
2.035	0.3347087(92)	0.280(10)
2.04	0.3298508(91)	0.285(15)
2.05	0.3321901(90)	0.275(15)
2.06	0.3236569(89)	0.285(15)
2.07	0.3054373(87)	0.295(15)
2.08	0.2949694(86)	0.315(15)
2.09	0.3121407(85)	0.280(10)
2.1	0.3047839(83)	0.285(15)
2.12	0.2971047(81)	0.285(15)
2.14	0.2820428(78)	0.295(15)
2.16	0.2801630(76)	0.280(10)
2.18	0.269303(13)	0.290(10)
2.2	0.2634137(79)	0.285(15)
2.21	0.2584991(92)	0.290(10)
2.22	0.2473085(70)	0.300(10)
2.23	0.2566864(92)	0.275(15)
2.24	0.2524211(95)	0.280(10)
2.25	0.2448761(92)	0.285(15)
2.26	0.240805(10)	0.285(15)
2.28	0.2325036(64)	0.285(15)
2.3	0.2334408(62)	0.275(15)
2.32	0.2234691(60)	0.275(15)
2.33	0.2234528(92)	0.275(15)
2.34	0.2173783(59)	0.275(15)
2.36	0.2112648(57)	0.275(15)
2.38	0.2075895(56)	0.270(10)
2.4	0.2017438(54)	0.270(10)
2.42	0.1974284(53)	0.270(10)
2.44	0.1908109(52)	0.275(15)
2.46	0.1871306(50)	0.270(10)
2.48	0.1784964(49)	0.275(15)
2.5	0.1780193(48)	0.270(10)
2.52	0.1705328(47)	0.270(10)
2.54	0.1647649(45)	0.275(15)
2.55	0.1635040(55)	0.275(15)

(contd.)

λ	$k_B\,T_c/\epsilon$	$\varrho_c\,\sigma^3$
2.56	0.1610674(44)	0.275(15)
2.57	0.1587360(55)	0.270(10)
2.58	0.1564089(43)	0.275(15)
2.59	0.1559131(49)	0.270(10)
2.6	0.1537577(42)	0.270(10)
2.62	0.1499922(41)	0.270(10)
2.64	0.1460387(40)	0.270(10)
2.66	0.1401607(39)	0.275(15)
2.68	0.1402388(38)	0.270(10)
2.7	0.1349930(38)	0.270(10)
2.72	0.1345349(37)	0.270(10)
2.74	0.1292534(36)	0.270(10)
2.75	0.1276306(61)	0.270(10)
2.76	0.1278133(35)	0.270(10)
2.78	0.1252788(34)	0.270(10)
2.8	0.1224374(34)	0.265(15)
2.82	0.1190511(33)	0.270(10)
2.84	0.1171284(32)	0.265(15)
2.86	0.1152180(31)	0.265(15)
2.88	0.1123890(31)	0.265(15)
2.9	0.1111786(30)	0.260(10)
2.92	0.1087431(30)	0.260(10)
2.94	0.1067793(29)	0.260(10)
2.96	0.1051046(28)	0.260(10)
2.98	0.1029332(28)	0.260(10)
3.0	0.1013445(27)	0.260(10)
3.025	0.0989655(31)	0.260(10)
3.05	0.0967575(46)	0.260(10)
3.075	0.0946991(31)	0.260(10)
3.1	0.0934158(46)	0.255(15)
3.125	0.0908478(31)	0.255(15)
3.15	0.0879250(23)	0.260(10)
3.175	0.0869965(31)	0.255(15)
3.2	0.0848534(23)	0.250(10)
3.225	0.0823944(31)	0.255(15)
3.25	0.0810376(24)	0.255(15)
3.275	0.0784332(31)	0.255(15)
3.3	0.0764185(24)	0.255(15)
3.325	0.0748260(31)	0.255(15)
3.35	0.0735229(24)	0.250(10)
3.375	0.0710968(31)	0.260(10)
3.4	0.0697437(24)	0.260(10)
3.425	0.0680145(31)	0.255(15)

(contd.)

λ	$k_B\,T_c/\epsilon$	$\varrho_c\,\sigma^3$
3.45	0.0662378(24)	0.260(10)
3.46	0.0656219(31)	0.255(15)
3.47	0.0650055(31)	0.255(15)
3.48	0.0643829(31)	0.255(15)
3.49	0.0638092(31)	0.255(15)
3.5	0.0631128(24)	0.260(10)
3.51	0.0625702(31)	0.260(10)
3.52	0.0619354(31)	0.260(10)
3.53	0.0613312(31)	0.260(10)
3.54	0.0607468(15)	0.260(10)
3.55	0.0601831(24)	0.260(10)
3.56	0.0595261(15)	0.260(10)
3.58	0.0586105(15)	0.260(10)
3.6	0.0572647(15)	0.260(10)

E.2. Critical temperature and density for square wells of variable range with $5+1$ basis functions

We here list the results on the critical temperature's λ-dependence in SWs as obtained with $N_{cc} = 5$ (other parameters as in section 4.8) as well as estimates of the reciprocal of $\beta_{max,\#}$, the lowest temperature where the program terminates normally, where available. The reader will notice not only that a larger fraction of the parameter range $1 < \lambda \leq 2$ is accessible to HRT than for $N_{cc} = 7$ (*cf.* section E.1) but also that the fluctuations in the critical temperatures are considerably higher. In the light of section 5.6 the behavior of $\beta_{max,\#}$ around $\lambda \sim 1.7$ is of particular interest, and the small-λ data, showing dramatically falling $\beta_{max,\#}$ for $\lambda \to 1+$, provides some support for the considerations of sub-section 5.2.1.

λ	$k_B\,T_c/\epsilon$	$1/\beta_{max,\#}\,\epsilon$
1.01	—	3.414(45)
1.02	—	1.574(54)
1.03	—	0.9884(38)
1.04	—	0.861(16)
1.05	—	0.7232(41)
1.06	—	0.6739(41)
1.07	—	0.6432(32)
1.08	—	0.563088(16)
1.09	0.5303591(17)	0.5255(39)

(contd.)

λ	$k_B\,T_c/\epsilon$	$1/\beta_{\mathrm{max},\#}\,\epsilon$
1.095	0.56064(15)	—
1.1	0.592238(18)	—
1.105	0.62573(19)	—
1.11	0.663002(88)	0.47(16)
1.12	0.75075(23)	0.379(56)
1.1225	0.581899(81)	—
1.125	0.592354(63)	—
1.13	0.613467(68)	—
1.135	0.635316(81)	0.598(27)
1.14	0.658241(74)	—
1.15	0.708210(80)	—
1.16	0.76849(37)	0.590(35)
1.18	0.784135(61)	0.57(15)
1.185	0.81496(33)	—
1.19	0.84992(10)	0.650(59)
1.195	0.887887(77)	0.690(24)
1.2	0.93015(11)	—
1.205	0.977566(94)	0.750(83)
1.2075	0.78558(30)	—
1.21	0.795868(82)	—
1.22	0.838574(84)	0.583(83)
1.23	0.886407(94)	—
1.24	0.943005(98)	—
1.26	0.95179(10)	—
1.27	1.01017(10)	—
1.28	1.07919(10)	—
1.29	1.16129(13)	—
1.2925	1.18416(34)	—
1.295	0.965582(91)	0.741(92)
1.3	0.984485(87)	—
1.32	1.07380(10)	—
1.34	1.07236(11)	0.87(13)
1.36	1.17318(10)	—
1.38	1.087623(85)	—
1.4	1.15735(11)	—
1.41	1.19872(34)	—
1.42	1.24397(10)	—
1.43	1.19174(34)	—
1.44	1.228172(92)	—
1.45	1.26693(39)	—
1.46	1.305492(99)	—
1.47	1.20562(33)	—
1.48	1.23139(17)	—

(contd.)

λ	$k_B\,T_c/\epsilon$	$1/\beta_{\mathrm{max},\#}\,\epsilon$
1.49	1.25888(35)	—
1.5	1.28732(17)	—
1.52	1.29559(17)	—
1.54	1.33876(18)	—
1.55	1.35624(35)	—
1.56	1.33770(16)	—
1.57	1.35591(17)	1.008(91)
1.575	1.36448(17)	1.019(93)
1.576	1.36599(17)	1.181(69)
1.578	1.36902(17)	1.181(69)
1.58	1.37218(17)	1.181(69)
1.59	—	1.3832(96)
1.6	—	1.468364(65)
1.608	—	1.49403(74)
1.616	—	1.8071(10)
1.625	—	1.9392(94)
1.65	—	2.289(13)
1.675	—	2.494(14)
1.7	—	2.7686(11)
1.725	—	2.891(17)
1.75	—	2.972(17)
1.775	—	2.793(15)
1.8	—	2.7153(16)
1.82	—	2.786(17)
1.84	—	2.588(11)
1.86	—	2.401(13)
1.88	—	2.2920(68)
1.89	—	2.174(14)
1.895	—	2.088(13)
1.896	2.13667(21)	1.94(19)
1.897	2.13847(21)	1.94(19)
1.898	2.14029(21)	1.94(19)
1.9	2.14415(11)	1.94(19)
1.92	2.18069(86)	1.59(22)
1.94	2.27428(88)	1.68(25)
1.96	2.31621(86)	—
1.97	2.33803(87)	—
1.98	2.36061(89)	—
1.99	2.4996(10)	—
2.0	2.52733(25)	—
2.02	2.5860(10)	—
2.04	2.7041(11)	—
2.06	2.7748(11)	—

(contd.)

λ	$k_B\,T_c/\epsilon$	$1/\beta_{\mathrm{max},\#}\,\epsilon$
2.08	2.9519(12)	—
2.1	3.03503(30)	—
2.2	3.6959(31)	—
2.3	4.41721(49)	—
2.4	5.22450(57)	—
2.5	5.887(21)	—
2.6	6.66916(76)	—
2.7	7.44070(83)	—
2.8	8.18652(87)	—
2.9	8.92347(96)	—
2.94	9.2563(39)	—
2.96	9.4069(40)	—
2.98	9.5890(40)	—
3.0	9.7371(10)	—
3.02	9.9620(42)	—
3.04	10.1193(43)	—
3.06	10.3178(44)	—
3.1	10.6301(11)	—
3.2	11.7840(12)	—
3.3	12.9604(14)	—
3.4	14.2922(15)	—
3.5	15.8032(17)	—
3.6	17.4047(19)	—
3.7	19.1095(21)	—
3.8	20.7190(22)	—
3.9	22.4488(25)	—
4.0	24.1788(26)	—

F. Notation, Conventions, and Abbreviations

In this appendix we summarize the mathematical, notational and presentational conventions used throughout this text, complete with pointers to the symbols' definitions and short descriptions, as well as some of the abbreviations used.

Much of the presentation below is in tabular form but interspersed in the text; in these lists, the first column gives the quantity to be defined, the second column (which may be missing) references the equation introducing it, and the third provides a short description of the quantity under consideration.

F.1. Notation

F.1.1. Modifiers for symbols

In view of the pivotal *rôle* a hierarchy of physical systems plays for the development of HRT it is natural to modify a given symbol's meaning by various super- and subscripts indicating the system or the thermodynamic state it refers to; in particular, for any quantity x, the following quantities are defined:

$x_{\#}$	quantity x in the context of numerical evaluation
$\tilde{x}$	three-dimensional Fourier transform of x
x_c	x at the system's critical point
x_v	x at the binodal's vapor branch
x_l	x at the binodal's liquid branch
x^y	x for the system indicated by y; in particular, as special cases we have:
$x^{(Q)}$	x for the system with cut-off Q
x^v	x for the system with potential v

Consequently, $x^{v^{(Q)}}$ and $x^{(Q)}$ are equivalent. — Among the labels that can take the place of y in the above list, the following are used frequently:

ref	(2.1)	reference system
hs	(2.1)	hard sphere system
core	(3.5)	system where w vanishes for $r > \sigma$
sw	(3.1)	square well system
st	(3.4)	general multi-step system
st′	(3.3)	general multi-step system (different parametrization than for "st")
hcy	(3.2)	hard-core Yukawa system

Note that the parameters these potentials depend on may be added in brackets; for the parameters appropriate for some of the potentials listed above, see the respective defining equations.

F.1.2. Symbols

The following sub-sections list those of the symbols used in the text the definition or meaning of which might not be self-evident, even though their use is standard practice for the most part; we do, however, leave out some symbols that are used only in a short passage and should thus easily be identified from context. Note that these symbols may still be modified according to sub-section F.1.1 where this makes sense, and that different entities of the same kind may be distinguished by indices.

F.1.2.1. Greek symbols

α	(2.17)	auxiliary quantity, related to third-order partial derivative of $\mathcal{A}$; table 2.1 only: critical exponent.
β		$1/k_B\,T$; table 2.1 only: critical exponent.
$\beta_{\max}$		maximum β amenable to HRT
$\beta_{\max,\#}$		maximum β accessible to the implementation of chapter 4
γ		table 2.1 only: critical exponent
γ_n	(2.15)	expansion coefficients in closure
ΔQ		step size in Q
$\Delta\varrho$		step size in ϱ
$\Delta Q\|_\infty$		limit of the pre-determined step sizes for infinite cut-off in the implementation of main part solver discussed in sub-section 4.6.2
δ		Dirac generalized function; parameter of potential $v^{\mathrm{st}'}$; table 2.1 only: critical exponent.
$\delta\gamma_0$		sub-section 2.4.1 only: a hypothetical small error introduced in γ_0
ϵ		energy-like potential parameter

$\epsilon_{\#}$		pivotal parameter governing the numerics, characteristic of maximum relative error admissible in any step
ε	(A.3)	auxiliary quantity
$\bar{\varepsilon}$	(A.3)	$\varepsilon - 1$
η		table 2.1 only: critical exponent.
Θ		Heaviside function
κ_T	(A.4)	isothermal compressibility
λ		dimensionless potential parameter indicative of the range in r-space of some component of the potential
ν		table 2.1 only: critical exponent.
ϱ		particle number density
σ	(2.1)	hard-core diameter
ϕ	(2.5)	$-\beta\, w$
ψ		an arbitrary function

F.1.2.2. Hebrew symbols

$\aleph_0$		cardinality of $\mathbb{Z}$
$\aleph_1$		cardinality of $\mathbb{R}$

F.1.2.3. Latin symbols

A		free energy
$\mathcal{A}$	(2.10)	modified free energy
$\mathcal{C}$	(2.11)	modified c_2
c_n		n-particle direct correlation function
d_0	(2.25)	sub-section 2.3.2 only: auxiliary function related to the total derivative of $f(Q, \varrho)$ with respect to Q, of order $\mathcal{O}(1)$ for large $\varepsilon(Q, \varrho)$.
d_{0i}	(A.5)	coefficients of the PDE in the form (2.23)
f	(A.1)	auxiliary function for re-writing the HRT-PDE in a form superficially resembling a quasi-linear one
g		pair distribution function
h		total correlation function
$\hat{\mathcal{I}}$	(D.9)	short-hand notation for certain integrals in Fourier space with discontinuous integrand
k		wavenumber
k_B		Boltzmann's constant
N_{cc}		number of basis functions vanishing outside the core
N_ϱ		the number of ϱ-intervals in the density grid, which is one less than the number of ϱ values considered

$\mathcal{O}(\cdots)$		terms of the order indicated
$p_y^{[x]}$		customization parameters of the numerical procedure for controlling some quantity x *via* some criterion identified by the label y
Q		cut-off wavenumber
Q_0		smallest Q considered numerically
Q_∞		largest Q considered numerically
r		distance
$\mathbb{R}$		the set of reals
T		thermodynamic temperature
u	(C.1)	basis functions in the expansion (2.15) for $\mathcal{C}$.
v		interparticle potential
w	(2.2)	perturbational part of potential $v^{(0)}$
x		section 4.6 only: a quantity monitored for choosing and assessing step sizes ΔQ
y		section 4.6 only: a quantity monitored for assessing convergence of corrector steps and indirectly affecting step sizes ΔQ
$\mathbb{Z}$		the set of integers
z		inverse screening length of Yukawa potential; section 2.1 only: fugacity

F.1.2.4. Miscellaneous

$a \propto b$		proportionality of a and b
$a \Longrightarrow b$		replacement of a by b
$[a, b]$		closed interval extending from a to b
$]a, b[$		open interval extending from a to b
$\|x\|_Q$	(4.2)	L_∞-norm of x on $]Q, \infty[$

As far as the notation for intervals is concerned, there are, of course, also the mixed cases not mentioned in the above list.

F.2. Mathematical conventions

One important convention regards the choice of constants in Fourier transformations; restricting ourselves to the spherically symmetric case in three dimensions, for any function $\psi(r)$ we define the Fourier transform $\tilde{\psi}(k)$ as

$$\tilde{\psi}(k) = \frac{4\pi}{k} \int_0^\infty \psi(r)\, \sin(kr)\, r\, \mathrm{d}r\,; \tag{1}$$

thus, the inverse transform is

$$\psi(r) = \frac{1}{2\pi^2 r} \int_0^\infty \tilde{\psi}(k)\, \sin(kr)\, k\, \mathrm{d}k\,. \tag{2}$$

F.3. Abbreviations

In the text we make use of a number of abbreviations, some of which are specific to this work while others are generally accepted in English prose or for the field of liquid theory but may be unfamiliar to some readers.

APT2	second-order perturbation theory
CAS	Computer algebra system
cf.	*confer*, compare
e. g.	*exempli gratia*, for example
et al.	*et alii*, and others; *et alibi*, and elsewhere
EOS	equation of state
FD	finite difference
FDE	FD equation
FSS	finite size scaling
GCMC	grand-canonical MC
GEMC	Gibbs-ensemble MC
GMSA	generalized mean spherical approximation
GH	Grundke-Henderson
HCY	hard-core Yukawa
HRT	Hierarchical Reference Theory
HSVDW	hard-sphere van-der-Waals
i. e.	*id est*, that is
LOGA	Lowest-Order γ-Ordered Approximation
MC	Monte Carlo
MD	molecular dynamics
MHNC	modified hypernetted chain
ODE	ordinary differential equation
ORPA	Optimized Random-Phase Approximation
OY	Okumura-Yonezawa
OZ	Ornstein-Zernike
PDE	partial differential equation
PY	Percus-Yevick
q. v.	*quod vide*, which see
SCOZA	Self-consistent Ornstein-Zernike approximation

SW	square well
TDSMC	thermodynamic- or temperature-and-density scaling MC
URL	uniform resource locator
v. i.	*vide infra*, see below
viz.	*videlicet*, that is to say, namely
v. s.	*vide supra*, see above
vs.	*versus*, against, compared to
YY	Yang-Yang

Note that the plural of an abbreviation is consistently formed by appending -s.

F.4. Presentation

Equations, tables, and figures are numbered on a per-chapter basis, and references to them are displayed in the form $(c.n)$, where c references the chapter and n is the number within the current chapter; for references within the same chapter, only the number n is shown. The same applies, with the obvious modifications, to appendices, where c now is an uppercase letter.

References to the literature are indicated as (lists of) numbers in brackets, referring to the bibliography (appendix G). Note that, as much of the work reported here is in the process of also being published as [26, 27], we generally do *not* include references to those.

Mono-spaced font is generally used for the main parts of our software (*cf.* chapter 4), for the names of programming languages and computer software, and in representing the dialog with the `Mathematica` CAS in appendix A.

G. Bibliography

In the following list of references we also give, where appropriate, URLs for electronically accessible material in monospaced font; pre-prints on `www.arXiv.org`, on the other hand, indicated in the form `arXiv:`*arch-ive/nnn*, are available via the URL obtained by substituting archive name (*e. g.* `cond-mat`) and article number (*e. g.* `0112035`) for "*arch-ive*" and "*nnn*", respectively, in `http://www.arXiv.org/abs/`*arch-ive/nnn/*. Note that line breaking within a URL is not indicated.

[1] C. Caccamo, Phys. Rep. **274** (1996) 1.
[2] A. Parola, L. Reatto, Adv. Phys. **44** (1995) 211.
[3] A. Parola, L. Reatto, Phys. Rev. Lett. **53** (1984) 2417.
[4] A. Parola, L. Reatto, Phys. Rev. A **31** (1985) 3309.
[5] A. Parola, A. Meroni, L. Reatto, Phys. Rev. Lett. **62** (1989) 2981.
[6] A. Meroni, A. Parola, L. Reatto, Phys. Rev. A **42** (1990) 6104.
[7] A. Parola, L. Reatto, Phys. Rev. A **44** 6600.
[8] D. Pini, A. Parola, L. Reatto, J. Stat. Phys. **72** (1993) 1179.
[9] A. Meroni, L. Reatto, M. Tau, Mol. Phys. **80** (1993) 977.
[10] A. Parola, D. Pini, L. Reatto, Phys. Rev. E **48** (1993) 3321.
[11] M. Tau, A. Parola, D. Pini, L. Reatto, Phys. Rev. E **52** (1995) 2644.
[12] L. Reatto, Phys. Lett. **72A** (1979) 120.
[13] A. Parola, J. Phys. C: Solid State Phys. **19** (1986) 5071.
[14] L. Lue, J. M. Prausnitz, J. Chem. Phys. **108** (1998) 5529.
[15] J. A. White, J. Chem. Phys. **113** (2000) 1580.
[16] J. A. White, Sh. Zhang, J. Chem. Phys. **103** (1995) 1922.
[17] J. A. White, Sh. Zhang, J. Chem. Phys. **99** (1993) 2012.
[18] K. G. Wilson, Phys. Rev. B **4** (1971) 3184.
[19] A. Parola, L. Reatto, J. Phys.: Condens. Matter **5** (1993) B165.
[20] D. Pini, A. Parola, L. Reatto, J. Stat. Phys. **100** (2000) 13.
[21] L. Reatto, A. Parola, J. Phys.: Condens. Matter **8** (1996) 9221.
[22] P. Gianinetti, A. Parola, Phys. Lett. A **268** (2000) 424.
[23] P. Gianinetti, A. Parola, Phys. Rev. B **63** (2001) 104414.
[24] P. Gianinetti, A. Parola, Phil. Mag. B **81** (2001) 1565.

[25] A. Brognara, A. Parola, L. Reatto, Phys. Rev. E **64** (2001) 026122-1.

[26] A. Reiner, G. Kahl, to appear in Phys. Rev. E; `arXiv:cond-mat/0112035`.

[27] A. Reiner, G. Kahl, to be published; preliminary version at `http://purl.oclc.org/NET/a-reiner/sci/texts/20011127-0/`.

[28] C. Caccamo, G. Pellicane, D. Costa, D. Pini, G. Stell, Phys. Rev. E **60** (1999) 5533.

[29] F. Barocchi, P. Chieux, R. Fontana, R. Magli, A. Meroni, A. Parola, L. Reatto, M. Tau, J. Phys.: Condens. Matter **9** (1997) 8849.

[30] D. Chandler, J. D. Weeks, Phys. Rev. Lett. **25** (1970) 149.

[31] D. Chandler, J. D. Weeks, H. C. Andersen, J. Chem. Phys. **54** (1971) 5237.

[32] H. C. Andersen, J. D. Weeks, D. Chandler, Phys. Rev. A **4** (1971) 1597.

[33] M. J. P. Nijmeijer, A. Parola, L. Reatto, Phys. Rev. E **57** (1998) 465.

[34] M. E. Fisher in: *Critical Phenomena. Proceedings of the Summer School Held at the University of Stellenbosch, South Africa, January 18-29, 1982*, ed. F. J. W. Hahne, Lecture Notes in Physics **186**, Berlin (Springer) 1983, pp. 1–139.

[35] G. Stell in: H. L. Frisch (ed.), *The equilibrium theory of classical fluids.* New York (Benjamin) 1964.

[36] L. S. Ornstein, F. Zernike, Proc. Akad. Sci. (Amsterdam) **17** (1914) 793.

[37] M. Campostrini, A. Pelissetto, P. Rossi, E. Vicari, unpublished; pre-print `arXiv:cond-mat/0201180`.

[38] G. Stell, Phys. Rev. **184** (1969) 135.

[39] G. Stell, J. Chem. Phys. **55** (1971) 1485.

[40] H. C. Andersen, D. Chandler, J. Chem. Phys. **55** (1971) 1497.

[41] M. E. Fisher, J. Math. Phys. **5** (1964) 944.

[42] L. Vega, E. de Miguel, L. F. Rull, J. Chem. Phys. **96** (1992) 2296.

[43] E. de Miguel, Phys. Rev. E **55** (1997) 1347.

[44] G. Orkoulas, A. Z. Panagiotopoulos, J. Chem. Phys. **110** (1999) 1581.

[45] N. V. Brilliantov, J. P. Valleau, J. Chem. Phys. **108** (1998) 1115.

[46] N. V. Brillantov *(sic!)*, J. P. Valleau, J. Chem. Phys. **108** (1998) 1123.

[47] J. R. Elliott, L. Hu, J. Chem. Phys. **110** (1999) 3043.

[48] A. Lomakin, N. Asherie, G. B. Benedek, J. Chem. Phys. **104** (1996) 1646.

[49] D. M. Heyes, P. J. Aston, J. Chem. Phys. **97** (1992) 5738.

[50] J. Chang, St. I. Sandler, Mol. Phys. **81** (1994) 745.

[51] A. L. Benavides, J. Alejandre, F. del Rio, Mol. Phys. **74** (1991) 321.

[52] G. Orkoulas, M. E. Fisher, A. Z. Panagiotopoulos, Phys. Rev. E **63** (2001) 051507.

[53] R. V. Gopala, D. Debnath, Colloid Polym. Sci. **268** (1990) 604.

[54] A. Lang, G. Kahl, Ch. N. Likos, H. Löwen, M. Watzlawek, J. Phys.: Condens. Matter **11** (1999) 10143.

[55] G. Foffi, E. Zaccarelli, F. Sciortino, P. Tartaglia, K. A. Dawson, J. Stat. Phys. **100** (2000) 363.

[56] L. Acedo, A. Santos, J. Chem. Phys. **115** (2001) 2805.

[57] E. Zaccarelli, G. Foffi, K. A. Dawson, F. Sciortino, P. Tartaglia, Phys. Rev. E **63** (2001) 31501.

[58] M. E. Fisher, G. Orkoulas, Phys. Rev. Lett. **85** (2000) 696.

[59] G. Orkoulas, M. E. Fisher, Cevat Üstün, J. Chem. Phys. **113** (2000) 7530.

[60] H. Okumura, F. Yonezawa, J. Chem. Phys. **13** (2000) 9162.

[61] J. S. Høye, G. Stell, J. Chem. Phys. **67** (1977) 439.

[62] J. S. Høye, G. Stell, Mol. Phys. **52** (1984) 1071.

[63] J. S. Høye, G. Stell, Int. J. Thermophys. **6** (1985) 561.

[64] R. Dickman, G. Stell, Phys. Rev. Lett. **77** (1996) 996.

[65] D. Pini, G. Stell, R. Dickman, Phys. Rev. E **57** (1998) 2862.

[66] D. Pini, private communication.

[67] D. Pini, G. Stell, N. B. Wilding, Mol. phys. **95** (1998) 483; reference according to [28].

[68] C. Caccamo, G. Giunta, G. Malescio, Mol. Phys. **84** (1995) 125; reference according to [28].

[69] Fortran standards committee ISO/IEC JTC1/SC22/WG5, `Fortran-90` standard ISO/IEC 1539:1991.

[70] Floating-point standard IEEE 754-1985, also published as IEC 559:1989.

[71] Fortran standards committee ISO/IEC JTC1/SC22/WG5, technical report TR 15580; also available from `ftp://ftp.nag.co.uk/sc22wg5/N1351-N1400/N1378.ps.gz` and `ftp://ftp.nag.co.uk/sc22wg5/N1351-N1400/N1378.pdf`; *cf.* `http://www.nag.co.uk/sc22wg5/TR15580.html`.

[72] J. L. Lebowitz, Phys. Rev. **133** (1964) A895.

[73] D. Henderson, E. W. Grundke, J. Chem. Phys. **63** (1975) 601.

[74] L. Verlet, J.-J. Weis, Phys. Rev. A **5** (1972) 939.

[75] N. F. Carnahan, K. E. Starling, J. Chem. Phys. **52** (1969) 635.

[76] R. Courant, K. O. Friedrichs, H. Lewy, Mathematische Annalen **100** (1928) 32.

[77] W. Auzinger, *Numerik partieller Differentialgleichungen. Eine Einführung*, lecture notes, Technische Universität Wien, 2001.

[78] W. H. Press, S. A. Teukolsky, W. T. Vetterling, B. P. Flannery, *Numerical recipes in Fortran 77: The Art of Scientific Computing.* 2nd ed., Cambridge (Cambridge University Press) 1992, also available from `http://www.nr.com/`.

[79] A. Lang, thesis, Technische Universität Wien, 2001.

[80] L. Reatto, A. Meroni, A. Parola, J. Phys.: Condens. Matt. **2** (1990) 121.

[81] A. Parola, A. Meroni, L. Reatto, Int. J. Thermophys. **10** (1989) 345.

[82] S. Wolfram, *Mathematica: A System for Doing Mathematics by Computer*, 4th edition (Wolfram Media/Cambridge University Press), 1999.

[83] V. K. Decyk, Ch. D. Norton, B. K. Szymanski, ACM Fortran Forum **16** (1997); also available from `http://www.cs.rpi.edu/~szymansk/OOF90/Forum.html`.

[84] A. Reiner, G. Kahl, poster P1-31 presented at 4th Liquid Matter Conference, Granada, Spain, July 3, 1999; available from `http://purl.oclc.org/NET/`

`a-reiner/sci/texts/19990630-0/`, abstract in Europh. Conf. Abstr. **23C** (1999) P1-31.

[85] D. Knuth, *Literate Programming*, Stanford University, Stanford, Calif., 1992.

[86] N. Ramsey, IEEE Software **11** (1994) 97.

[87] I. S. Gradstein, I. M. Ryshik, *Tables*, Moscow (MIR) 1981, Thun–Frankfurt (Harri Deutsch) 1981.

[88] M. Frigo, S. G. Johnson, International Conference on Acoustics, Speech and Signal Processing (ICASSP) conference proceedings **3** (1998) 1381.

Lebenslauf

Am 27. Februar 1971 geboren, wuchs ich als nach meiner Schwester DSA Ulrike Reiner zweites Kind der AHS-Lehrer für Englisch und Französisch Prof. Mag. OStR. Friederike Reiner (geborene Ott) und Prof. Dr. Erwin Reiner in Wien auf. Dort besuchte ich zunächst die Öffentliche Volksschule in 1070, Zieglergasse 21, danach vier Jahre lang das Bundesgymnasium und -realgymnasium BGRG VI (1060, Rahlgasse 4) sowie ebenfalls vier Jahre das Öffentliche Schottengymnasium der Benediktiner in Wien (1010, Freyung 6), letzteres im Herbst 1987 unterbrochen durch einen dreimonatigen Aufenthalt in New York samt Schulbesuch an der Fiorello H. LaGuardia High School of Music and the Arts–Performing Arts im Rahmen meiner Teilnahme am Ronald S. Lauder "Young Diplomats" Schüleraustausch. Nach der Matura mit Auszeichnung inskribierte ich 1989 zunächst Rechtswissenschaften an der Universität Wien, wandte mich jedoch bald ausschließlich dem Studium der Technischen Physik an der Technischen Universität Wien zu. Im Rahmen der Vorbereitung meiner Diplomarbeit, die unter Anleitung von ao.Univ.Prof. Dr.phil. Heinz Oberhummer der Entwicklung eines potentialbasierten **R**-Matrixansatzes zur Beschreibung der Neutron-Kern-Streuung bei mittleren Energien anhand von ^{208}Pb gewidmet war, besuchte ich im Jänner 1997 gemeinsam mit Univ.Doz. Ass.Prof. Dr.phil. Peter Riehs die ORELA-Anlage am Oak Ridge National Laboratory (Oak Ridge, Tennessee, U.S.A.). Nach Ablegung der zweiten Diplomprüfung mit ausgezeichnetem Erfolg im Dezember 1997 wandte ich mich dem mir bereits durch Lösung der Percus-Yevick-Gleichungen für ein ternäres additives Hartkugelsystem vertraut gewordenen Gebiet der Flüssigkeitsphysik zu, auf dem ich mich im Rahmen eines von ao.Univ.Prof. Dipl.-Ing. Dr.techn. Gerhard Kahl betreuten Doktoratsstudiums der Hierarchical Reference Theory widmete; in diese Zeit fielen neben dem vom 2. November 1999 bis 30. Juni 2000 an der ABC-Abwehrschule des Österreichischen Bundesheeres abgeleisteten Grundwehrdienst auch ein dreimonatiger Forschungsaufenthalt in der Gruppe von Prof. George Stell, B.S. Ph.D., an der State University of New York in Stony Brook (New York, U.S.A.) sowie auf Einladung von p. t. D.Ph. Giorgio Pastore ein einwöchiger Besuch am Dipartimento di Fisica Teorica dell' Università degli Studi di Trieste (Triest, Italien); außerdem nahm ich im Juli 1998 an der NATO-ASI School on New Approaches to Old and New Problems in Liquid State Theory (Patti Marina, Italien) und im Juli 1999 an der 4$^{\text{th}}$ Liquid Matter Conference (Granada, Spanien) teil. Seit Sommersemester 2001 halte ich — im ersten Jahr noch gemeinsam mit DI Martin Ertl — an der Technischen Universität Wien unter dem Titel "Symbolische Mathematik in der theoretischen Physik" Vorlesungen und Übungen über Computeralgebrasysteme und funktionale Programmierung.